Two *C. elegans* high mobility group genes, *hmg-12* and *hmg-1.1*, function in neural postembryonic development and cell survival

Dissertation
zur Erlangung des Doktorgrades
der Mathematisch- Naturwissenschaftlichen Fakultäten
der Georg- August- Universität zu
Göttingen

vorgelegt von

Abd-elNasser Elashry
aus

Sharkia/Ägypten

Göttingen 2004

D7

Referent: PD. Dr. E. Schulze

Korrerent: Prof. Dr. M. Kessel

Tag der mündlichen Prüfung: 30.4.2004

TABLE OF CONTENTS

1. INTRODUCTION....1

2. MATERIALS AND METHODS....15

2.1 MATERIALS....15
2.1.1 C. elegans genes studied in this study....15
2.1.2 C. elegans strains....15
2.1.2.1 Strains from CGC center....15
2.1.2.2 Strains made in our laboratory....16
2.1.3 The bacterial strains....16
2.1.4 Vectors and plasmids....17
2.1.4.1 Basic cloning vectors....17
2.1.4.2 Recombinant plasmids....18
2.1.4.2.1 Plasmids for RNAi techniques....18
2.1.4.2.2 Recombinant plasmids used for other purposes....19
2.1.5 PCR amplification....20
2.1.5.1 Oligonucleotide sequences....20
2.1.6 Reagents for antibody staining of C. elegans embryos....20
2.1.6.1 Primary antibodies....20
2.1.6.2 Secondary antibodies....21
2.1.7 Databases and Softwares....21
2.1.8 Equipments for fluorescence light microscopy....22
2.1.8 Bombardment equipment....23
2.1.9 The compositions of solutions used in this study....24
2.1.10 Antibody purification....26
2 METHODS....27
2.2.1 Culturing worms in plastic petri dishes....27
2.2.2. Culturing worms on plastic petri dishes for feeding experiment....28
2.2.3 Extraction of the eggs from the adults....29
2.2.4 RNA interference by feeding....30
2.2.4.1 The cloning of cDNA....30
2.2.4.2 The RNAi feeding (standard)....30
2.2.4.3 The RNAi feeding (collective scoring)....30
2.2.4.4 The RNAi feeding (individual scoring)....31
2.2.5 RNAi microinjection....31
2.2.5.1 Preparation of agarose coated cover slips (pads)....31
2.2.5.2 Preparation of the cDNA template....32
2.2.5.3 Transcription of the cDNA....33
2.2.5.4 Microinjection of the dsRNA....34
2.2.6 Cloning....34
2.2.6.1 Preparation of the competent *E. coli* DH5α bacteria....34
2.2.6.2 Restriction enzymes analysis....35
2.2.6.3 Agarose-gel electrophoresis....35
2.2.6.4 Ligation of DNA for transformation into the competent *E. coli* cells....36
2.2.6.5 Transformation of ligated plasmid into competent *E. coli* cells....37
2.2.6.6 Isolation of plasmids from transformed *E. coli* cells....37
2.2.7 DNA transformation of C. elegans (Fire, 1986)....38
2.2.7.1 Creating transgenic animals by microinjection technique....39

2.2.7.2 Creating transgenic animals by bombardment....40
2.2.7.2.1 The preparation of the gold beads....41
2.2.7.2.2 Coating the prepared gold beads by DNA....42
2.2.7.2.3 Putting worms on plates....42
2.2.7.2.4 Putting beads on macrocarriers and bombardment....43
2.2.7.2.5 Post-bombardment care of worms....43
2.2.2.8 Freezing and recovery of the *C. elegans* strains....44
2.2.2.9 Cleaning of contaminated *C. elegans* strains....44
2.2.2.10 Growing the *C. elegans* worms in liquid culture....45
2.2.2.11 Preparation of agarose coated cover slips for microinjection....46
2.2.2.12 Preparing the slides for microscopic observation....47
2.2.2.13 Preparation of polylysine-coated glass slides....47
2.2.2.14 Staining the DNA with DAPI....48
2.2.2.15 The acridine orange staining....48
2.2.2.16 The extraction of the total protein from *C. elegans* worms....48
2.2.2.17 Agarose Gel Extraction Protocol with QIAEX II kit....49
2.2.2.18 GST purification....50
2.2.2.18.1 Culturing the bacteria....50
2.2.2.18.2 Incubation....50
2.2.2.18.3 Elution....51
2.2.218.4 Dialysis....51
2.2.2.19 Bradford assay....51
2.2.2.20 The antibody purification....52
2.2.2.20.1 The reduction of the protein....52
2.2.2.20.2 Coupling protein to gel....52
2.2.2.20.3 Blocking Nonspecific Binding Sites on Gel....53
2.2.2.20.4 Washing the column....53
2.2.2.21 The affinity purification of protein....54
2.2.2.21.1 Column preparation....54
2.2.2.21.2 Sample purification....54
2.2.2.21.3 Regenerating and storing the affinity column....54
2.2.2.22 Immunostaining....55
2.2.2.23 The separation of the proteins with SDS-PAGE....56

3. RESULTS....57

3.1 STUDIES ON *HMG-12* (*HMG-1B*)....57
3.1.1 Phenotypes that resulted from hmg-12 RNA interference (RNAi)....57
3.1.1 Phenotypes that resulted from the microinjection of N2....57
3.1.1.1 Depletion of *hmg-12* caused defective touch response....57
3.1.1.1.1 Head-tail touch....58
3.1.1.1.2 Touching the head of the animals....63
3.1.1.1.3 Response to the tail touch....66
3.1.1.1.4 Head touch response of L2 larvae....66
3.1.1.2 Turning defect....67
3.1.1.3 Uncoordination....68
3.1.1.4 Fast foraging activity....69
3.1.1.5 Partial egg laying defect....69
3.1.1.6 Embryonic and oocyte lethality....69
3.1.2 Feeding of hmg-12 dsRNA to N2 animals....70
3.1.2.1 Effect of *hmg-12* dsRNA feeding on chemotaxis....70

3.1.3 Microinjection of hmg-12 dsRNAi into him-8 ..... *70*
3.1.4 Microinjection of hmg-12 dsRNAi into KP987 (glr-1::gfp): *73*
3.1.5 Expression pattern of hmg-12 ..... *74*
3.1.5.1 Expression pattern of *hmg-12* in EC700 and EC701 strains 74
3.1.5.2 Expression pattern in L1 and L2 75
3.1.5.3 Expression pattern in the dauer larva 76
3.1.5.4 Expression pattern in the hermaphrodites 76
3.1.6 Expression pattern in EC705 ..... *77*
3.1.7 Depletion of hmg-12 in EC700 ..... *79*
3.1.8 Immunostaining of HMG-12 ..... *80*
3.2 STUDIES ON *HMG-1.1* 81
3.2.1.1 Phenotypes that resulted from *hmg-1.1* dsRNA feeding 81
3.2.1.1.1 Phenotypes from *hmg-1.1* dsRNA feeding of N2 animals 82
3.2.1.1.2 The phenotypes from *hmg-1.1* dsRNA application of *rrf-3* 85
3.2.1.1.3 The *hmg-1.1* dsRNA microinjection effect on *him-8* 86
3.2.1.5 Effect of stresses on the *hmg-1.1* dsRNA fed animals 91
3.2.1.1.5.1 Effect of the starvation stress on the *hmg-1.1* dsRNA fed animals 91
3.2.1.5.2 Effect of heat shock on the *hmg-1.1* dsRNA fed animals 93
3.2.1.5.3 Effect of the *hmg-1.1* dsRNA feeding on the brood size of N2 93
3.1.1.3 Phenotypes that resulted from microinjection 97
3.1.1.4 Phenotypes that resulted from the microinjection of *him-8* 97
3.1.1.4.1 Male defects 97
3.2.1.5 The relationship between *hmg-1.1* and necrosis 99
3.2.1.5.1 The effect of L1 starvation stress on *crt-1* strain 100
3.2.1.5.2 The effect of *hmg-1.1* dsRNA feeding on the defecation period of N2 and *crt-1* adults 101
3.2.1.5.3 The effect of the *hmg-1.1* dsRNA feeding on strains from the necrotic death pathway 101
3.2.1.6 studying the relationship between *hmg-1.1* and apoptosis 102
3.2.1.6.1 The effect of starvation stress on a *ced-3* mutant fed with *hmg-1.1* dsRNA 102
3.2.1.6.2 Effect of the *hmg-1.1* dsRNA feeding on mutants of the programmed cell death pathway 103
3.2.2 Expression pattern of hmg-1.1 in the strain EC715 ..... *105*
3.2.2.1 *hmg-1.1::gfp* expression in the embryos 105
3.2.2.2 The *hmg-1.1::gfp* expression in the larval stages 110
3.2.2.3 The *hmg-1.1::gfp* expression in the adults 111
3.2.3 Effect of overexpression on the embryonic lethality *112*
3.2.4 Depletion of the expression in hmg-1.1::gfp using RNAi *112*
3.2.5 Immunostaining *113*

4. DISCUSSION 115

4.1 STUDIES OF THE HMG-12 FUNCTIONS 115
4.1.1 Touch-response defect of RNAi animals *115*
4.1.1.1 Nature of the touch response behaviour in the control N2 animals ... 115
4.1.1.2 Nature of the touch response behaviour in HMG-12 RNAi animals . 120
4.1.2 The relationship between HMG-12 functions and the germline: *125*
4.2 STUDIES OF THE FUNCTIONS OF HMG-1.1 125
4.2.1 The relationship between HMG-1.1 and necrosis *125*
4.2.2 The relationship between HMG-1.1 and apoptosis *130*

4.2.3 HMG-1.1 and cell cycle 131
5. ABSTRACT 135
6. BIBLIOGRAPHY 136
7. ABBREVIATIONS 148
8. ACKNOWLEDGMENT 150
9. LEBENSLAUF 115

1. Introduction

High mobility group (HMG) proteins are a diverse group of nuclear proteins. Based on their structure, HMG proteins were grouped under three families, HMGI(Y), HMG14/17, and HMG1/2. HMGI(Y) and HMG1/2 interact with several transcription factors. Proteins from both families, HMGI(Y) and HMG1/2, are considered architectural factors because of their ability to bind to the DNA minor groove and bend the DNA segment to which they are bound (Tjian and Maniatis, 1994).

HMG1 is a very abundant and highly conserved non-histone protein that is present in all vertebrate nuclei (Bianchi, 1995; Bustin and Reeves, 1996). HMG2 protein is also ubiquitously expressed and has overlapping functions with HMG1 (Vaccari *et al.*, 1998). HMG1 and HMG2 establish protein-protein contacts with TFIIA-TFIID, several HOX and OCT proteins, and the progesterone nuclear receptor to facilitate the binding of these transcription factors to target sites on DNA and transcriptional activation. (Onate *et al.*, 1994; Shykind *et al.*, 1995; Zappavigna *et al.*, 1996; Zwilling *et al.*, 1995).

Historically, HMG proteins were discovered as highly mobile bands, which were scored when chromatin-proteins were separated with polyacrylamide gel electrophoresis. However the first observation of the high mobility group proteins described them as contamination or acidic impurities in histone H1 preparations (John, 1964), the recent studies describe them as critical cell components, which serve many cellular functions (Wisniewski and Schwanbeck, 2000, and Bustin and Reeves, 1996).

It was reported that HMG protein family members stimulate human immunodeficiency virus type 1 (Hindmarsh *et al*., 1999). It was proved that, HMGI(Y) and HMGI-C genes are expressed in neuroblastoma cell lines and tumors (Andersson et al., 2000). HMG1 can assist recombination reactions, DNA replication, transposition, and DNA repair (Bustin and Reeves, 1996; Bustin, 1999; Grasser, 2003; Müller *et al*., 1999).

The initial grouping of these proteins was done based on their molecular weight. These four groups seemed to fall into two categories: HMG1 and 2, which contain aromatic amino acid residues and which have a molecular weight of approximately 28 kDa, and HMG14 and 17 which are less than half of this value and does not contain

aromatic amino acid residues. It was expected that these differences would reflect on the nature of their functions.

The four major proteins were found in several calf tissues and it was shown that there is no qualitative tissue specificity. It was revealed that HMG1 and 2 are very similar proteins and that no extensive regions of sequence similarity exists between the histones and any of the HMG 1 and 2, however limited similarities were found between H1 and HMG 14 and 17 (John *et al*., 1982).

Goodwin and his colleagues identified some more HMG proteins and called them HMG18, HMG19A, and HMG19B (Goodwin *et al*., 1980). One of the HMG proteins that were previously identified as HMG20 (John, 1982) is now known as ubiquitin, one of the very widely distributed proteins in the cells of the higher organisms. HMG1 and HMG2 proteins are very acidic, hence, it was suggested that it could be involved in a complex formation with the very basic regions of histones and complexes between HMG1 and histone H1 (Smerdon and Isenberg, 1976; Cary *et al*., 1979). However, the possibility that these acidic regions may bind calcium has not been discussed (John *et al*., 1982).

The binding of HMG1 to DNA is reversible and on adding DNA to a complex HMG1/DNA the protein re-equilibrated itself between all of the DNA molecules (Shooter *et al*., 1974).

It was found by Bustin and his colleagues that HMG-1/2 proteins have a three-part domain structure (Bustin *et al*., 1990). Two of these domains, a terminal amino domain (A-domain), a basic domain (B-domain), are the HMG boxes and the third domain is a terminal Carboxy-domain (C-domain) (Landsman and Bustin, 1993).

Some other researchers went further investigating the specific structure of HMG-1/2 by NMR spectroscopy. They found that it consists of three α-helices, which are forming a L-shape structure (Read *et al*., 1993; Weir *et al*., 1993). This highly charged domain (HMG-box domain) was found to be HMG1 sequence independent DNA binding structure (Bianchi *et al*., 1992).

HMG-1/2-proteins bind both double-stranded DNA (dsDNA) as well as the single stranded DNA, however they bind preferentially to dsRNA (Einck and Bustin 1985). Furthermore, they bind to none-B-DNA-structures such as palindrome, B-Z-DNA-junctions, crosswise DNA, four-way-junctions (4WJ) and cis-diamindichloroplatine (II) (cisplatine) modified DNA (Hamada and Bustin 1985, Hughes *et al*., 1992). Thus

they show a functional relationship to the bacterial proteins IHF (integration host factor) and HU (Bianchi, 1994). It was found later that the binding with the cisplatine-modified protein would be enhanced by the presence of the tumour suppressor *p53* in human being (Imamura et al., 2001).

Additionally to the recognition of the bent and distorted DNA structures HMG-1/2-proteins can bend the DNA, insert loops into linear or circular DNA and in the presence of topoisomerase it causes supercoils in closed DNA conformations (Stros *et al*., 1994, Sheflin *et al*., 1993).

Studying the similarity between HMG1/2 proteins and other proteins revealed a link between the proteins from this family and other proteins that can play a role in the regulation of the chromatin architecture (Thomas and travers, 2001). Soullier and his colleagues published a phylogenetic tree (see Fig. 1.1) showing the phylogeny of the proteins from the different HMG families (Soullier *et al*., 1999).

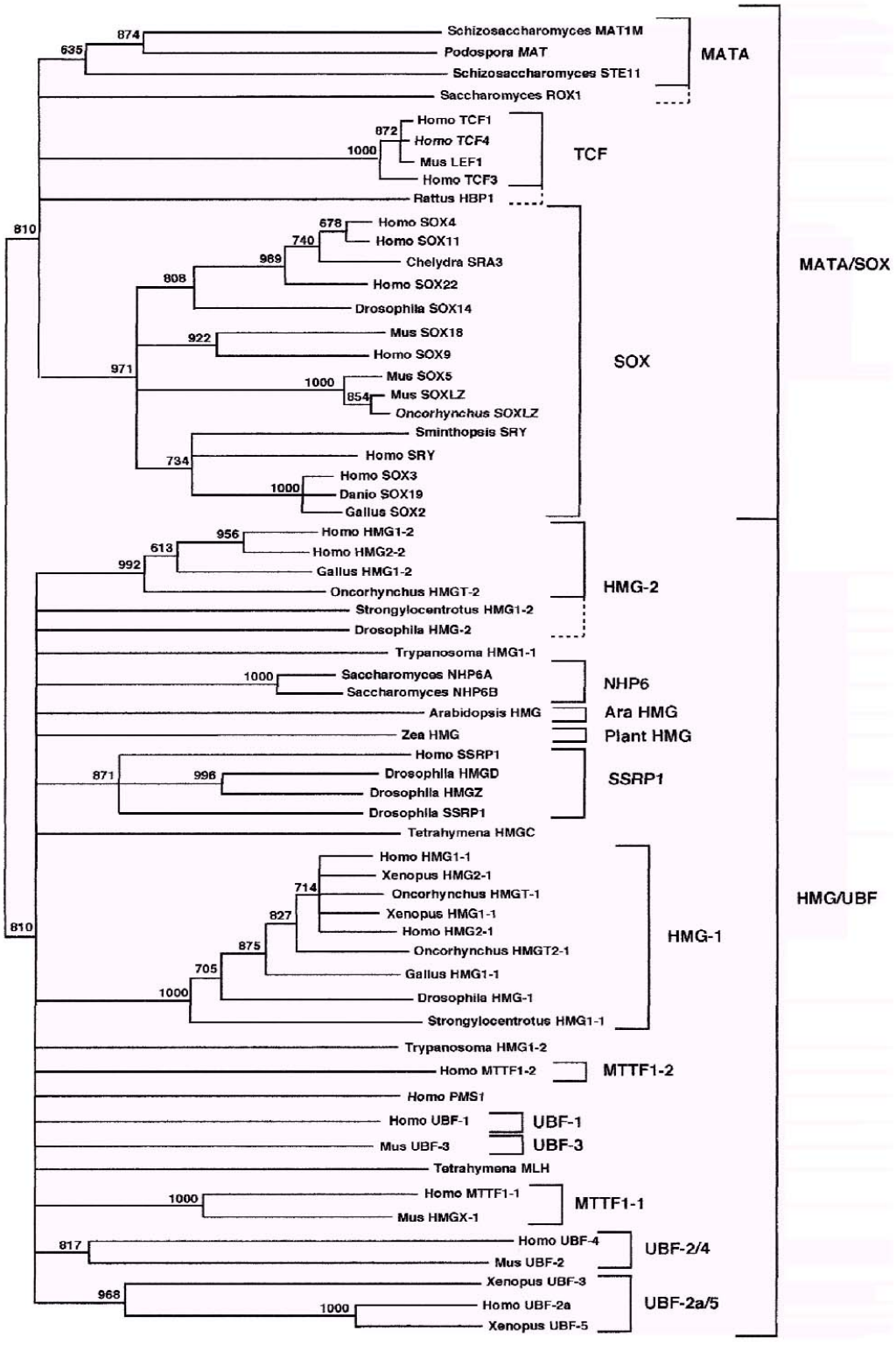

Fig. 1.1: A phylogenetic neighbour-joining-tree of HMG-1 superfamily. This phylogenetic tree is taken from (Soullier *et al*., 1999).

Based on the results of the phylogenetic studies, HMG box super family can be divided into two sub-families, SOX/MATA/TCF and HMG/UBF families (Soullier *et al*., 1999). The degree of specificity to bind DNA and the number of the HMG boxes differ between the proteins that belong to the two families.

The proteins belong to the SOX/MATA/TCF family contain only one HMG box and can bind specifically to DNA. This family includes, the gender defining factor SRY of mammals as well as homologues in insects and vertebrates (SOX) (Sinclair *et al*., 1990), and the T-lymphocyte-specific transcription factors TCF1 and LEF1 (Waterman *et al*., 1991)

Members of the HMG/UBF-family have one or more HMG boxes and indicate no or only very little sequence specificity of the DNA linkage. Members of the HMG/UBF-family have one or more HMG boxes and indicate no or only very little sequence specificity of the DNA binding. The HMG/UBF-family includes, the classical HMG-1/2-proteins, the SSRP (structure specific recognition protein) proteins, the eukaryotic UBF (upstream binding factor) transcription factors of RNA polymerase I, the chromatin proteins NHP6A/B of yeast *Sacharomyces cerevisiae*, and the mitochondrial transcription factors ABF2 of yeast (Soullier *et al*., 1999).

The sub-groups of the HMG/UBF family defined by (Soullier *et al*., 1999) correspond to those, which were found by Baxevanis and Landsman by using structural alignments of HMG-1-Boxes (Baxevanis and Landsman, 1995). An alignment, which was made based on tertiary structure similarities instead of sequence homologies, showed that no rigid sequence preservation is necessary in order to maintain the conformation of the HMG-1 Box, but stabilisation is achieved mainly by hydrophobic interactions (Baxevanis *et al*., 1995).

HMG1/2 proteins function as positive or negative regulatory factors. HMG-1 was implicated as a ligand for the monocyte receptors for advanced glycated proteins (RAGE). RAGE receptor ligand interaction with glycated proteins can indeed activate macrophages (Ichikawa et al., 1998). Furthermore, lymphocytes are a specific target for the cytokine-inducing activity of HMG-1 (Andersson *et al*., 2000). Hence, they are involved in the replication, transcription and repair of the DNA. DNA bending can be used in the regulation of the transcription. By that, it increases the accessibility of the bent DNA for the function of the transcription factors to take place (Onate *et al*., 1994).

Furthermore, it was found that HMG1/2-proteins possess the ability to bind at linker DNA between neighbouring nucleosomes and that they are able to replace histone H1 in defined regions (Ner and Travers, 1994). By their interaction with TBP (TATA-box-binding protein) the transcription of genes can be restrained reversibly by RNA polymerase II (Ge and Roede, 1994).

A reasonable number of researchers from different groups proved that HMG-1 has a link with inflammation and necrosis. It was found that HMG-1 functions as a late extracellular mediator during endotoxemia, but normally acts intracellularly as DNA binding protein (Angello, *et al*., 2002).

Some other researchers investigated the role that HMG-1 plays in necrosis and apoptosis. They found that HMG-1 would function in the crossroads between apoptosis and necrosis. The HMG1 binding to RAGE in the neural cells activates the Ras-MAP kinase and leads ultimately to the activation of NF-kB, the transcription factor that linked to inflammatory process (Huttunen et al., 1999). The release of HMG-1 by the necrotic cells triggers inflammation in HeLa cells. However, HMG-1 stayed linked to the chromosomes in the cells that destined to apoptosis. Accordingly, HMG-1 spelling from the chromosomes versus attaching firmly to it can be a signal differentiating necrotic- from apoptotic-cell death, respectively (Scaffidi *et al.*, 2002).

Calogero and his colleagues showed by their studies on HMG-1$^{-/-}$ mice that the lack of HMG-1 does not disrupt cell growth because these mice were born. However, these mice died shortly after they were born. The analysis showed that they had hypoglycaemia (Calogero *et al*., 1999).

One of the recent studies showed, with the use of the fluorescence of HMG-1 fused to GFP or to DSRed, that HMG-1 that HMG-1 is associated with the mitotic chromatin in HeLa cells (Pallier *et al*., 2003). These results were contradicting the previous knowledge that HMG-1 is not associated with mitotic chromosomes based on immunofluorescence studies (Falciola *et al*., 1997).

In *C. elegans*, Jiang and Sternberg found that the disruption of *son-1*, a HMG-1-like protein, function by RNAi results in a male spicule defect. This defect is the same spicule defect that caused by overexpression of POP-1, a TCF/LEF class HMG protein. It is known that POP-1 acts downstream of the Wnt signaling pathway. These results revealed a possibility that SON-1 and POP-1 might act in the Wnt responding cells to regulate gene transcription in opposite directions (Jiang and Sternberg, 1999).

After the discovery of the previously mentioned two families, HMG-1/2 and HMG-14/17, another protein that is similar in its physicochemical properties and abundances to the HMG-14 and HMG-17 proteins has been discovered. This protein was isolated by two different groups, the first group isolated it from HeLa cells and designated it HMGI (Lund *et al*., 1983); and the second group isolated it from the African green monkey CV-1 cell culture, and designated α-protein (Strauss and Varshavsky. 1984).

At that time, another protein was discovered which was designated HMGY (Lund *et al*., 1983). Then, the cDNA of HMGI and HMGY were cloned (Johnson *et al*., 1988 and Johnson *et al*. 1989). Later a third protein was identified in hepatoma cells and designated as HMGI-C that was found to have a different structure in comparison with the previously identified HMG proteins (Manfioletti *et al*., 1991, and Giancotti *et al*., 1991).

All HMGI/Y proteins have multiple copies of a DNA binding domain called AT hook domain, which consists of K/RXRGRP amino acid residues. HMGI/Y proteins characteristically have 20-25% positively charged residues and 12-15% negatively charged residues with a number of proline residues. The net charge of the N-terminal residues up to the first AT-hook and in the region between the first and the second AT hooks are between –1 to +1. In contrast, the protein region between the second and the third At-hooks is strongly basic. The C-terminal region of the HMGI/Y proteins is negatively charged and that was the reason to call it the acidic tail (Wisniewski and Schwanbeck, 2000).

HMGI/Y proteins have a structure-specific binding ability to the DNA within the minor groove. The binding of HMGI/Y to the DNA affects the DNA conformation and facilitates binding of transcription factors. HMGI/Y proteins bind preferentially to AT-rich DNA. This might lead to consider the HMGI/Y binding as unspecific, however, the high binding affinity of HMGI/Y occurs only if the tracts are appropriately spaced (Maher and Nathan, 1996).

Mammalian HMGI/Y and the insect HMGI from *Chironomus tentans* contain three AT-hook domains. The second AT-hook domain plays the main role in binding to the DNA and the other two domains are optionally involved in protein-DNA contacts (Piekieko *et al*., 2000).

HMGI/Y proteins are involved in a number of specific cellular functions, which is mainly the regulation of gene transcription. These functions can be either positive or

negative regulation. One of the examples of the positive regulation function of HMGI/Y proteins is regulating the interferon-β gene (Thanos and Maniatis, 1992). One of the examples for the functions of HMGI/Y as a repressor is their binding to the promoter element of interleukin 4 gene, where HMGI/Y probablycompete with the transcription factor NF-AT (Klein-Hessling *et al*., 1996).

The HMGI(Y) proteins play a special role during the generation of cancer. By localisation of the human HMGI(Y) protein on the short arm of chromosome 6 (6p21), it appears in a region, which is known for frequent translocational events and responsible for different types of cancer (Friedmann *et al*., 1993). It was observed with human lymphomas and leukaemia that the AT hook motive fusion with oncoproteins can lead to the generation of cancer (Cleary, 1991).

Furthermore, a connection was determined between high HMGI(Y) expression and neoplastic transformation of normal cells or increased metastasis potential of tumor cells respectively. Normal differentiated somatic cells indicate a very small content of HMG-I/Y proteins and their mRNA, whereas neoplastically transformed as well as undifferentiated embryonic cells show exponential quantities of HMG-I/Y (Giancotti *et al*., 1987). The HMG-I/Y content varies in normal cells with their division rate. It is very small in resting cells and rises with exponential growth up to the quadruple amount (Johnson *et al*., 1990).

Furthermore, HMGI(Y) in the host cell is needed for the integration of HIV-1 and other kinds of retroviruses into the genome (Farnet and Bushman, 1997). In tumor cells the HMGI/Y content is independent from the division rate and 15 to 50 times higher than in normal cells.

In mice the HMGI-C protein is involved in the control of growth. In case of the pygmy phenotype (dwarf mouse) the causative mutation has been identified as a HMGI-C null-allele mutant (Zhou *et al*., 1995).

Finally, HMG-I/Y is multifunctional chromosomal protein and causally involved in tumor progression and malignant transformation by its engagement in the regulation of many genes involved in the function of many transcription factors (Wisniewski and Schwanbeck, 2000).

It was important to use *C. elegans* to investigate the functions of HMG proteins because of its helpful features to use it as a model organism (Brenner, 1974). It facilitates the direct observation of the HMG expression by its transparency. This can

be done using *gfp* fusion with the gene of interest. It is easy to culture it in the laboratory.

It has a small size, about 1.3 mm, and because of its short life cycle (51 hours at 25°C) it is easily possible to produce massive cultures from which also larger protein quantities can be wxtracted. Especially, to study the functions of HMG in development *C. elegans* is considered to be an optimal selection because of the knowledge about their cell identification and location.

Also, the relatively small number of somatic nuclei in the worms, which are 959 with hermaphrodites and 1031 with the rare males, can ease the investigation of the nature and the location of the HMG expression. *C. elegans* fertilization is normally done by self-fertilization, which makes it easy to screen and identify mutants and/or transgenic animals. At last, having the complete sequence of the *C. elegans* genome is quite important for the investigation of the protein function and many other targets.

The transcription factor POP-1 was identified in C. *elegans*. It was found that POP-1 has a HMG-box DNA binding domain, which is similar to the one of T-cell-factor 1 (TCF-1) in vertebrates and to the one of the lymphoid specific enhancer-binding factor 1 (LEF-1) in mice (Lin *et al*., 1995). POP-1 possesses important functions for the pattern formation in *C.elegans*. It is needed for the specification of the MS-fate. It functions at the division of the EMS-cell into the MS-cell, from which the mesodermal cell types are being derived, and the E-cell, which is the precursor of the endoderm.

Furthermore, it was shown that POP-1 has an important function for the cell fates after anterior-posterior cell divisions (Lin *et al*., 1998, Schroeder *et al*., 1998) and downstream the Wnt signal transduction, which controls the fates of cells resulting from anterior-posterior divisions and is under the control of *mom-4* and *lit-1* (Thorpe *et al*., 1997, Rocheleau *et al*., 1999, Meneghini *et al*., 1999).

In this study, two of HMG proteins will be investigated, HMG-1.1 and HMG-Iβ (HMG-12), the first protein belongs to the HMG-1/2-protein family that contain HMG-box and the second belongs to HMG-I/Y proteins that contain AT hook domains.

HMG-1.1 is located on chromosome II at the position 14250602-14250951 bp. The unspliced gene contains 350 bp and it has one intron. The molecular weight of that

protein is 10.6 kDa and it has 95 amino acids residues. It is inferred from its electronic annotation that it can bind the DNA to work as a transcriptional regulator.

Kim and his colleagues found that HMG-1.1 is located in the microarray topographic map of *C. elegans* on mountain 5, which is enriched with proteins associated with lipid metabolism and biosynthesis proteins (Kim *et al*., 2001). Two large screens of the *C. elegans* chromosomes by using RNAi, which were made by two different groups, showed that the HMG-1.1 depleted animals were wild type animals (Kamath 2003, and Maeda *et al.*, 2001).

A phylogram of HMG box proteins shows the distance between a member of HMG box proteins in *C. elegans* HMG-1.1 and some other HMG box proteins from *C. elegans*, human, mouse, and plants (Fig. 1.2). The search for the HMG box protein was performed with hmmsearch program from hmmer version 2.2g based on the result of the HMG_box ACC (PF00505) profile from PFAM 12 database. The protein database used to build up this tree was Wormpep 119 (Sanger Center, UK).

The phylogram shows that the nearest proteins from *C. elegans* to HMG-1.1 are two of the *C. elegans* proteins, HMG-3 and HMG-4. Both HMG-3 and HMG-4 function in embryonic and larval development. The nearest protein to HMG-1.1 that comes from *Arabidopsis thaliana* was SSRP-ARATH-1. The nearest mammalian proteins to HMG-1.1 were HMG1, HMG2, and HMG4 from human and mouse. These 6 HMG proteins and the *C. elegans* protein HMG-1.2 formed together the nearest separate cluster to HMG-1.1 (Fig. 1.2).

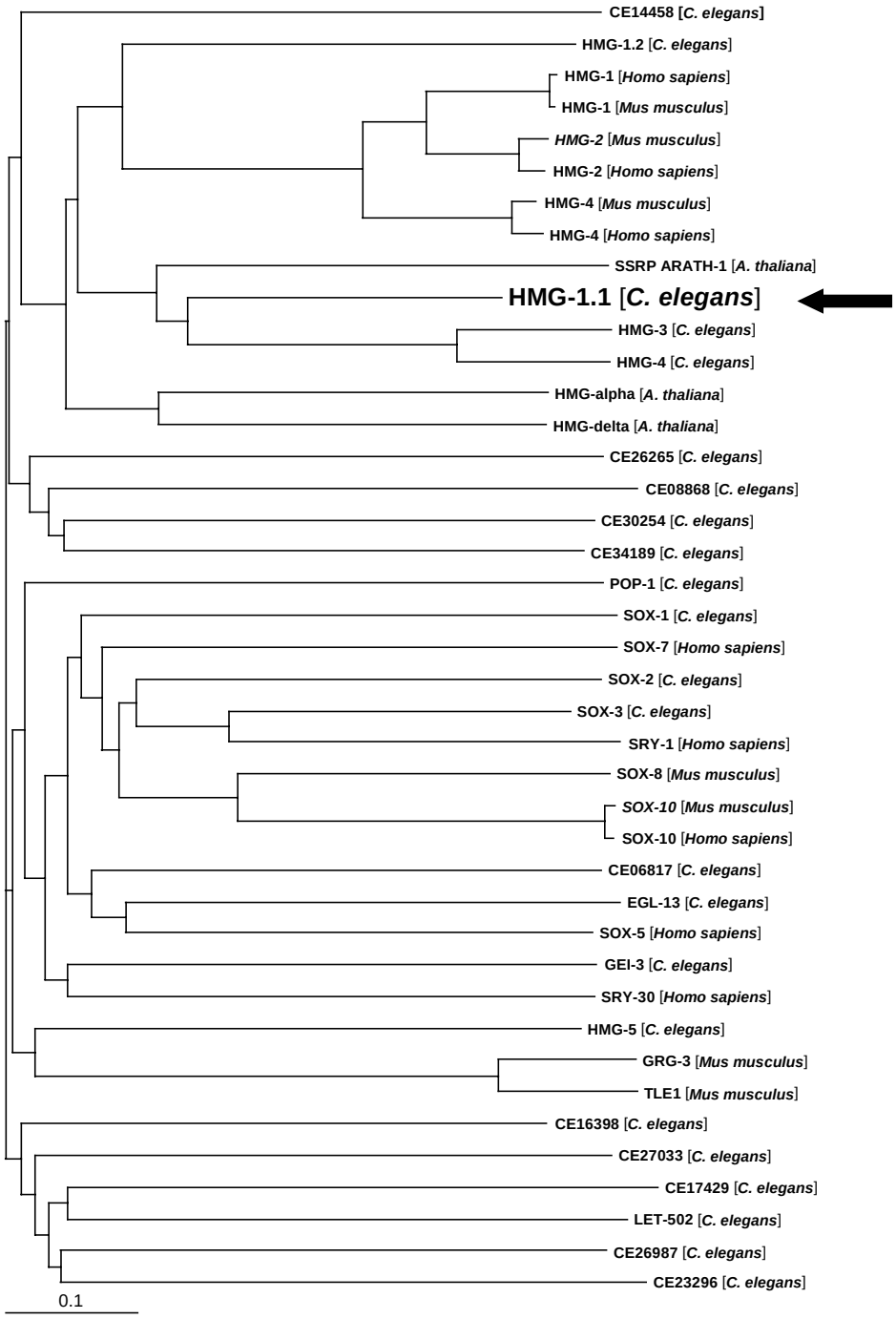

Fig. 1.2: A rectangular phylogram shows the distance between HMG-box proteins from different species. The numbers preceded by (CE) are the designated number for *C. elegans* proteins.

hmg-12 is located on chromosome II at the position 11916411-11917408 bp. This protein has 2 introns and it has 315 amino acids residues. It belongs to HMGI/Y family and it has its AT hook motifes at residues 95-107. However, a large chromosomal screen RNAi of genes on chromosome II showed that depleting HMG-12 resulted in *emb* phenotype (Piano, 2002). Another similar screen by Kamath showed that HMG-12 depleted animals showed no phenotype (Kamath, 2003).

Kim and his colleagues showed that HMG-12 is located on the microarray topology map at mountain 7, which is enriched with germline proteins (Kim, *et al*., 2001). Some proteins, which are homologous to HMG-12 were scored in other species. Table 1.2 shows the degree of the similarities between these genes and HMG-12, their description and further information.

The phylogram in Fig. 1.3 shows the distance between HMG-12 and other HMG AT hook proteins from *C. elegans*, human, mouse, and plant. The determination of the HMGI/Y proteins in *C. elegans* was done by the pattern program (Cockwell and Giles, 1989). The proteins that were determined by the program were the HMG proteins that contain at least three AT-hook domains out of the wormpep119 database (Sanger Center, USA). These proteins were aligned with other proteins with clustalX program (Thompson *et al.*, 1997) and the phylogram was represented from that alignment with the tree view program version 1.6.6.

The phylogram in Fig.1.3 shows that the nearest proteins to the *C. elegans* AT-hook protein (HMG-12) are the *Chironomus tentans* protein (A55819) and the *Drosophila melanogaster* protein (D1). The three HMGI/Y proteins of *Oryze sative*, *Zea mays* and *Pisum sativum* formed a separate cluster which were the nearest to three isoforms, alpha, beta, and gamma, of the human HMGI-C. In the nearest cluster to HMG-12, two proteins with unidentified biological function from C. brigssae (Gupta and Sternberg, 2003) were cluster with HMG-11.

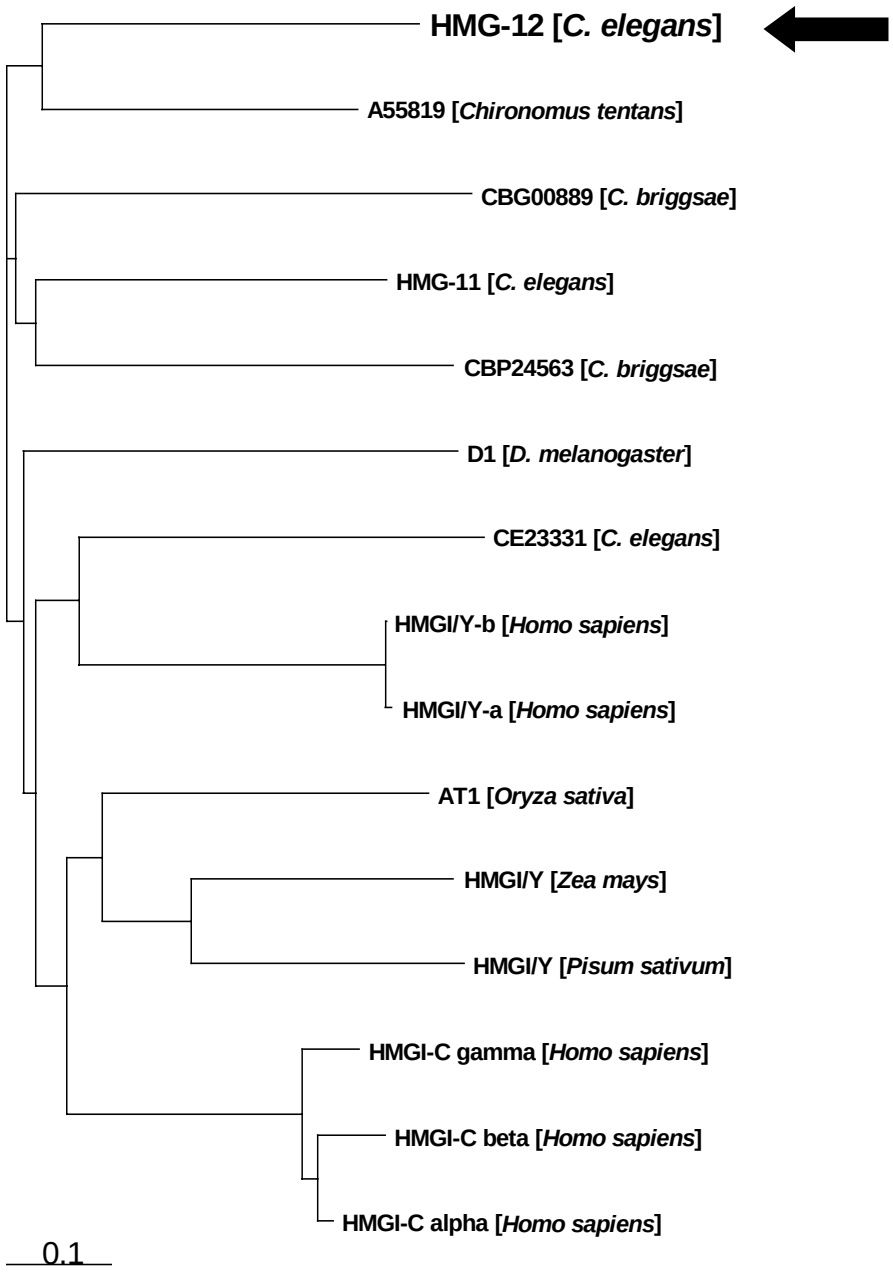

Fig. 1.2: A phylogram shows the distance between HMG AT hook proteins from different species. The number preceded by (CE) is a designated number for *C. elegans* proteins.

In this study, the effect of depleting HMG-1.1 and HMG-12 proteins will be studied with the RNAi method and the expression pattern of these proteins with transgenic worms that contain these proteins fused to GFP or YFP beside using the immunostaining methods. The method of double-strain-RNA-mediated gene knockouts (RNAi, RNA interference) used here is a relatively new method, whose reliability is generally recognized, although the functional mechanisms have not yet completely been clarified (Fire 1999).

A remarkable characteristic of the RNAi is its ability to be active not only within the cell, but also beyond its boundaries (Fire *et al*., 1998), as far as the microinjection of the double-stranded-RNA has not to be in the target organ. Additionally, this allows absorption of double-stranded-RNA from the environment or the intestine (Timmons and Fire 1998). Moreover, the RNAi effect is passed on to the descendants of the injected animal. The same way as it was mentioned for the microinjection, feeding with the dsRNA from a certain gene can make reasonably the same effect like microinjecting the dsRNA.

2. Materials and methods

2.1 Materials

2.1.1 *C. elegans* genes studied in this study

The *C. elegans* genes studied in this study and their specifications is shown in (Table 2.1)

Table 2.1: The *C. elegans* high mobility group proteins used in this study and their specifications.

Common name	Another name	Protein domain	Gene model	Protein	Amino Acids residues
hmg-12	*HmgIβ*	AT hook	y17g7a.1	WP:CE21378	315 aa
hmg-1.1	*hmg-1.1*	HMG box	y48b6a.14	WP:CE29377	95 aa

2.1.2 *C. elegans* strains

2.1.2.1 Strains from CGC center

N2, variation Bristol wild-type (Brenner, 1974)
CB1489 *him-8*(*e1489*)*IV*
ZB1028 *crt-1*(*bz29*)*V*
ZB1029 *crt-1*(*bz30*)*V*
MT1522 *ced-3*(*n717*)*IV*
MT1440 *ced-1*(*n691*)*I*
MT4952 *ced-2*(*n1994*)*IV*
MT4434 *ced-5*(*n1812*)*IV*
MT4433 *ced-6*(*n1813*)*III*
MT2121 *lin-33*(*n1043*)*IV*
MT4982 *ced-7*(*n1892*)*III*
NL2099 *rrf-3*(pk1426)*II*
AZ212 *unc-119*(*ed3*) ruIs32[*unc-119*(+) pie-1::GFP::H2B]*III*
KP987 *lin-15*(*n765*) nuIs1 X*[pV6 glr-1::GFP]*
SK4005 *zdIs5 I [mec-4::GFP]*
HC75 *ccIs4251* I; *sid-1*(qt2)*V*

2.1.2.2 Strains made in our laboratory

EC705 *eeEx705 [hmg-12::eyfp]*: This strain was made by microinjecting complete genomic coding sequence of *hmg-12* cloned into the pEYFP-N1 plasmid (pYB) into the wild type strain (N2). The complete coding sequence of *hmg-12* was made by amplifying genomic DNA with the primers ESMG74 and TKMG10. It expresses the complete HMG-12 protein (315 amino acid residues) fused to the N-terminus of EYFP.

EC715 *unc-119*(*ed3*) *III*; *eeIs715[unc-119(wt) hmg-1.1::egfp]*: This strain contains an integrated transgene, which was established by bombardment of the *unc-119*(*ed3*) mutant strain (DP38) with the HMG1.1-pEGFP-N1-unc119 rescue plasmid (this plasmid was provided from E. Schulze). This strain expresses the complete HMG-1.1 fused to EGFP.

EC807 *eeEx807 [hmg-12::egfp]*: It was made by microinjecting the *hmg-12::egfp* plasmid (HMGIβPromotor) into the wild type strain (N2) (Kurz, 1999). It expresses a partial HMG-12 that lacks 85 amino acid residues from its N-terminal. This strain was made to determine the expression pattern of HMG-12 by inspecting GFP fluorescence.

2.1.3 The bacterial strains

***E. coli* OP50:** A strain of *E. coli* with auxotrophy for uracil, which has limited growth on NGM agar plates (Brenner, 1974). It is used for culturing worms because their limited growth helps in having good observation conditions and efficient mating of the animals (CGC, USA).

***E. coli* OP50-1:** A streptomycin resistant derivative strain of OP50, which is used for growing *C. elegans* in bulk. This strain was made by Johnson C, Axys Pharma., NemaPharm Div., So. San Francisco, CA. This strain was obtained from CGC (USA).

***E. coli* DH5α(LTI):** A strain of *E. coli* used for cloning. It has the following genotype: *6, 7 F´/ endA1 hsdR17 (rK–mK+) glnV44 thi- 1recA1 gyrA (Nalr) relA1 .(lacIZYAargF) U169 deoR (80 dlac.(lacZ)M15)* (Hanahan, 1985).

***E. coli* OP50-GFP:** A strain of OP50 containing a GFP plasmid (pFVP25.1), which is very fluorescent. It is resistant to ampicillin. This strain was used as food for the worms and for the inspection of the bacteria inside the worm (Labrousse, *et al.* 2000).

***E. coli* BL21(DE3)(N):** A strain used as an expression host. It has the following genotype: *17 F– ompT gal [dcm] [lon] hsdSB (rB– mB–;* an *E. coli B* strain) with DE3, a prophage carrying a T7 RNA polymerase structural gene under the control of the *lac* promotor (Studier *et al.*, 1990).

***E. coli* HT115(DE3):** *F-, mcrA, mcrB, IN(rrnD-rrnE)1, rnc14::Tn10(DE3 lysogen: lavUV5 promoter -T7 polymerase)* (IPTG-inducible T7 polymerase) (RNAse III -). It is tetracycline resistant. This strain is used in RNAi feeding experiments (Timmons *et al.*, 2001).

2.1.4 Vectors and plasmids

2.1.4.1 Basic cloning vectors

pET-41c: This vector was used for making a fusion of the coding sequence of *hmg-1.1* to the coding sequence of the GST protein (Studier and Moffatt, 1986).

L4440: This vector has double T7 promotors flanking the multiple cloning site in opposite orientation. It was used for generating dsRNA from the DNA inserted into the polylinker. This was done either by *in vitro* transcription or *in vivo* in *E. coli* HT115 (DE3) bacteria and used for RNAi experiments (Timmons *et al.*, 2001).

pBluescript II KS+: This phagemid vector was used in cloning steps. It contains T3 and T7 RNAi polymerase promotors and it has an ampicillin resistance gene (Stratagene, La Jolla, USA).

pBluescript II KS-: This phagemid vector is the same like pBluescript II KS+ but differs in its f1 origin orientation. (Stratagene, La Jolla, USA.).

pEGFP-N1: This vector contains enhanced green fluorescent protein coding sequence and a kanamycin resistance gene. It is 4.7 kb (Clontech, CA, USA).

pEYFP-N1: This vector is the same like pEGFP-N1 but differs in having the coding sequence of enhanced yellow fluorescent protein (YFP) instead of the enhanced GFP coding sequence. YFP coding sequence differs from GFP coding sequence in containing several point mutations. It is 4.7 kb (Clontech, CA, USA).

pEGFP-N1-unc-119: This plasmid contain *unc-119* coding sequence that can rescue UNC-119 mutant fused to the pEGFP-N1 vector. This coding sequence was inserted in into *Hin*dIII and *Xba*I restriction sites of pEGFP-N1. The *unc-119* coding sequence was digested using H*in*dIII and *Nhe*I (by E. Schulze).

2.1.4.2 Recombinant plasmids

2.1.4.2.1 Plasmids for RNAi techniques

2.1.4.2.1.1 Plasmids used for the synthesis of dsRNA for RNAi feeding

L4-HMG1.1: This plasmid is L4440 vector with the coding sequence (complete cDNA) of *hmg-1.1* inserted into the *Xba*I and *Xho*I restriction sites. It was used for *hmg-1.1* dsRNA feeding after transforming it into *E. coli* HT115(DE3) strain (this plasmid was made by E. Schulze).

L4-HMGIα-yk: This plasmid is L4440 vector with the coding sequence (complete cDNA) of *hmg-11* inserted into the *Xba*I and *Xho*I restriction sites. It was used for *hmg-11* dsRNA feeding after transforming it into *E. coli* HT115(DE3) strain (this plasmid was made by E. Schulze).

pBL44: This plasmid is L4440 vector with the coding sequence of *hmg-12* inserted into *Xba*I and *Xho*I restriction sites. This plasmid was used for *hmg-12* dsRNA feeding after transforming it into *E. coli* HT115(DE3).

2.1.4.2.1.2 Plasmids used for the synthesis of dsRNA for microinjection

pSKHMGI.α-yk: It is pBluescript II KS+ vector containing the coding sequence (the complete cDNA) of *hmg-11* cDNA inserted into *Eco*RI and *Xho*I restriction sites (Kurz, 1999).

pSKHMGIβ-yk: It is pBluescript II KS+ vector containing the coding sequence (complete cDNA) of *hmg-12* cDNA inserted into *Eco*RI and *Xho*I restriction sites (Kurz, 1999).

pSKHMG1.1-yk: It is pBluescript II KS+ vector containing the coding sequence (complete cDNA) of *hmg-1.1* cDNA inserted into *Eco*RI and *Xho*I restriction sites (Kurz, 1999).

2.1.4.2.2 Recombinant plasmids used for other purposes

pBpSK: It is pBluescript II KS+ vector containing the complete coding sequence of *hmg-12* which was amplified from genomic DNA using ESMG74 and TKMG10 primers. It was used to generate the *hmg-12*::eyfp worms by microinjecting it into the germline of N2 worms. *hmg-12* was inserted into *Kpn*I and *BamH*I restriction sites.

pYB: It is pEYFP-N1 vector containing the complete genomic coding sequence of *hmg-12*. This coding sequence was digested out of pBluescript II KS+ from the construct (pBpSK) and cloned into pEYFP-N1 by insertion into *Kpn*I and *BamH*I restriction sites. It was used to generate the *hmg-12*::eyfp worms by microinjecting it into the germline of N2 worms.

HMG1.1Promotor: It is pEGFP-N1 vector containing the complete coding sequence of *hmg-1.1*. This coding sequence was inserted in pEGFP-N1 into *Kpn*I and *BamH*I restriction sites. It was used to generate the *hmg-1.1*::egfp transgenic lines (Kurz, 1999).

HMGIβPromotor: It is the vector used to make the strain CE700 and EC701. The *hmg-12* sequence was inserted in EGFP-N1 into *Kpn*I and *BamH*I restriction sites. Expression that vector produce a partial HMG-12 protein that lacks The expression of that vector results in a partial HMG-12 protein that lacks 85 amino acid residues.

HMG1.1-pEGFP-N1-unc119: It is pEGFP-N1 vector containing the coding sequence of *hmg-1.1*. This coding sequence was digested out of pEGFP-N1 from the construct (HMG1.1Promotor) and cloned into pEGFP-N1-unc-119 by insertion into *Kpn*I and *BamH*I restriction sites. It was used to generate the *[unc-119(wt) hmg-1.1::egfp*] strains by the bombardment transformation technique (by E. Schulze).

pET41c-hmg1.1cDNA: This is the vector pET41c containing the coding sequence of *hmg-1.1* cDNA which was inserted into *EcoR*I and *Xho*I restriction sites. This plasmid was used to transform *E. coli* DH5α strain first and then transfered to the *E. coli* BL21 strain. It was useful in the purification of the polyclonal antibody against HMG-1.1 and pull down assay.

2.1.5 PCR amplification

2.1.5.1 Oligonucleotide sequences

ESMG74 CGGGATCCGCGTCTGAGCCATCGAAGAAGGC

TKMG10 GGGGTACCAGCTCTGACCATTACAGCAT

ESMG67 CGCGCGTAATACGACTCACTATAGGGCGAATTG
CCCTCACTAAAGGGA

T7 TAATACGACTCACTATAGGG

2.1.6 Reagents for antibody staining of *C. elegans* embryos

2.1.6.1 Primary antibodies

In this study, two primary antibodies were used. They were made to be used in the immunofluorescence techniques to stain HMG-12 and HMG-1.1. The anti-HMG-12

and anti-HMG-1.1 were prepared by injecting rabbits with HMG-12 or HMG-1.1 recombinant proteins, respectively (Kurz, 1999). HMG-1.1 antibody was purified by using the GST purification procedure.

2.1.6.2 Secondary antibodies

Goat anti-Rabbit IgG (H&L): This secondary antibody is Cy2-conjugated. It was used in the final concentration of 500 µg/ml (Jackson ImmunoResearch, USA).

2.1.7 Databases and Softwares

ACeDB database

The database ACeDB is provided by the Sanger center (USA) and was the main source of the *C. elegans* biological information in this study. This database is available freely and can be used either through an internet search or through a self standing database program which can be used offline. This database contains information about the *C. elegans* genome and related studies.

PCGENE program

PCGENE version IGI 3064 (IntelliGenetics Inc.) was used for the protein analysis, the primer design, and the restriction site analysis for many of the sequences used in this study.

LSM (510)

The laser scanning microscopy (LSM) was used for recording 3D-stacks of micrographs and/or time series of micrographs. This instrument was adjusted and its processes were performed using a special program (version 2.50.0929) developed by Zeiss.

Spot camera basic and advanced programs

For scoring and processing two-dimensional (2D) photos digitally, the Spot-Camera (Diagnostic instruments, Inc.) was used. The spot camera program was used for processing and adjusting the photos (version 3.0 for Windows).

Photoshop and Microsoft office

General editing steps were done using different windows 2000 office programs. Microsoft word for editing text and Microsoft excel for editing tables and graphs. For processing photos, Adobe Photoshop (version 6) was used.

SPSS program

For statistical analysis, SPSS (version 11) was used.

2.1.8 Equipments for fluorescence light microscopy

The documentation of most photomicrographs was performed with a Zeiss Axioplan 2 microscope equipped with Zeiss confocal laser scanning module Zeiss 510 (Jena, Germany). It is equipped with three laser excitation systems and confocal optics. The acquisition of data is through a 12-bit 1024/1024 frame buffer. Image processing was carried out by image analysis software developed by Zeiss.

Therefore, conventional and Laser scanning microscopy and epifluorescence of specimen were performed with Zeiss LSM510. The Axioplan 2 is equipped with a set of several lenses with magnification of 10 x Plan-Neofluar (NA of 0.3), 20 x Plan-Neofluar (NA of 0.5), 40 x Neofluar (NA 1.3, oil), 63 x Plan-Apofluar (NA of 1.4 oil), and 100 x Plan-Neofluar (NA of 1.3, oil).

Some images were captured with a charge coupled digital (CCD) camera (spot Camera, Diagnostic Instruments, Sterling Height, MI). To examine the specimen on the slides, a mercury high-pressure lamp (Zeiss) of LSM 510 was used.

The worm samples were excited with a Laser beam 351 nm and 364 nm for DNA staining, 488 nm for GFP and Cy2, 514 nm for YFP, and conventional Nomarski-DIC light photo. The micrographs were taken with the appropriate filters that are shown in Table 2.2.

Table 2.2: The spectrum of chromophores from fluorescent proteins and dyes with the appropriate band-pass set of confocal laser scanning microscope 510.

Fluorochrome	**Fluorochrome excitation max. (λ), nm**	**Band-pass (λ), nm**	**Emission max. (λ), nm**
H33342	364	385-470	465
Cy2	489	505-530	505
GFP	488	505-530	509
YFP	513	505-550	527

A coaxial fluorescence attachment (dissection) stereomicroscope SZX-RFL2 from Olympus (Tokyo, Japan) was used to screen the *C. elegans* culture plates. This microscope is equipped with a mercury high-pressure lamp (HBO USH-102D, Ushio, Japan) and filters for observation of CFP, GFP, and YFP expression pattern in worm (Table 2.4).

Table 2.4 The filter set of the stereomicroscope SZX-RFL2 for observation of fluorescent proteins in transgenic animals in this study.

Fluorescent protein	Band-pass excitation, λ nm	Band-pass emission, λ nm
CFP (Haas *et al.*, 1996, Yang *et al.*, 1996)	460-490	BA510-550
GFP(Chalfie *et al.*, 1994)	460-560	590
YFP (Orm*et al.*, 1996)	540-580	BA610

To screen different obvious phenotype on the culture plates for everyday purpose a dissecting stereomicroscope (Wild-Heerbrugg, Switzerland) has been used. This stereomicroscope was equipped with a transmitted light source, 10x eyepieces, and a lens revolver ranging from 5 x to 50 x magnification.

2.1.8 Bombardment equipment

We used a Biolistic PDS-1000/He, which required the following materials:

1) Rupture discs: 1350 psi disks were used in this study.

2) Macrocarriers: They are the plastic discs, which carry the gold beads till bombarding the worms. They were sterilized before usage by dipping them into 100% EtOH and allowed to dry under sterile conditions.

3) Macrocarrier holders: These holders are metal rings holding the macrocarriers inside them. They were sterilized by dipping in 70% EtOH and flaming them before each run of bombardment.

4) Stopping screens: They look like small pieces of window screen. It was placed in front of the macrocarriers, in between the macrocarriers and the worms. It was used to avoid the macrocarrriers from hitting the worms and the NGM agar media on the plates. They were sterilized by dipping in 70% EtOH and flaming them. They were kept in sterilized plastic container until using them.

2.1.9 The compositions of solutions used in this study

50x TAE buffer

2 M Tris, 2 M Acetic acid, 50 mM EDTA, and autoclaved

10x T4-ligation buffer

400 mM Tris-HCl, 100 mM $MgCl_2$, 100 mM, DTT, 5 mM ATP, pH 7.8

Sample buffer

20 mM Tris-HCl, pH 6.8, 480 ng/ml SDS; (1:250 v/v) glycerol; 5 µg/ml bromophenol blue and twentieth part of β-mercaptoethanol was freshly made

TBS

10 mM Tris-HCl, 150 mM NaCl, pH 7.4, and autoclaved

Transfer buffer

25 mM Tris-HCl, 192 mM glycine, 20% methanol, 0.1% SDS at pH 8.3.

Bleaching solution

900 µl of 3% NaOCl diluted in egg-salt, and 100 µl of 500 mM NaOH

Destaining solution

70 ml MilliQ water, 20 ml methanol and 10 ml acetic acid

Cathode buffer

25 mM Tris pH 9.4; 40 mM aminocapron acid; 20% methanol; and 0.1% SDS

Coomassie blue

1 mg/ml Coomassie Blue G-250, 50% methanol and 10% acetic acid

Egg-salt

118 mM NaCl, 48 mM KCl, ddH2O for solutions, and autoclaved

Electrode buffer

250 mM Tris-HCl, 1.92 M glycine, and 0.1% SDS

Extraction buffer

Tris-HCl 20 mM pH 6.8, glycerin 4 mM, SDS 1.66 mM, bromophenol blue 29.9 µM

LB Laura-Bertani (LB) medium

To prepare 1liter medium, 5 g NaCl, 10 g peptone, and 5 g yeast extract were added to 1 liter dH_20. Then, the pH was adjusted to pH7.2, and the medium was autoclaved

LB-Agar

1 liter of LB medium was prepared as previously mentioned in LB medium preparation added to15 g agar. The pH was adjusted to be pH7.2 (Miller, 1972)

LB-ampicillin

For each 1 liter preparation 100 µg/ml ampicillin were added to 1 liter autoclaved LB medium.

LB-kanamycin

For each 1 liter preparation 70 µg/ml kanamycin were added to 1 liter autoclaved LB medium.

opti-gro medium

The same preparation like it with NGM agar with:

6 g pepton and 2 ml cholestrol (5mg/ml Ethanol) and 100 µg/ml nystatin for 1 liter of the medium.

Loading buffer

0.25% xylene cyanol, 0.25% bromophenol blue, approximately 30% ficoll, 500 mM EDTA

Lysis buffer

200 mM NaCl, 100 mM Tris-HCl, pH 8.5, 50 mM EDTA, 0.5% SDS

M9 solution

3 g KH_2PO_4, 6g Na_2HPO_4, 5 g NaCl, and1 liter dH_2O was added and autoclaved. Then, 1 ml of sterilized 1 M $MgSO_4$ was added.

PBS

140 mM NaCl, 2.7 mM KCl, 4.3 mM Na_2HPO_4, 1.47 mM KH_2PO_4,

pH 7.2, and autoclaved

10x PCR buffer

500 mM Tris-HCl pH 9.2, 17.5 mM $MgCl_2$, and 160 mM (NH_4) 2 SO_4

Buffer P1 (resuspension buffer)

50 mM Tris·Cl, pH 8.0; 2–8°C, 10 mM EDTA; 100 µg/ml RNase A. It was Stored at 4°C.

Buffer P2 (lysis buffer)

200 mM NaOH, 1% SDS (w/v). It was Stored at room temperature.

Buffer P3 (neutralization buffer)

3.0 M potassium acetate pH 5.5. It was stored at room temperature.

Buffer FWB2 (QIAfilter wash buffer)

1 M potassium acetate (pH 5.0). It was Stored at room temperature.

Buffer QBT (equilibration buffer)

750 mM NaCl; 50 mM MOPS, pH 7.0; 15% isopropanol (v/v), 0.15% Triton X-100 (v/v). It was Stored at room temperature.

Buffer QC (wash buffer)

1.0 M NaCl; 50 mM MOPS, pH 7.0; and 15% isopropanol (v/v). It was stored at room temperature.

Buffer QF (elution buffer)

1.25 M NaCl; 50 mM Tris·Cl, pH 8.5; 15% isopropanol (v/v). It was stored at room temperature.

Buffer QN (elution buffer)

1.6 M NaCl; 50 mM MOPS, pH 7.0; 15% isopropanol (v/v). It was stored at room temperature.

TE

10 mM Tris·Cl, pH 8.0; 1 mM EDTA.

STE

100 mM NaCl; 10 mM Tris·Cl, pH 8.0; 1 mM EDTA.

RIPA-buffer

(20 mM TRIS pH 7.5, 500 mM NaCl, 5 mM EDTA, 1% Triton X 100, and with 5 mg/ml lysozyme. Each 30 ml of RIPA buffer was supplemented with a full set of protease inhibitors (Boehringer Mannheim).

2.1.10 Antibody purification

In order to purify HMG-1.1antibody rabbit serum, SulfoLink kit (Pierce, Rockford, USA) was used.

The contents of SulfoLink Kit

SulfoLink coupling gel

6% cross-linked beaded agarose supplied as a 50% slurry in storage buffer (10 mM EDTA-Na, 0.05% NaN_3, 50% Glycerol), 5 x 2 ml columns

SulfoLink sample preparation buffer

0.1 M sodium phosphate, 5 mM EDTA-Na, pH 6.0, 7.5 ml

SulfoLink coupling buffer

50 mM Tris, 5 mM EDTA-Na, pH 8.5, 500 ml

SulfoLink wash solution

1.0 M NaCl, 0.05% NaN3, 120 ml

SulfoLink reductant

2-mercaptoethylamine•HCl (2-MEA, MW = 113.61), 5 x 6 mg

L-cysteine HCl

100 mg

D-salt polyacrylamide desalting columns

They were 5 ml columns that has exclusion limit of 1,800 MW.

Polyethylene porous discs

They were used for topping the gel bed after coupling process. It prevents the column from running dry.

Serum separation

It aids in placement of top discs in protein-coupled columns.

Column extender

It allows larger volumes of buffer to be applied to columns.

12% SDS-PAGE separating gel

18.7 ml acrylamide solution, 29.1% w/v acrylamide, 0.9% biscaryamide (dissolved in ddH2O), 18.1 ml of ddH_2O, and 9.3 ml of a 1.875 M Tris-HCl pH 8.8

5% SDS-PAGE stacking gel

2.4 ml polyacrylamide solution, 10.8 ml ddH_2O, and 1.5 ml of 1.25 M Tris-HCl (pH 6.8). After degassing the resulting solution the following chemicals were added:
150 µl 10% SDS, 15 µl TEMED, 15 µl 30% amonium persulphate (APS)

2 Methods

2.2.1 Culturing worms in plastic petri dishes

Three different sizes of plates were used in this study as following:

1. Plates with 3 cm in diameter, which were used mainly for crossing worms.
2. Plates with 6 cm in diameter, which were used mainly for culturing worms and experiments if nothing else is mentioned.

3. Plates with 10 cm in diameter, which were used mainly for thawing worm strains or generating large amounts of worms.

Worms were cultured on NGM agar plates. A liter of NGM agar medium contains: 3 g NaCl, 2.5 g peptone from casein, and 17 g agar completed up to 1 L by adding H_2O. The medium was autoclaved at 120 °C for 20 minutes. Then, incubated in a 50°C water bath for about 15 minutes.

Before pouring the media on plates other chemicals were added. One of these chemicals, 1 ml cholestrol, was not added directly after autoclaving the media because of its sensitivity to the high temperature. The rest of the chemicals, 25 ml KH_2PO_4, 1 ml $MgSO_4$, 1 ml $CaCl_2$ (1M), were not added before autoclaving the media to avoid precipitation.

After mixing all together, the medium was poured directly into the plastic dishes. It was left to solidify and cool down till reaching room temperature and then each plate was covered by its led. This step is important to avoid water condensation on the lids, which might cause contamination later. Ready plates with NGM agar can be seeded directly with bacteria or otherwise be kept at 4 °C till usage.

The bacteria used for culturing were: *E. coli* OP50, OP50-I, or OP50-GFP. Tiny amounts of the frozen bacterial cultures were used to inoculate 5 ml LB medium. The inoculated LB medium was incubated at 37 °C overnight with shaking at 250 rpm.

For seeding the plates about 25 µl from this culture had been added to each plate and streaked on it with a Drigalski spatula. It was left to dry. The seeded plates were left over night to have the bacteria growing. Alternatively, the plates were incubated at 37°C for 1 hour. At that stage the plates were ready with the bacteria for adding the worms.

2.2.2. Culturing worms on plastic petri dishes for feeding experiment

Culturing worms for feeding experiments was done on feeding NGM agar medium. It is the same media in composition as it was mentioned previously about NGM agar but after the sterilization of the media 2.5 ml of 10 mg/ml carbencillin and 1 ml 1M IPTG had to be added for each liter before plating the media. The bacteria used for RNAi feeding were specific for the target gene, which needed to be depleted.

2.2.3 Extraction of the eggs from the adults

To get the developmentally synchronized L1 stage larva, eggs were extracted from the adult hermaphrodites and left overnight for hatching. Leaving the hatched L1 without bacteria will make them starving hence arresting their development in L1 stage. Out of that, it was possible to collect developmentally synchronized starved L1.

The extraction of the eggs from the adults was done using alkaline sodium hypochlorite, which was made out of 5 ml 5M KOH and 20 ml NaOCl (6%) in water up to 100 ml. It is very important to degas this solution before using it to minimize the toxic effect of the free Cl_2 in the newly prepared solution, which can lead to kill much of the collected embryos.

Furthermore, all egg preparations were checked after the overnight incubation for any dead L1. Any preparation that contained dead L1 was discarded. These dead L1 worms means that the embryos faced too high concentration of the bleaching solution that caused its death after hatching.

Using such preparation would produce misleading results. These misleading results can happen due to performing the egg extraction of each preparation separately, to work fast enough through the procedure. So that, using exact chemical concentrations and having fast and accurate bleaching steps were critical to have a successful egg preparation.

Collecting the adults from the plates with cold M9 in 10 ml plastic falcon tubes helped avoiding loosing much of the adults in the solution because the low temperature didn’t allow the worm to swim and float in the solution.

Before extracting the eggs, the adults were washed in cold M9 3-4 times with precipitating them in between each time by centrifugation for 1 minute at 500 x g at 4°C to reduce the amount of bacteria in the M9 used from the plates as well as the bacteria which attached to their cuticle. This helps to have clean embryos.

Then, The worms were shaked vigorously in the alkaline sodium hypochlorite solution for exactly 1 minute, followed by a precipitating step by centrifugation as mentioned before and resuspending in cold M9 followed by centrifugation. The supernatant was wasted fast and 10 ml of alkaline sodium hypochlorite was added, shacked and centrifuged like previously mentioned.

The collected eggs from this step need fast and intensive washing. The washing steps were done repetitively in as many as 6 cycles of shaking vigorously in M9 for 1

min. and centrifugation like previously mentioned. The collected eggs from the last washing time were incubated in M9 on a shaker at 250 rpm at room temperature overnight.

2.2.4 RNA interference by feeding

2.2.4.1 The cloning of cDNA

The RNAi feeding technique was done in its standard way in this study by cloning the complete coding sequence of the cDNA of each protein into pBluescript II KS+ vector by the standard method of cloning mentioned previously.

The resulting plasmid was transformed into *E. coli* DH5α strain bacteria. Later, the cloned cDNA was cut from pBluescript KS+ II vector and cloned into the L4440 vector, which contains double T7 promotor.

The resulting plasmid from the last cloning step was extracted from DH5α and subsequently transformed into *E. coli* HT115(DE3) strain bacteria which lack the RNAse III which is responsible for digesting dsRNA in the bacterial cell. Furthermore, the used plasmid has T7 RNA polymerase. All of the previous conditions lead to an enrichment of effective dsRNA ready to be fed to the worms. Feeding the worms with a high concentration of the dsRNA helps to enhance the RNAi effect.

2.2.4.2 The RNAi feeding (standard)

The standard feeding of the dsRNA was done by growing L4 stage or adult worms (P0) on NGM feeding plates. Then, after incubating the plates for at least 12 hours at 20°C, the adults were transferred to a new feeding plate (in case of no other temperature will be mentioned) to a new feeding plate. The P0 worms were left on the plate for 12-24h at the same temperature as the first incubation temperature.

Then, the adults were either discarded or transferred to new feeding plates or scored for resulting RNAi phenotypes. Generally, the resulting phenotypes were scored from these plates, which contain worms of F1 and/or F2 generations.

2.2.4.3 The RNAi feeding (collective scoring)

This procedure was used to score phenotypes impossible to be scored using the standard RNAi feeding method. It was used to study the response of the worms

toward different stress conditions like temperature and starvation of RNAi fed animals.

Scoring the resulting phenotypes was performed on the F1 worms. The F1 eggs were extracted from P0 adults after incubating the adults for 2 days at 25°C on feeding plates. The egg extraction was done by alkaline sodium hypochlorite solution as previously mentioned. This incubation period was useful to extract only the F1 eggs that were exposed from their very early developmental stages to the RNAi effect.

Adding ampicillin (end concentration 100 µg/ml) to M9 solution, in which the eggs were collected, helped to reduce the risk of having contaminating bacteria. The bacteria can sometimes influence negatively the ability to count correctly the dead L1 by covering them by its dense colonies.

For calculating the death ratio, 50 µl from the egg suspension were transferred to standard 9 cm NGM agar plates seeded with OP50 bacteria and left 2 days at 20-25°C. After these 2 days, the alive and the dead worms were counted to calculate the death ratio. A worm has been counted as dead only if it does not make any movement after touching its body.

2.2.4.4 The RNAi feeding (individual scoring)

This procedure of applying the dsRNA through the feeding procedure was done exactly like the standard technique with some small changes. Scoring for the phenotypes in that approach was done on individual F1 worms. These worms resulted from dsRNA fed worms.

Each worm was followed by a daily transfer to a new plate. The differences between it and the worms from the control plates were scored. Whether the plates, which the worms were transferred to, were NGM feeding plates or standard NGM agar plates, differed from an experiment to another experiment. It will be mentioned for each experiment individually in the chapter “Results”.

2.2.5 RNAi microinjection

2.2.5.1 Preparation of agarose coated cover slips (pads)

It is important to have different concentrations of agarose pads for microinjection because each concentration can be suitable for a certain stage of worms.

On the other hand, using too high concentration of the agarose can lead to break down the worms through the process of reorienting it in a good position for microinjection, or it can be killed by extensive dehydration.

An agarose 0.075 to 0.15% (Roth, Germany) was boiled in dH_2O in a microwave oven, a drop of it was dispensed onto a 24 x 40 mm cover slip (Menzel-Glaeser, Germany), and air-dried over night at room temperature. Breathing over the cover slip surface moisturized its agarose before using it. Also, this breathing eased the discrimination of the cover slip side that was coated by the agarose pad.

2.2.5.2 Preparation of the cDNA template

In this technique, all used plastic materials and solutions must be RNase free with only diethyl pyrocarbonate (DEPC)-treated plastic materials and wearing gloves to prevent the degradation of dsRNA. The DEPC treatment for plastic materials was done by incubating it for several hours at room temperature 0.1% DEPC in water. Then, it was autoclaved for 20 min at 121°C.

The PCR technique was used to amplify the complete cDNA coding sequence, which was used in the preparation of the dsRNA for microinjection. The plasmids pSKHMGI.α, pSKHMGIβ, and pSKHMG1.1 were used as a template for amplifying the cDNA of *hmg-11*, *hmg-12*, and *hmg-1.1* respectively.

The PCR amplification was done for each one of the 3 different cDNAs in total reaction volumes of 200 µl using T7 and ESMG67 primers. The PCR components for each reaction was as following: 2 µl of each primer (50 pmol), 4 µl of DNA (10 ng/ µl), 4 µl of dNTPs (2.5 µM), 20 µl 10x reaction buffer, 10 µl $MgCl_2$, 4 µl Taq polymerase and 160 µl RNAse-free H_2O.

After overlaying the mix with drops of mineral oil, the reaction was run based on the following program: denaturation at 95°C for 5 min., low annealing temperature of 45°C for 20 sec., then, followed by 30 cycles of annealing temperature of 51°C for 60 sec., polymerization temperature of 72°C for 90 sec, and denaturation temperature of 94°C for 60 sec. About 5 µl of the PCR reaction was run on a 1% agarose gel to check for the resulting DNA quality.

The resulting DNA was extracted from the PCR reaction with the same volume of chloroform:isoamyl alcohol 96:4. Then, all components were mixed well but not vigorously. Then, centrifuging it in a microfuge on 12,000 x g at 4°C for 10 minutes. Then, the upper phase was collected in a new Eppendorf tube and equal volume of

isoamylalcohol was added to it. The same steps of vortexing, centrifugation and collecting the upper phase were repeated.

The resulting DNA was precipitated with 20 µl of 3 M sodium acetate pH 5.5 added to 400 µl EtOH at –20°C for 3 hours. Then, the DNA was collected by centrifugation at 12,000 x g, at 4°C for 30 minutes and the supernatant was discarded. The DNA was washed with 100 µl of 70% ice-cold ethanol. After centrifugation at the same conditions as previously mentioned, the DNA pellet was dissolved in 30 µl TE buffer and the amount of DNA was measured by the spectrophotometer (260 nm).

2.2.5.3 Transcription of the cDNA

The complete cDNA sequence was amplified and transcribed *in vitro* with MEGAscript™ High yield transcription T7-kit (Ambion Inc., USA). It was done with about 1 µg of DNA of each gene, which was transferred to a sterile and DEPC rinsed reaction tube with 2 µl 10 x reaction buffer, 2 µl ribonucleotides ATP, CTP, GTP, and UTP each, nuclease-free H_2O, and 2 units of the T7 RNA-polymerase enzyme were added. The amount of the DEPC-treated water that would be needed to for a final reaction volume 20 µl was calculated and added as a first component in the reaction.

This mixture was then incubated for 6 hours at 37°C. The DNA was digested with 1 µl of DNase. After mixing the reaction, it was incubated for 15 min at 37°C. The RNA was recovered by adding 115 µl nuclease-free water and 15 µl 5 M NH_4Ac stop solution and mixed thoroughly.

To extract the dsRNA from the reaction, an equal volume of phenol (pH 4.0)/chloroform was added and mixed well. Then, it was centrifuged at 12,000 x g for 5 minutes and the upper phase was collected in a new tube. An equal volume of chloroform was added to it and the same conditions of mixing and centrifugation and collecting were applied.

The dsRNA was precipitated by adding 1 volume of isopropanol and mixing gently. It was then incubated at -20°C for not less than 1 hour. It was centrifuged at 10000 xg for 15 min at 4°C. The resulting pellet was collected in a careful way to avoid loosing the pellet or part of it.

The dsRNA pellet was dissolved with RNase-free water. The concentration of the dsRNA was determined with the UV spectrophotometer at 260 nm. The dsRNA was loaded on a 0.7% agarose gel to test its quality. The dsRNA solution was stored at -80°C.

2.2.5.4 Microinjection of the dsRNA

Before using the dsRNA solution for microinjection, 2 min. spin at 12,000 x g at room temperature was used to clarify the solution. This was useful in minimizing the risk of blocking the microinjection needle.

Microinjecting dsRNA can be done into any part of the worm and is preferentially done into the gonads. Early adults and L4 were the best stages for microinjection.

After microinjecting the worms, they were incubated on NGM agar plates at 20°C or 25°C for 12 h. Then, the worms were transferred to a new NGM agar plate and the embryos resulting from the first 12 h of incubation were discarded. The adults then were allowed to lay eggs for 24 to 36 hours after microinjection. The offspring was scored for resulting phenotypes, which did not appear in the control. The control was done by microinjecting worms of the same genotype by DEPC-treated H_2O.

2.2.6 Cloning

2.2.6.1 Preparation of the competent *E. coli* DH5α bacteria

The preparation of the competent bacteria, *E. coli* (DH5α), was done by growing a tiny amount of DH5α bacteria, taken from a frozen culture, over night in 5 ml sterilized LB medium at 37°C with shaking at 250 rpm. Then, 1 ml of the resulting culture was added to 50 ml of LB medium and incubated at 37°C with shaking at 250 rpm.

Every 30 minutes, 1 ml of this culture was taken to measure its optical density (OD) at the wavelength 600 nm. The resulting OD was compared with the OD value of a control, sterilized LB medium, till the OD of the culture reached OD 0.3.

Then, the cells were harvested by centrifugation at 4°C and 3600 x g for 10 minutes and the supernatant was discarded. The cells were resuspended with sterile 50mM $CaCl_2$ and incubated on ice for 15 min (this step was repeated twice). Then, the cells were centrifuged under the previously mentioned conditions and the supernatant was discarded. The pellet was resuspended in 20 ml of 50 mM $CaCl_2$ with 20% glycerol and kept on ice. Finally, with continuous mixing by shaking, aliquots of 100µl bacterial suspension were made in Eppendorf tubes and frozen directly in liquid nitrogen and stored at –80°C.

2.2.6.2 Restriction enzymes analysis

A successful DNA digestion depends on multiple factors. One of these factors is the purity of the DNA that needs to be digested. Therefore, purifying the DNA from chemicals like phenol and ethanol or from other cell components like proteins was done with a kit called Nucleobond AX (Macherey-NAGEL GMBH&Co. KG, Germany). This kit was provided with special columns that can trap the DNA from the samples. Then, after washing the column several times, the clean DNA was eluted from the column.

Furthermore, other critical factors for efficient DNA digestion were taken into consideration: using the appropriate buffers, sterilizing all plastic materials and solutions to destroy the DNase, and avoiding using too much amount of DNA or restriction enzymes.

For each 30 µl-reaction, 1 µg DNA, 3 µl of the appropriate 10 x restriction enzyme buffer, and 3 U of restriction enzyme were used. Then, the needed amount sterilized water to make the reaction up to 30 µl was added as a first component of the reaction. Te reaction was mixed well. All of the previous steps were done on ice. The reaction was incubated at the appropriate incubation temperature for 3 h.

2.2.6.3 Agarose-gel electrophoresis

For scoring the digestion results, 10-20 µl of the reaction was loaded into 0.7% low melting agarose gel. Each gel included 1 or 2 lanes of appropriate DNA marker(s). The loaded DNA was differentiated by electrophoresis using 100 v for 1-2 h. After the run finished, the DNA was inspected with a 360 nm UV light lamp. Then, the gel was photographed using LCD camera. Finally, the DNA bands, which will be used for ligation were cut out from the gel and collected into new sterile Eppendorf tubes (Dretzen *et al.*, 1981).

The low melting point agarose gel was prepared by boiling 0.35 g low melting agrarose powder (Peqlab, Erlangen, Germany) in 50 ml 1x TAE. It was mixed and cooked in the microwave oven, and left to cool down for about 3 minutes at room temperature. Then, ethidium bromide (Roth, Karlsruhe, Germany) was added to the gel to a final concentration of 100 µg/ml. The gel was poured and left till it solidified. Then, it was submerged in an electrophoresis chamber containing 1 x TAE buffer.

The digested DNA has been differentiated on the gel that included as well a control lane made out of linearized plasmid (the same plasmid that was double digested to be

used for cloning). Furthermore, a lane or more of the appropriate standard DNA marker(s) was applied to the gel.

In this study, two standard DNA markers were used; one of them is the λ-DNA marker (self-made ladder that was made out of λ-DNA digested by *Hind*III and *Eco*RI by the same conditions as mentioned in the restriction enzyme part) and GeneRuler 1 kb DNA ladder (Fermentas, Germany). All loaded DNA solutions in the gel were mixed previously with loading buffer and applied to the gel-lanes that were created by the appropriate comb.

2.2.6.4 Ligation of DNA for transformation into the competent *E. coli* cells

The success of the following method depends on the agarose patch and the end concentration of the agarose in the DNA sample that will be ligated. So that, when it didn't end up to a successful cloning with this method, a kit called Qiaex II (Qiagen) was used for the DNA extraction from the agarose gel before using it for the ligation step. The details of the method and the materials of the kit can be found under a separate point in this chapter.

The ligation was done by adding a ligation mix which contains 2 µl of 10 x T4-ligation buffer, 7 µl ddH2O, and 2 µl T4 DNA ligase (1 u/µl) to a mix of the digested vector and the coding sequence which needed to be inserted into that digested vector (vector & insert solution). The first solution, the ligation mix, was kept all the time on ice till insert & vector solution was prepared and mixed with it on ice as well.

The vector & insert solution was prepared by incubating the cutted piece of the low melting agarose gel, which contains the desired DNA band, and the other piece which contains the digested vector, in separate Eppendorf tubes, at 65°C. The tubes were left at that temperature till the gel pieces were completely melted.

Then, 3 µl of vector solution were mixed with 6 µl of the insert solution very well. The temperature of that mixture was cooled down by holding the tube containing it in hand for short time till it is slightly worm.

Finally, the vector & insert solution was added to the ligation mix solution on ice and mixed as fast as possible before the low melting agarose solidifies and incubated for about 1 minute on ice. The tubes were incubated in the water bath (RM20-Lauda, Germany) over night at 14°C.

Beside the ligation reaction, a negative control reaction was done. This negative control was made by making the same steps like in the ligation reaction with one difference: using distilled water instead of the insert.

2.2.6.5 Transformation of ligated plasmid into competent *E. coli* cells

In this procedure, the ligation reaction was brought into a Jublowater- bath (W. Krannich, Goettingen, Germany) for 5 min at 65°C to melt the gel pieces. Then, it was cooled down in hands before adding it to the previously thawed DH5α cells.

For each transformation one 100 µl-aliquot was taken out from –80°C to be thawed on ice. The whole amount of the ligation reaction, after cooling it down till 37°C, was added to one of the aliquot tubes. Then, after mixing the ligation reaction and the bacterial cells, the mix was incubated for 40 min on ice.

After the incubation time, a heat-shock treatment was applied to the reactions. It was done by taking the tubes directly from the ice to be put into a water bath at 42°C for exactly 2 min. Followed by an incubation period at room temperature for 10 min. Then, 500 µl of LB medium was added and the solution was incubated in Heraeus-incubator (Hanover, Germany) at 37°C for 1 hour and plated on LB plates containing the appropriate selecting antibiotic.

Single colonies were taken from the plates for making plasmid DNA mini preparation. The DNA was digested using the same previously used restriction enzymes or others to have the possibility to figure out the size of the inserted DNA sequence. The molecular size fractionation of DNA was carried out in agarose gels like previously mentioned in the digestion step but with a standard agarose instead of low melting point agarose gel.

2.2.6.6 Isolation of plasmids from transformed *E. coli* cells

After selecting single colonies from the LB agar plates, which contain the appropriate selecting antibiotic, it was transferred to glass tubes that contain 5 ml of LB with the previously used selecting antibiotic. The tubes were incubated over night at 37°C with shaking, using the shaker B. Braun (Melsungen, Germany), at 220 rpm.

About 4 ml LB from each tube were collected and centrifuged in the Labofuge Heraeus 6000 (Heraeus, Hannover, Germany) at 12000 x g for 1 min to pellet the bacterial cells. The supernatant was removed and the pellet was resuspended, completely without leaving any part of the pellet intact, in 300 µl buffer P1.

Then, 300 µl of buffer P2 was added and mixed well and left for maximum 5 min at the room temperature. Fast after the incubation time finished, 300 µl of buffer P3 was added to each tube and mixed well and centrifuged twice in the Eppendorf centrifuge, 5415R (Eppendorf, Germany) at 12000 x g for 15 min at 4°C. In each time, the supernatant was transferred carefully to a new Eppendorf tube avoiding taking any amount of the resulting pellet.

At last, the supernatant was transferred to an Eppendorf tube and 750 µl of room temperature isopropanol was added to precipitate the DNA. The solution was centrifuged immediately at 12000 x g for 30 min at 4°C. The supernatant was discarded and the pellet was washed with 1 ml 70% ethanol, and resuspended in 25 µl autoclaved MilliQ-water (ddH_2O) or TE buffer.

Finally, 1 µl of the resulting DNA was digested by the restriction enzymes that were previously used for cloning. The digested DNA was examined on 0.7% agarose gel with the previously mentioned procedure.

After analyzing the results of the DNA digestion resulting from each selected bacterial colony, it was needed for further usage of the DNA to have higher amount and quality of the extracted plasmid. This was done with Qiagen DNA midi preparation Kit and Nucleobond PC 100 Kit (Macherey-Nagel, Düren, Germany), which involved using anion exchange column for extracting highly pure DNA.

The harvested DNA was washed with 70% ethanol, dried in a speedvac Hetovac (Hettich, Hannover, Germany) and resuspended in 50 µl ddH2O. The concentration of the DNA was determined with the spectrophotometer (Kontron Instruments, Milan, Italy) at a wavelength of 260 nm and at 280 nm for measuring the protein concentration, which can be used later to measure the degree of the DNA purity.

2.2.7 DNA transformation of *C. elegans* (Fire, 1986)

It was important for studying the expression pattern of the studied genes to make transgenic worms. These transgenic worms used in this study have been produced by microinjection and bombardment techniques.

The worm transgenic lines fall into two categories:

1. Extrachromosomal array lines that contain the inserted sequence with no integration into its genome, therefore, it is not to be hereditized according to

the Mendelian Laws and not equally hereditized cell by cell in the offspring of the worms.

2. Integrated lines that contain the inserted sequence as an integrated sequence into its genome, therefore, it is to be hereditized according to the Mendelian Laws and existed in every cell of the worm's offspring.

2.2.7.1 Creating transgenic animals by microinjection technique

In this technique, to get a considerable number of successful transgenic lines, the worms that will be microinjected should be healthy by growing it in optimum conditions and being not too old. All worms were kept at 16-20°C on fresh NGM agar plates seeded with *E. coli* (OP50) bacteria and only early adults or L4 larvae were used.

A highly pure DNA must be used for microinjecting worms, therefore, only DNA which was extracted as a midi preparation with the Nucleobond AX, (Macherey-Nagel GMBH & Co. KG, Germany) kit was used. The amount of microinjected DNA is critical as well. Generally, the solution used for microinjection contained a mixture of DNA plasmids. 1) The plasmid contains the sequence of the gene of interest fused to one of the fluorescent protein sequences with a final concentration of 20 ng/µl. 2) The plasmid pRF4, which contains *rol*-6 (*su1006*) with concentration of 70 ng/µl.

For microinjecting worms an inverted microscope (Zeiss, Axiovert 35, Germany) attached to microinjecting controller was used. Either self made needles or Femtotip II (Eppendorf, Hamburg, Germany) needles were used. These fine needles were loaded with microloaders (Eppendorf, Hamburg, Germany). To avoid the DNase activity the used DNA solutions were always kept on ice.

To microinject worms, an early adult or a L4 larva can be selected from the plates with the dissecting microscope Wild-Heerbrugg (Switzerland) provided with 50 x magnification power. The selected worms were transferred from the plate by a sterilized worm pick to unseeded plates and left for about 30 min at room temperature to get rid of some of the bacteria attached to its cuticle.

Later these worms were microinjected, one by one, by transferring a worm onto a glass slide that has a dried drop of 0.075 to 0.15% agarose located on its center and covered by a drop of mineral oil. The worm was positioned in the best position to show the gonads clearly.

The glass slide was taken to the axiovert microscope (Zeiss, Germany) and worms were centered in the vision field with using enough magnification power to show the details of the gonads. The microinjecting needle manipulated with micromanipulator PMZ 20 and positioned with mother steering (Zeiss, Germany) to point the tip of the needle exactly into the gonad-rachis.

A DNA was microinjected with a pressure of 2-3 hPa. One or both gonads were microinjected as fast as possible to avoid dehydration of the worm and death. The microinjection process must be done carefully to avoid causing a big damage to the tissues of the worm.

Finally, the microinjected worm was picked to a new NGM agar plate seeded with OP50 and incubated at 20°C. After 2-3 days, the offspring (F1) on the plates, which contained the microinjected worms, were checked with the dissecting microscope by normal light, to check for having rolling worms, and by UV to check for their fluorescence.

Some of these worms, which were fluorescent roller worms were taken separately on new NGM agar plates to observe their offspring and make sure that it is still fluorescent and rolling. In this case, it means that those can be considered as a stable line, which contains extrachromosomal array of the microinjected plasmids.

A single fluorescent rolling worm from F2 that was produced from a single microinjected mother was transferred to new NGM agar plate and incubated to form a transgenic line.

2.2.7.2 Creating transgenic animals by bombardment

This method was used in this study to create an integrated transgenic line expressing *hmg-1.1* fused to *gfp*. It is possible to introduce DNA into the *C. elegans* germ line using microparticle bombardment. On the other hand, it is much easier to generate low copy integrated lines than using the microinjection procedure because the microparticle bombardment introduces DNA in small aliquots, which are less effective for creating extrachromosomal arrays.

In our study we used a selectable cotransformation marker, *unc-119*, to help observing the rare worms that can be selected to form the integrated line later (Maduro and Pilgrim, 1995). The worms used for bombardment were *unc-119(ed3)* mutants. These worms were bombarded with plasmid HMG1.1-pEGFP-N1-unc119.

The advantage of using a *unc-119(ed3)* strain is that it does not form dauers and the adult worms are paralyzed. This means that after 2-3 weeks of incubation at 20-25°C. The adult worms will be starved and died leaving the transgenic worms. The transgenic worms that are containing at least one copy of the wild type *unc-119* gene would be crawling as wild type animals, which can ease the determination of the transgenic worms.

This made it possible to differentiate the transgenic line from the non-transformed worms. The transgenic lines that their offspring did not contain any paralyzed worms are the integrated lines. The other worms that produced a number of paralyzed worms beside the transgenic worms were considered transgenic worms that contain extrachromosomal array.

There is a possibility to have a heterozygous integrants, so that, about 20 worms were selected from the main plates and every worms were kept individually on an NGM agar plate. The percentage of the offspring animals that shows fluorescence was measured. If the percentage of these animals were 50% this would mean that the mother is heterozygous integrant. About 10 of F1 fluorescent animals were incubated individually on plates. The worm that has all of its offspring with fluorescence considered to be homozygous integrant and can be used to culture an integrated line.

2.2.7.2.1 The preparation of the gold beads

First, the gold beads must be prepared to be ready to have it possible that the DNA can be carried on it. It was prepared by weighing 15 mg of 1 micron gold beads into siliconized Eppendorf tube. It was important to have siliconized tubes to avoid loosing much of the gold beads on the walls of the tube. For washing the gold beads, 1 ml of 70% ethanol was added to the gold beads and the tube was vortexed strongly for at least 5 min.

Then, the tube was left at room temperature for 15 min to allow the gold beads to settle down and a 3-5 seconds spin in a microfuge was applied and the supernatant was discarded. These washing steps were repeated for 3 times. Then, 1 ml of dH_2O was added and the tube was vortexed for 1 min and centrifuged briefly for 3-5 seconds and the supernatant was discarded carefully not to loose the pellet. Then, 250 µl 50% glycerol was added to the pellet of the beads.

The prepared gold beads were directly coated with the DNA, or stored for a maximum time of 2 weeks at room temperature to be used later for bombardment. This amount was enough for 25 bombardments.

2.2.7.2.2 Coating the prepared gold beads by DNA

For putting the DNA on the previously prepared gold beads, the beads were vortexed at least for 5 min. For each bombardment, 10 µl from the prepared beads was taken into a new Eppendorf tube. This step should be fast not to let the beads settle in the main tube and at the same time carefully done to take the exact amount needed.

Then, adding the following amounts in the same order and with vortexing for 1 min in between each addition: 1 µl DNA (1 mg/ml), 10 µl 2.5 M $CaCl_2$, and 4 µl 0.1 M spermidine (store frozen at -20°C). After all chemicals were added to the beads, the tube was vortexed for at least 3 minutes and left to settle. A brief spin for 3-5 seconds was applied and supernatant was removed.

The pellet was resuspended in 30 µl 70% ethanol and care was taken to collect as much as possible of the beads stuck to the walls of the tube with a pipet tip. After a small spin of 3-5 seconds, the beads pellet was resuspended by adding 10 µl of 100% ethanol and vortexing at least 3 minutes. It is very critical to have the beads resuspended very well to have a successful bombardment. So, it was observed with the microscope till it had no clumps.

2.2.7.2.3 Putting worms on plates

It is very important to use the suitable developmental stage of worms to get integrated lines by bombardment technique. The best stages for bombardment are L4 stage and early adults. So, worm cultures that have mainly these stages were used for transformation.

The worms were grown on opti-gro plates, which is NGM agar medium containing double amount of peptone and cholesterol with adding 100 µg/ml nystatin to avoid contamination on plates. The worms were washed off from the plates with egg salts buffer and were left to settle in 15 ml tube for 5 min. The supernatant was removed carefully to avoid loosing many worms. A small amount of the supernatant left over the pellet helped to spread the worms on a monolayer on the opti-gro plates. It was enough to use 50 µl from the worm pellet for each bombardment.

2.2.7.2.4 Putting beads on macrocarriers and bombardment

The macrocarrier holders and stopping screens were sterilized by dipping them in 100% EtOH and flamed. The macrocarriers were sterilized by dipping them in 100% EtOH. Later, it was air-dried under sterile conditions. The macrocarriers were pushed into macrocarrier holder with a special tool. All of the 10 µl gold beads resuspended in 100% EtOH were spread over the central region of each macrocarrier and left under sterile conditions to dry.

For bombardment a Bio-Rad-1000/He instrument was used with a gap distance of 1/4". Also, 1350 psi rupture disk was used and a vacuum of 28 inches Hg was applied. In all bombardment shots, the plates were put on the second shelf from the bottom. The bombardment was done under sterile conditions to avoid contaminations in the plates.

2.2.7.2.5 Post-bombardment care of worms

The bombarded plates were kept for 1 hour at room temperature to allow the animals to recover from the bombardment process. The worms were washed off the bombarded plates and distributed on 2 or more 100 mm opti-gro plates. The original bombarded plates were also kept and scored later for having transgenic worms.

All plates were incubated for 2-3 weeks at 20-25°C and screened later for having transgenic worms. The non-*unc* transformed worms, which were rescued by the wild type *unc-119* gene were moving like wild type animals. So, it was easy to select the transformed worms by differentiating them from the uncoordinated animals.

From each plate, 10-15 worms were selected and kept individually on a new NGM agar plate. The offspring of these worms was inspected with the fluorescent dissecting microscope. Homozygous integrated transgenic worms were the worms that didn’t segregate uncoordinated worms.

The plates can contain heterozygous integrated transgenic worms. F1 of these worms should have 25% of their offspring as uncoordinated worms and the rest is wild type. In this case, 20 of F1 worms were kept individually on new NGM agar plates and one of the fluorescent worms that had an offspring of 100% coordinated fluorescent worms was kept to make an integrated transgenic line.

Furthermore, bombarded plates can contain worms with extrachromosomal array. Only one transgenic worm, which contained an extrachromosomal was collected from these plates to form separate transgenic line.

Each separate integrated line must be resulting from a single worm that was produced in a single bombarded plate. A worm that has an extrachromosomal array can be kept and its offspring can be designated as a separate extrachromosomal array transgenic line.

2.2.2.8 Freezing and recovery of the *C. elegans* strains

Freezing and recovery of the *C. elegans* strains is a very important technique to store the strains for long time. For freezing the *C. elegans* cultures, a freezing medium was used. This freezing medium was made as it is described in Sulston and Brenner, 1974.

The worms were collected from their plates with M9 and an equal volume of the freezing solution was added and mixed well. This mix was directly transferred to a new Eppendorf tube and put into a box made out of foam and kept at –80°C. The foam box is helping to have a gradual cooling of about 1°C/min which is need to have a successful freezing of worms.

Generally, the most recommended stage to be used for this procedure is starved L1. So, the worms prepared for freezing, were kept for some days at 20°C till they had many of the starved L1 worms. Every time to freeze worms, an extra aliquot from the strains frozen was kept at –80°C overnight and then, thawed and poured onto a new NGM agar. Then, the plate was inspected for the efficiency of the freezing procedure by scoring the ratio of the worms that survived.

To thaw a frozen strain, the tube containing it was left at room temperature till the worm suspension was totally thawed. Then all of the suspension was poured onto a new NGM agar plate. The plate was left open under sterile conditions till all the solution dried and then covered. The worms were observed with the microscope for having alive worms to be picked onto new plates to start growing the culture cleanly.

2.2.2.9 Cleaning of contaminated *C. elegans* strains

Contaminated *C. elegans* cultures with other bacteria, yeast, or fungi should be cleaned. Some of these contaminating microorganisms can infect the worms, affect it negatively, or in some cases make the observation of worms and the scoring phenotypes very difficult.

To clean contaminated worm cultures, a drop of alkaline sodium hypochlorite solution was added to the center of a fresh NGM agar plate seeded with OP50. Adult worms, which contain many eggs, were transferred from the contaminated plates to this drop. After a few minutes, the drop dried out leaving died adults and their eggs on the plates.

This bleaching solution shouldn't affect the embryos in the same strength like the adults because embryos are surrounded with a thick shell that is able to protect them for longer time from the bleaching solution. The clean plate was incubated overnight at 20°C and was observed for having a survived L1 stage worms to start the new culture from.

2.2.2.10 Growing the *C. elegans* worms in liquid culture

It was important to have a big number of worms, as a target for the bombardment technique because the event of having the bombarded DNA integrated into the *C. elegans* genome is rare. Therefore, bombardment of a high number of worms helped to increase the probability of getting integrated lines.

The standard method for culturing the worms on NGM agar plates was not efficient to get the needed number of worms. For that reason, culturing the worms with the liquid cultures was used. In order to prepare the bacterial food for the worms, 1,25 L of *E. coli* bacterial culture was prepared. The bacteria used were *E. coli* DH5α contain pEGFP plasmid or OP50-1. It was used to have the ability to add the suitable antibiotics in the culture to avoid a possible contamination.

The bacterial media were made out of 2 separate solutions that were autoclaved separately to avoid precipitation. Solution (A) contained the following chemicals: 15 g Bactotrypton (Difco), 30 g yeast extract (Difco), 10 ml Glycerin solution 50 %, and 1125 ml distilled water. A liter of Solution (B) contained 23.2 g KH_2PO_4 and 125,4 g K_2HPO_4.

After autoclaving, both solutions were incubated into the water bath at 60°C for about 30 min. Then, 1125 ml of solution (A) was added to 115 ml of solution (B) and mixed well.

This media was inoculated by about 3 ml of *E. coli* culture and left to grow overnight at 37°C with shaking at 240 rpm. The same incubation conditions were applied to the newly inoculated media and the resulting bacteria were collected on the

next day. Collecting the bacteria was done by centrifugation at 3500 x g at 4°C. The pellet was resuspended in 2-4 ml S-basal media and left shaking in falcon tubes for about 20 min to be homogenized at 4°C.

Culturing of the worms was done in S-basal media. The S-basal media was prepared out of mixing different solutions, which were autoclaved separately. The main media solution contains, in 1 liter, 5,8 g NaCl, 50 ml 1 M KH_2PO_4 (brought to pH 6.0 with KOH), 950 ml double distilled water, 1 ml cholesterol solution (5 mg cholestrol/ml of 95 % EtOH).

The metal solution contained in 500 ml: 0,346 g $FeSO_4$ x 7 H_2O, 0,930 g Na_2EDTA, 0.098 g $MnCl_2$ x 4 H_2O, 0.144 g $ZnSO_4$ x 7 H_2O, 0.012 g $CuSO_4$ x 5 H_2O. This solution was autoclaved separately and stored always in dark.

In order to complete the preparation of the S-basal media the following, separately autoclaved, solutions had to be added to 1 liter of the main media solution: 3 ml of 1M $MgSO_4$, 6 ml of 0.5M $CaCl_2$, 10 ml of 100x Metal solution, 10 ml 1 M potassium citrate pH 6.0, 10 ml of (100 x) Penicillin-Streptomycin-Neomycin (Gibco), 10 ml of (100 x) nystatin (Gibco)

The prepared S-basal media was poured into 1 or 2 liter sterilized-flasks in a way that the amount of the media never exceeds the third of the total volume of the flask. This was important to have good aeration into the media, which helps in getting healthy worms. Furthermore, 5-8 growing plates of *unc-119* mutant worms and 30 ml bacterial suspension were added to the S-basal media. Then, the culture was left shaking at 250 rpm at 20-25°C.

It was very critical, to have good reproduction rate in the culture. So, the cultures were checked everyday for having enough food. New bacterial food had to be added when dauer larvae start to appear in the culture.

2.2.2.11 Preparation of agarose coated cover slips for microinjection

Different concentrations of agarose (ultra-quality, Roth, Germany) solution ranging between 0.075 and 0.3% in dH_2O were prepared by boiling them in a microwave oven. A drop of it was dispensed onto a cover slip (24 x 40 mm, Menzel-Glaeser, Germany), and air-dried over night at room temperature. Before every use, the agarose-coated cover slip was moistured by breathing over the surface. This makes it obvious, which side of the cover slip the agarose pad is fixed to.

2.2.2.12 Preparing the slides for microscopic observation

A solution of 4% agarose in M9 buffer was used to prepare the glass slides for worm microscopic observation. Some glass slides were covered by 1 or 2 layers of plastic adhesive tape to have them slightly thicker than the plain glass slides. For each plain slide, 2 glass slides with adhesive tape were used to flank it from both of its long sides.

With the microwave oven, the prepared 4% agarose in M9 buffer was melted. A drop of the melted 4% agar buffer was placed on to the plain glass slide. Another plain glass slide was placed very fast, before the drop solidified, on the agar drop in a way forming a cross with the other plain slide and having each of its ends laying on one of the glass slides with adhesive tape.

The slides were left for 1 minute to be ready. Then, all of the plain slides were collected in pairs having the agar pad in between them. One glass slide, the one carrying the agarose pad on it, from each glass slide-pairs was used for microscopic observation. These slides were made always fresh because the agarose pads were unusable after drying out.

To use these slides for microscopic observation, about 5 µl M9 contains 10 mM sodium azide were placed on the agarose pad. Then, a number of worms, which should be observed microscopically, were transferred on the agar pads. A cover slip was placed immediately on the agar pad. Within a few minutes the worms stopped moving, which made it possible to observe them and to make photos.

2.2.2.13 Preparation of polylysine-coated glass slides

These slides were used for the antibody staining technique. The worms are sticking to the polylysine-coated glass slide that makes it possible to make the staining and washing steps without loosing many of the worms. The polylysine solution, which made out 1mg polylysine in 1 ml water, had to be prepared fresh in the day of using the slides.

The slides were cleaned from any traces of grease on them by dipping them into detergents and then washing them with water. Then, the glasses were heated in a heating block at 80°C. The polylysine solution was distributed on the slides making a

thin layer. The slides were heated till the polylysine dried. Then, it was ready to be used after leaving it to cool down at room temperature for about 30 min.

2.2.2.14 Staining the DNA with DAPI

DAPI (diamidophenylindole) is a DNA-intercalating dye. The worms were stained by DAPI staining to inspect the DNA contents with the fluorescent microscope. The staining was done by picking the worms that needs to be inspected into few drop of the DAPI staining solution into a glass watch. The DAPI staining solution was 150 ng/ml DAPI in methanol or ethanol (diluted from 1 mg/ml stock).

The worms were left into the DAPI staining solution for at least 15 minutes at room temperature. Then, the worms were rehydrated by incubating the worms into M9 buffer for at least 10 min. Then, the worms were picked out for inspection on a glass slide and covered by a cover slip.

2.2.2.15 The acridine orange staining

The acridine orange staining was used to stain the apoptotic cells. In this technique, 1 ml of 100 µg/ml acridine orange was added to a glass watch. The worms were transferred to the glass watch and incubated in the solution at room temperature for about 4 hours.

Then, all worms were picked out from the glass watch and transferred to standard NGM agar and incubated at 20°C for at least 1 hour or overnight to reduce gut fluorescence. The worms were mounted on agarose pad with a drop of 20 mM sodium azide to be inspected by Nomarski microscope. The worms were observed with the fluorescent dissecting microscope with either the red or green channel. The nuclei undergoing programmed cell death were bright.

2.2.2.16 The extraction of the total protein from *C. elegans* worms

The worms, which were grown onto 5-10 NGM agar plates, were collected with cold M9 buffer. It was washed for 3-4 times in cold M9 by centrifugation at 500 x g for 1 minutes at 4°C. The supernatant was collected after each centrifugation and new M9 buffer was added and mixed well and centrifuged again under the same conditions previously mentioned. After the last wash, the amount of worms was measured and a double volume of lysis buffer solution added to it.

The worms were mixed well into the buffer by brief vortexing and boiled in water bath for 3 min. Then, the tube containing the total lysate was centrifuged at 12,000 x g for 1 min to clarify the solution from the cell debris. The supernatant was collected in a new tube and enough volume was loaded into SDS-PAGE gel or stored in –80°C till it can be used.

2.2.2.17 Agarose Gel Extraction Protocol with QIAEX II kit

The DNA band was excised from the agarose gel with a clean and sharp scalpel. Then, the gel slice was weighed in a colorless tube. For 1 volume of gel for DNA fragments 100 bp – 4 kb, 3 volumes of Buffer QX1 were added. In case of having a bigger band than 4 kb, 3 volumes of Buffer QX1 plus 2 volumes of H_2O was added.

QIAEX II was resuspended by vortexing for 30 seconds and added to the sample according to the expected DNA amount which was going to be extracted as follows: 10 µl of QIAEX II was added when expecting less than or equal to 2 µg DNA, or 30 µl of QIAEX II was added when expecting 2–10 µg DNA and an additional 30 µl of QIAEX II was added for each additional 10 µg DNA.

To solubilize the agarose and bind the DNA, the tube that contained the agarose slice was incubated at 50°C for 10 min. It was mixed by vortexing every 2 minutes to keep QIAEX II in suspension. In order to proceed with the procedure, the color of the mixture must be yellow. If it was not yellow 10 µl 3M sodium-acetate (pH 5.0) was added and the reaction continued for additional 5 minutes, at least.

The sample was centrifuged for 30 sec at 10,000 x g at 4°C and the supernatant removed carefully with a pipet. The pellet was resuspended in 500 µl of Buffer QX1 for washing it. Then, it was centrifuged, under the previously mentioned conditions, and supernatant was removed with a pipet. This wash step removed residual agarose contaminants.

The resulting pellet was washed twice with 500 µl of Buffer PE by the same way used in the last wash with buffer QX1. This step was important to remove residual salt contaminants. The pellet was air-dried by opening the lid of the tube and leaving it for 10–30 min at room temperature or until the pellet becomes white.

The DNA was eluted by resuspending the pellet in 20 µl of 10 mM Tris·Cl, pH 8.5 or H_2O. Then, the tube was incubated for 5 minutes at room temperature, if the extracted band was smaller or equal to 4 kb; or at 50°C, if the extracted band was 4-10 kb.

Finally, it was centrifuged for 30 seconds at 10,000 x g and the supernatant, which contains the purified DNA, was transferred to a new tube. The DNA was stored at 20°C.

2.2.2.18 GST purification

2.2.2.18.1 Culturing the bacteria

A tiny amount of the frozen bacterial culture of *E. coli* BL21 containing pET41c-hmg1.1cDNA plasmid, which produce HMG-1.1 fused to GST was used to inoculate 60 ml LB medium contains 70 µg/ml kanamycin. The LB medium was incubated at 37°C on the shaker at 250 rpm. The bacterial concentration was measured from time to time with the spectrophotometer at 600 nm till its OD value reached OD 0.6-1.

All of the 60 ml LB medium was used to inoculate 540 ml LB medium supplemented with 70 µg/ml kanamycin. The medium was incubated at 35°C and the bacterial concentration was measured by spectrophotometer at 600 nm till it had OD 0.5. Then, it was incubated at 30°C till the value of its OD measured at 600 nm reached OD 0.8-0.9.

2.2.2.18.2 Incubation

The induction was done by adding IPTG to the LB medium at final concentration 1 mM. The bacterial cells were harvested by centrifugation at 10000 xg for 15 min. at 4°C. The pellet was washed in 50 mM Tris (pH 7.5) with vortexing till it was fully homogenized. The cells were collected by centrifugation (under the previously mentioned conditions).

The pellet was resuspended in 10 ml RIPA-buffer and incubated at room temperature for about 5-10 min. After the incubation period finished the tube containing the suspension was quickly put into liquid nitrogen, and then, thawed on wet ice.

The suspension was sonicated 3 times for 10 seconds. Then, it was transfered into 30 ml COREX-tubes, spin at 39,000 x g for 20 min. The supernatant was transferred into 15 ml Falcon-tube. 400 µl of 50/50 slurry of Glutathione sepharose 4B (Pharmacia, USA) was transferred to 50 ml falcon tube.

The beads were washed 3 times in PBS and 1 time in RIPA-buffer. It was incubated overnight on a rocker at 4°C. The beads were centrifuged at 500 x g for 5 minutes at

4°C. The supernatant was collected and 30 ml PBS was added. These washing steps were repeated for 3 times.

2.2.2.18.3 Elution

For eluting the protein from the beads, 1 ml of (10 mM Glutathione in 50 mM Tris-HCL, pH 8.0) was added and left at room temperature for 10 minutes. Then, it was centrifuged at 500 x g for 5 minutes at 4°C. The supernatant was collected in a new falcon tube. This elution steps were performed for a total of 3 times. The protein concentration was measured by spectrophotometer at 280 nm by Bradford assay (Bradford, 1976).

2.2.218.4 Dialysis

It was important to get rid of the glutathione in the protein sample by dialysis before using it. The dialysis was done in 3 rounds, which were done with the dialysis solution (0.01 M Na_3PO_4, 0.5 M EDTA, pH 6) at 4°C with stirring. For each round of dialysis 3 L of the dialysis solution were used.

The sample was loaded carefully into the dialysis bag and the bag was closed well. The first round was done by adding the dialysis solution and incubated for 2 hours. In the second round, the dialysis solution was exchanged by a new dialysis solution and incubated overnight. Third round was done by the same way like the second round but with incubation for 3 hours. The protein sample was collected and lyophilized. Then, it was dissolved in 1x TBS and measured with Bradford assay.

2.2.2.19 Bradford assay

This assay was used to measure accurately the protein concentration. The Bio-Rad protein assay, dye reagent concentrate (Bio-Rad, USA), and different BSA concentrations as standards were used. The Spectrophotometer was warmed up for at least 15 minutes before usage.

The samples were diluted with buffer to an estimated concentration of 1-20 µg/ml. Standards containing a range of 1-20 µg BSA were prepared (200 µl from each). Then, 800 µl coomassie brilliant blue G-250 were added to each vial and incubated at room temperature for 5 minutes.

The protein concentration was measured with the spectrophotometer at 280 nm for all vials of the standards and the protein sample. A curve was plotted out of the

resulting OD values of the BSA standards. The protein concentration in the sample was measured by plotting its OD value on the curve of the BSA standards (Bradford, 1976)

2.2.2.20 The antibody purification

The rabbit serum collected from rabbits that were injected with recombinant HMG-1.1 was purified with an affinity column technique. This was done with the SulfLink kit (Pierce, Rockford, USA), as following:

2.2.2.20.1 The reduction of the protein

In this method, all buffers running through any column were degassed to avoid introducing air bubbles. About 5 mg protein were diluted in 1 ml of sample preparation buffer. The protein solution was added to the vial containing 6 mg of reductant (results in 50 mM 2-MEA). The mixture was incubated at 37°C for 1.5 hours. The mixture was cooled to room temperature.

Washing the desalting column with 20 ml of coupling buffer was used to equilibrate the column. The excess reductant was removed from the reduced protein and the previously prepared mixture was added to the equilibrated desalting column and the solution was allowed to flow into the column.

Coupling buffer (3 ml) was added to the column and the solution that flew from the column was collected. The desalting column was washed either with 20 ml of coupling buffer for immediate usage or 20 ml of coupling buffer with 0.05% sodium azide (NaN_3) for storage.

2.2.2.20.2 Coupling protein to gel

It was important to keep the gel bed wet throughout the entire procedure. To avoid drying of the gel an additional solution was added, or the bottom cap was replaced on the column whenever the buffer drains down to the top of the gel bed. For the determination of the coupling efficiency a small sample of the protein solution was retained

The SulfoLink coupling gel column was equilibrated to room temperature. The column caps were removed, top cap first then the bottom cap. Then the column was placed in a collection tube and the storage buffer was allowed to drain from the column.

The column was equilibrated with 8 ml of coupling buffer. The bottom cap was replaced and the reduced protein sample was added. The top cap was replaced and the column contents were mixed by rocking and end-over-end mixing at room temperature for 15 minutes.

The column was incubated at room temperature for additional 30 minutes without mixing. The top and bottom column caps were removed and the solution allowed draining from the column into a clean tube. The column was placed over a new collection tube and the column was washed with 6 ml of coupling buffer.

The coupling efficiency was determined by comparing the protein concentration in the retained amount of the protein sample before coupling to the gel with the protein concentration of the sample after coupling to the gel. The determination of the protein concentration in both samples was done by measuring the UV absorbance at 280 nm with Bradford assay.

2.2.2.20.3 Blocking Nonspecific Binding Sites on Gel

One of the porous discs provided with the kit was placed just above the gel bed to prevent the column from drying out by automatically stopping the column flow when solution has drained down to the top of the gel bed. The disc also prevented resuspension of the packed gel bed when adding solution to the column.

Then, the bottom cap was replaced and 15.8 mg L-Cysteine HCl added to 2 ml of the coupling buffer (0.05 M cysteine). 2 ml cysteine solution was added later to the column and the top cap was replaced.

The solution and the gel in the column were mixed together for 15 minutes at room temperature. Then, the reaction was incubated without mixing for an additional 30 minutes at room temperature.

2.2.2.20.4 Washing the column

The top and bottom caps were removed and the buffer was allowed to drain from the column. The column was washed with at least 12 ml of wash solution. The column was washed with 4 ml of degassed buffer Tris buffered saline (TBS) containing 0.05% sodium azide. The bottom cap was replaced and additional 2 ml of TBS containing 0.05% sodium azide added.

The top porous disc was inserted and it was slided within 1 mm of the gel bed using the open tube end of a serum separator. At that step, the ligand was covalently

coupled to the support through its sulfhydryl groups and used for affinity purification. The top cap was replaced and the column was stored upright at 4°C. Alternatively, in case of proceeding with the steps of the procedure, the bottom cap was removed.

2.2.2.21 The affinity purification of protein

2.2.2.21.1 Column preparation

The protein-coupled column was equilibrated to room temperature. The top cap was removed first to avoid drawing air into the gel bed. Then, the bottom cap was removed and the excess storage solution was allowed to drain from the column. The column was washed with 6 ml of degassed TBS buffer to equilibrate it.

2.2.2.21.2 Sample purification

To purify the sample, 1.5 ml of sample was applied to the column and it was allowed to completely enter the gel bed. Alternatively, the gel can be removed from the column and incubated batch-wise with the entire sample volume. After applying 0.2 ml of sample buffer and allowing it to enter the gel bed, the bottom cap was replaced.

Then, 0.5 ml of sample buffer was applied to the column and the top cap was replaced. The column was incubated at room temperature for 1 hour. After the incubation periods, the top cap was removed from the column then the bottom cap and the column was washed with 12 ml of sample buffer. The bound protein was eluted by applying 8 ml of glycine buffer (100 mM, pH 2.5-3.0) and 0.5 ml fractions were collected.

The eluted fractions were neutralized by 100 µl of 1 M Tris, pH 7.5. The elution was monitored by UV absorbance at 280 nm. The fractions of interest were pooled together.

2.2.2.21.3 Regenerating and storing the affinity column

The column had to be regenerated as soon as possible after chromatography to prevent damage to the immobilized molecule because of the low pH of the elution buffer. The column was washed with 16 ml of PBS to remove any residual protein and reactivate the gel.

It was equilibrated with 8 ml of degassed TBS buffer containing 0.05% sodium azide. The bottom cap was replaced and 2 ml of degassed storage buffer were added to the column and the top cap was placed. The column was stored upright at 4°C.

2.2.2.22 Immunostaining

For the immunostaining of HMG proteins in germline, we used the following protocol with small variations for each protein to reach the best staining:

A fresh solution of 10% paraformaldhyde (pH 7) was prepared directly before performing the immunostaining. This paraformaldhyde solution was diluted in 1 x sperm salts to a final concentration of 2%.

About 30-40 adult worms were placed in 10 µl of 2% paraformaldehyde (PFA), in 1x sperm salts to a final concentration of 1% PFA on a positively-charged glass slide, SuperFrost plus (Menzel-Glaser, Germany).

A cut between the pharynx and gonad was made using a needle. This cut makes it possible to see the gonad clearer because it is pushed outside the adults' cuticle and better access for the antibody staining to reach it.

The slide was incubated for 5 minutes. A cover slip (18 mm x 18 mm) was placed on top of the worms and frozen in liquid nitrogen for 5 to 10 minutes. The cover slip was removed quickly with a blade. The slide was immediately placed for 1 minute in 95% ethanol, which was previously cooled in a –20°C freezer. This step was done carefully not to loose the worms.

Then, the slide was incubated in PBST for 10 minutes. The PBST buffer was discarded. The washing step was repeated twice. The PBST buffer was wicked off from the slide surface. Through the last step, it was important to avoid worms from getting dry.

The primary antibody was diluted 1:50 in PBST with a final concentration of 0.5 mg/ml BSA and 10% of the goat sera were added. The slide was placed in a humid chamber and incubated overnight at 4^0C. The slide was washed twice in PBST for 10 minutes. The PBST was wicked off in the same way like before.

Carefully, in dark or under indirect dim light, 50 µl of secondary antibody, diluted in PBST, was added. The slide was placed in humid chamber and incubated overnight at 4^0C. It was washed in PBST twice for 10 minutes. The PBST was wicked off and 10 to 20 µl of SlowFade Light Antifade Kit supplemented with DAPI (Molecular Probes, Eugene, USA) were added to the slide. The cover slip (18 mm x 18 mm) was placed on top and the slide was sealed with fingernail polish. At that stage, the slide was ready to be observed or, alternatively, to be stored for maximum of 1 week at –20°C.

2.2.2.23 The separation of the proteins with SDS-PAGE

The separation of the proteins was performed in 12% SDS polyacrylamide gel electrophoresis (SDS-PAGE) as it was previously described (Laemmli, 1970). To run the total protein sample of *C. elegans,* 10 µl from it were mixed to equal volume of loading buffer including 10 µl β-mercaptoethanol, molecular biology grade, from Applichem (Darmstadt, Germany). The same was done to the protein standard marker before running it, 8 µl of Promega's Mid-Range protein molecular weight marker or 2 µl of premixed protein molecular weight marker (Roch, Germany) were mixed with equal amount of the previously mentioned loading buffer.

Then, all samples were incubated for 3 minutes in a DAGLEF-PATZ water-bath (Holstein, Germany) at 95-100°C. After quick centrifugation at 12,000 x g for 1 minute at 4°C the samples were loaded into the slots of the gel with the Hamilton-syringe (Bonaduz Microliter, Switzerland), and overlaid with electrode buffer.

The electrophoresis was done in an electrophoretic SE 600 chamber (Hoefer Scientific Instruments, San Francisco, USA). The electrophoresis was performed at 50 V and 20 mA, till the sample went through all of the stacking gel for about 1.5 hours, then at 250 V and 40 mA for 4-5 hours, after passage of the stacking gel till the end of the run.

Gels were removed from the gel plates, and the protein bands were stained in 1 mg/ml Coomassie Blue G-250 (Serva, Heidelberg, Germany) with slow shaking on a KS250 basic-shaker (W.Krannich, Göttingen, Germany) at 50 rpm for 6 hour and destained by submerging it in the destaining solution (50% methanol and 10% acetic acid) for 4 hours at room temperature with the same shaking conditions like it was used in the staining step. The gels were photographed with a Polaroid CCD camera.

3. Results

3.1 Studies on *hmg-12* (*hmg-Iβ*)

3.1.1 Phenotypes that resulted from *hmg-12* RNA interference (RNAi)

In this study, animals were exposed to *hmg-12* dsRNA by microinjection and feeding techniques.

3.1.1 Phenotypes that resulted from the microinjection of N2

The *hmg-12* dsRNA was synthesized from the pSKHMGIβ-yk plasmid. The microinjection was done in adults, L4 and L2 larvae. The animals were microinjected as described below.

3.1.1.1 Depletion of *hmg-12* caused defective touch response

The first offspring generation (F1) of the wild type animals (N2) that were microinjected with *hmg-12* dsRNA was tested for their response to different touch stimuli in comparison with the N2 control animals that were microinjected with DEPC water.

Touches on the animals' bodies were applied by using the fine tip of an eyelash hair to measure and analyze quantitatively the behavioral differences between the F1 of *hmg-12* dsRNA microinjected animals and the control animals.

This experiment was done with adults. For each animal, 3 different ways of touches were applied onto the body of the animals: 1) alternating touches on the head and tail (head-tail touches), 2) touches on the head, and 3) touches on the tail.

The touches were applied onto the body of the offspring (F1) of wild type strain (N2) animals that were laid 12-36 hours after the time of microinjecting their mothers. The microinjection was done with *hmg-12* dsRNA (3 µg/µl) into the gonad arms. In the control animals, the microinjection was done with DEPC water. The animals were touched several times. The time between two touches was about 1 second. The maximum number of touches was 40.

3.1.1.1.1 Head-tail touch

In this experiment, successions of touches were applied to the head and tail of each animal. Through the course of touching, the animals were left for a second after applying the touch to have enough time to express their response.

Every touch course started with head touch. The animals showed different types of responses, which were categorized into two main groups, normal responses, and abnormal responses. Moving backward after touching the head or forward after touching the tail was scored as normal response. On the other hand, the abnormal responses involved 2 different types of responses as following: 1) acceleration response, and 2) pause response.

The animals that showed acceleration response were moving forward after a head touch and backward after a tail touch. The animals that showed pause response were not responding to the touches by movement but rather by stopping their movement and staying with no movement after applying the corresponding touch.

Also, some other abnormal responses were scored such as the response by moving very slowly or the response by moving for very short distance and then stopping. These latter responses were hard to be calculated quantitatively. Generally, they were found more often in the F1 offspring of the *hmg-12* injected P0 than in that of the control animals.

As shown in Fig. 3.1, the percentage of the animals that showed abnormal responses after head hits (the odd numbers) was higher in case of the dsRNA treated animals than the percentage that was scored in the control animals. 40 animals were scored in every single experiment. The percentage of abnormally reacting animals increased in case of the RNAi animals till it reached its highest value, nearly 45%, at the hit number 19.

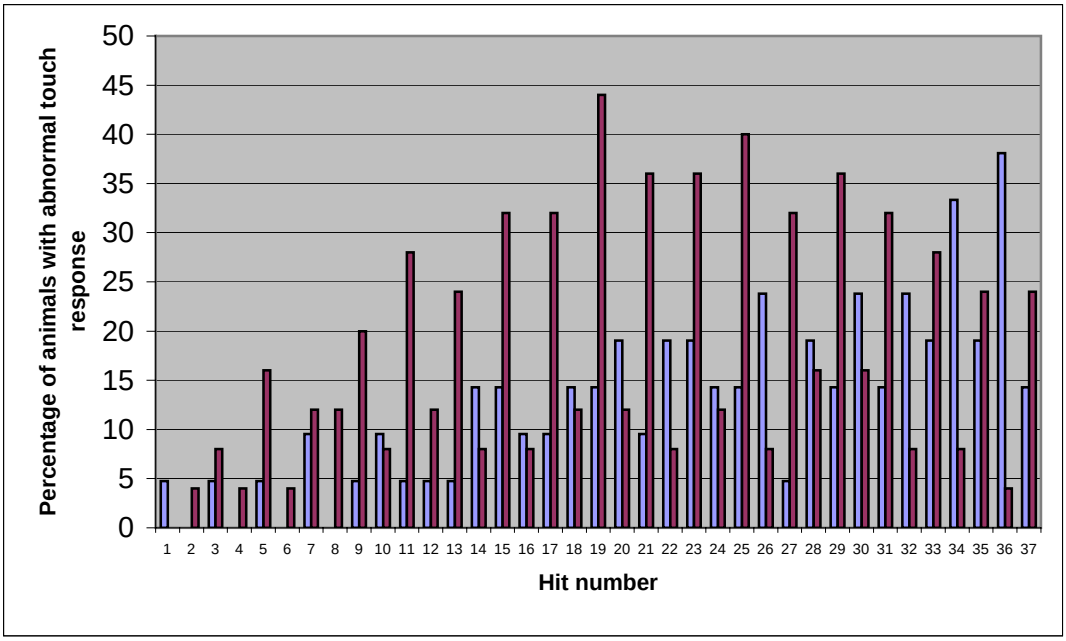

Fig. 3.1: The percentage of the animals that showed abnormal response in the head-tail touch response experiment. The *hmg-12* RNAi-interfered animals are shown in dark red and the control animals in blue (n=40). The odd numbers represent the head touches, the even numbers the tail touches.

In order to determine whether the head or the tail was the reason for the previously mentioned abnormal behaviour, the head and the tail responses for the control and the dsRNA treated animals were separated, analyzed and drawn in separate graphs. The head response was shown in Fig. 3.2 and the tail response was shown in Fig. 3.3.

Fig. 3.2 showed that the percentage of the abnormally reacting dsRNA treated animals was in every hit higher than that in the control and was increasing constantly with increasing hit numbers to reach its highest value after the hit number 19. On the other side, the scored percentages in the control were up and down in a way that they didn’t form one big peak but rather few small peaks.

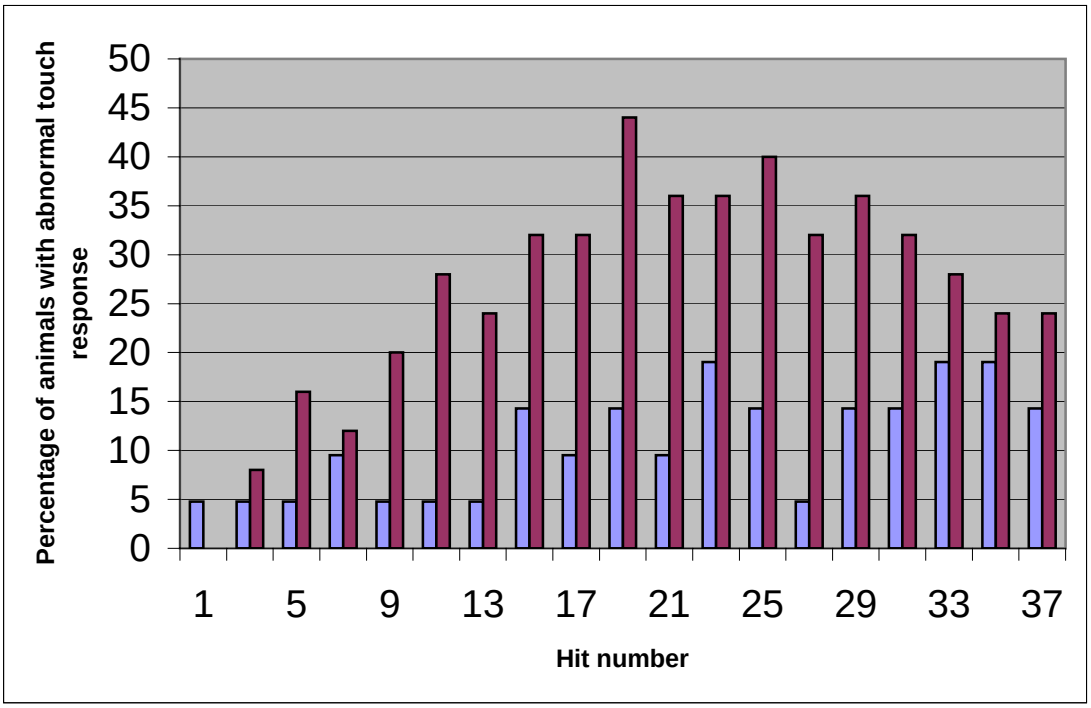

Fig. 3.2: The percentage of the animals that showed an abnormal response to a head touch in the head-tail touch response experiment. The *hmg-12* RNAi-interfered animals are shown in dark red and the control animals in blue (n=40).

Abnormal responses to the tail touches started much earlier, already after the second hit, in the RNAi animals in comparison with the control animals, which showed the first abnormal reaction at the 10th hit (Fig. 3.3). The dsRNA treated animals didn't show constant increase of the percentage of the animals that had this abnormal response through the entire touch course. The percentage of the dsRNA treated animals that showed an abnormal tail response was smaller than that of the control animals with one single exception at hit number 12.

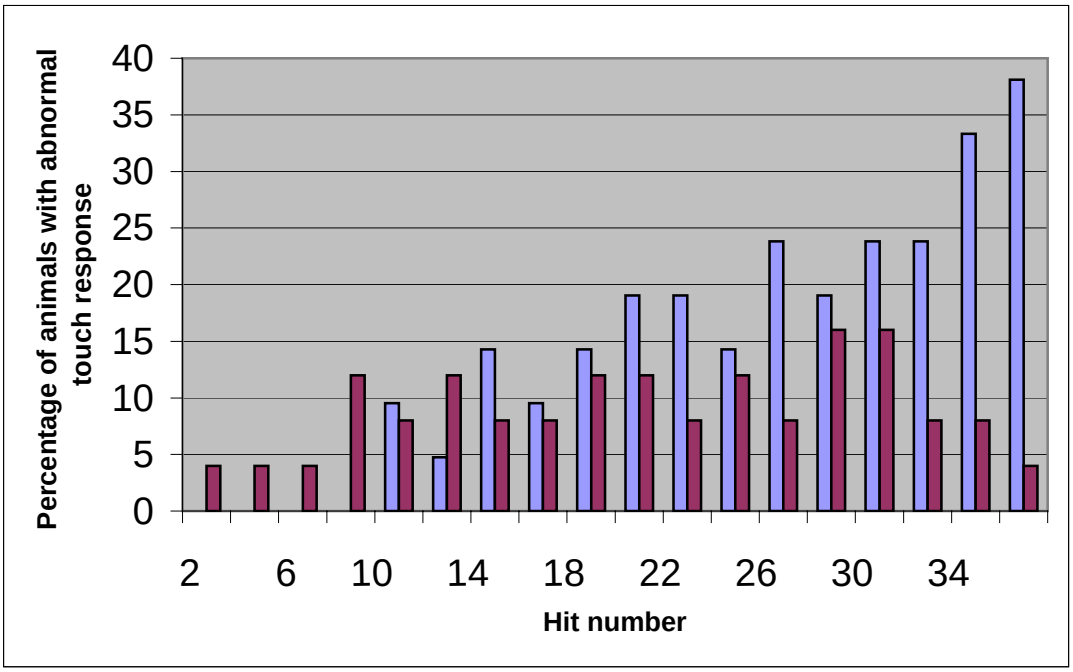

Fig. 3.3: The percentage of the animals with an abnormal tail response in the head-tail touch response experiment. The *hmg-12* RNAi-interfered animals are shown in dark red and the control animals in blue (n=40).

Based on that analysis the animals' heads were the source of the abnormal response rather than the tail. Another data analysis was done to investigate the source of this abnormality in the head. Fig. 3.4 shows the percentage of the animals that showed an acceleration response to the head touches and Fig. 3.5 shows the percentage of the animals that showed head pause response to head touches.

As shown in Fig. 3.4, the percentage of the RNAi animals that showed a head acceleration reaction was increasing till it reached its highest values (28%) at hits 15, 19, and 25. In contrast to that, the highest percentage occurred in the control was 14% and the hits didn't form a one clear curve like they did for the dsRNA treated animals.

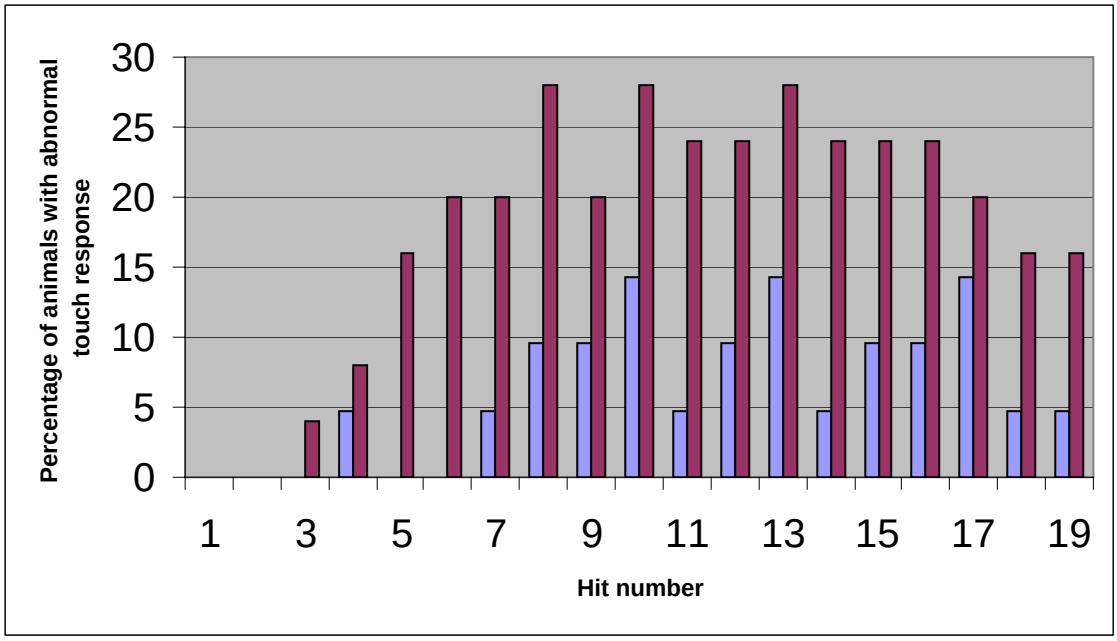

Fig. 3.4: The percentage of the animals that showed an acceleration response in the head-tail touch response experiment. The *hmg-12* RNAi-interfered animals are shown in dark red and the control animals in blue (n=40).

A comparison between Fig. 3.4 and Fig. 3.5 shows that in general the percentage of the animals that showed a pause response was smaller than that with an acceleration response. The highest percentage of the dsRNA treated animals with head pause response (Fig. 3.5) was 16% at hit number 10, and 14% in the control at hit number 18.

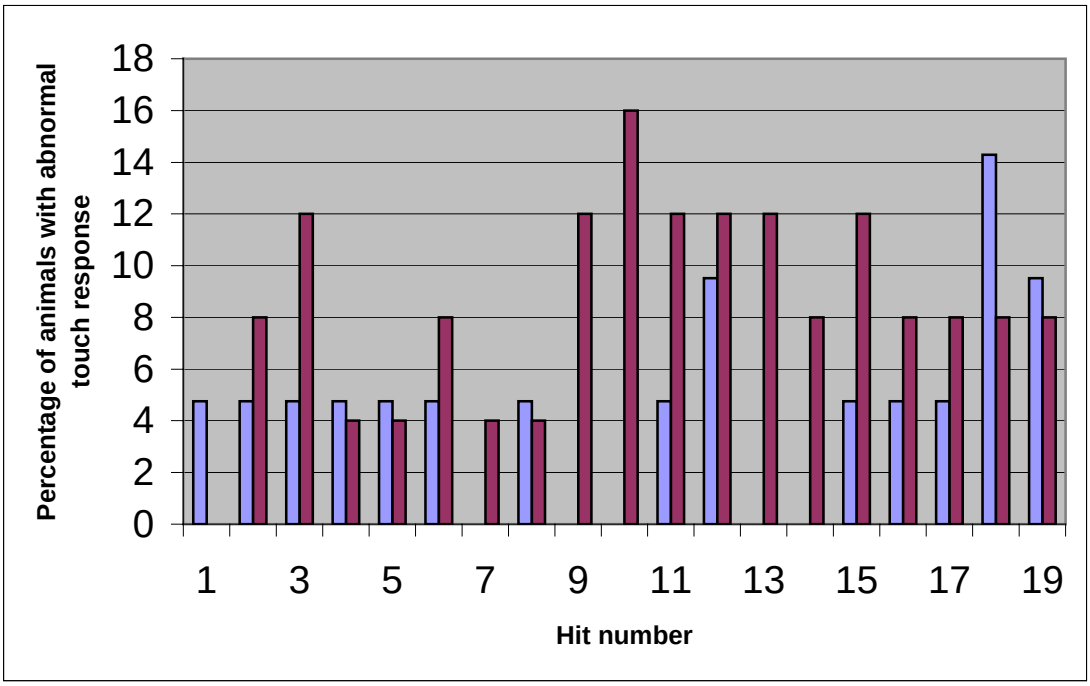

Fig. 3.5: The percentage of the animals with head pause reaction in the head-tail touch response experiment. The RNAi interfered animals are in dark red and the control animals are in blue (n=40).

3.1.1.1.2 Touching the head of the animals

In this experiment the touches were only applied to the animals' heads for several times in a touch course of maximal 40 touches. The period between two touches was about 1 second. The backward movement after touching the head of the animals was scored as normal response.

The abnormal movement response could appear in 3 different ways: 1) the worm stopped its movement and stayed with no movement through several touches (pause), 2) the worm did not respond to the touch at all and kept on crawling (acceleration), and 3) the worm stopped shortly and then continued to crawl.

The results of this experiment are shown in Fig. 3.6. The dsRNA treated worms showed earlier and more consistent abnormality in their head response to the head touches in comparison with the control worms. The abnormal behavior was first seen in the dsRNA treated animals at the hit number 4 (3.8%) and in the control animal fraction at hit number 10 (9.5%).

The percentage of the dsRNA treated animals with an impeded touch response was constantly increasing till the hit number 20 (19.2%), then it decreased to smaller

percentages (7.7-11.5%) at the hits number 21-24 but increases again to form another peak with its highest value (30%) at hit number 26. The percentage of the impeded control animals was generally smaller and not continuous.

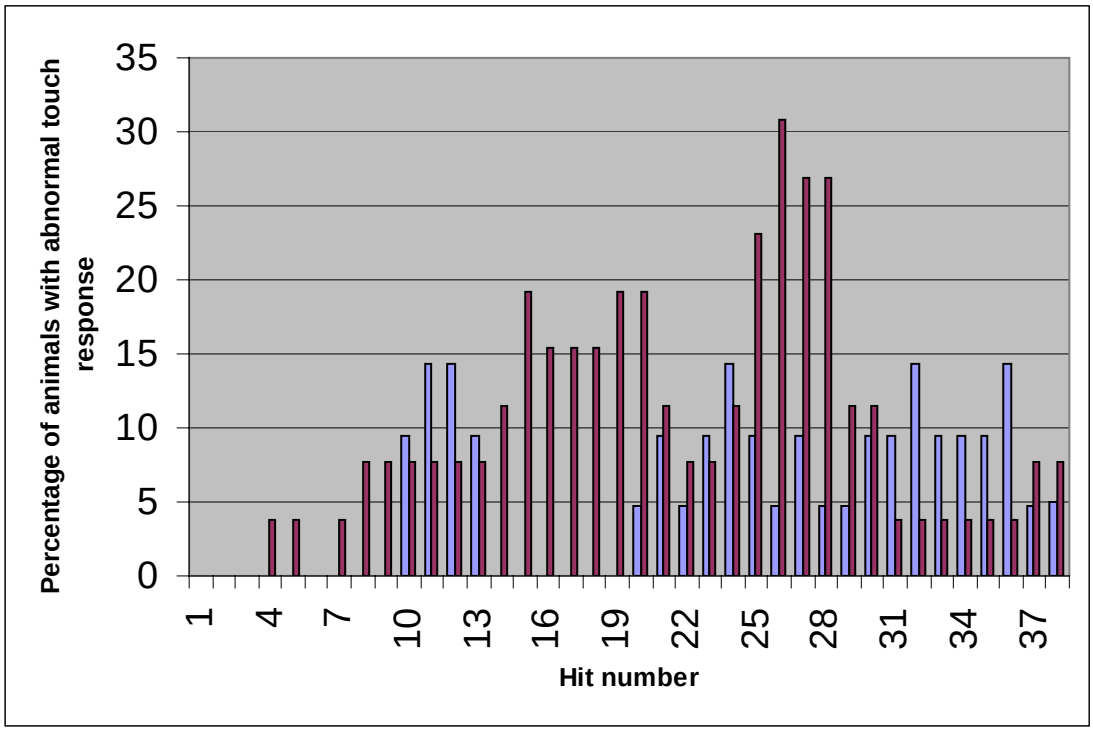

Fig. 3.6: The percentages of the animals with an abnormal response in the head touch response experiment. The *hmg-12* RNAi-interfered animals are shown in dark red and the control animals in blue (n=20).

For further analysis of the head response, the values of the head acceleration and pause reaction were separately analyzed to further define the reason behind the abnormal head response. Fig. 3.7 shows the percentage of the animals with a head acceleration reaction and Fig. 3.8 shows the percentage of the animals that had head pause response. The animals showed no considerable consistency in the increase or continuity of the acceleration response through progress of the touch course (Fig. 3.7).

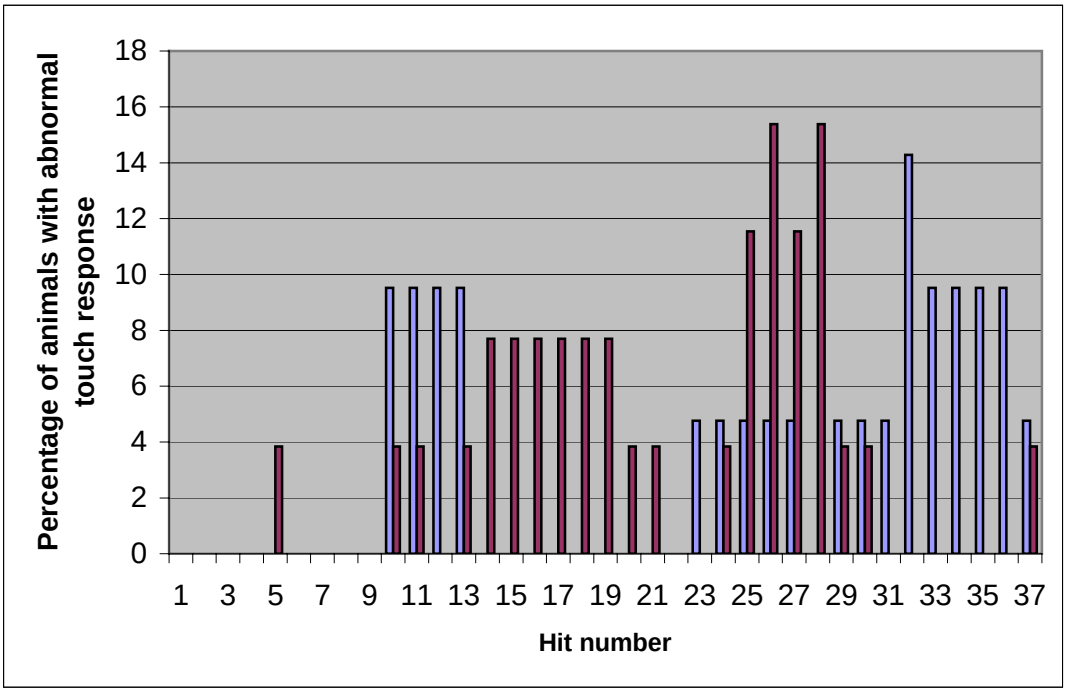

Fig. 3.7: The percentage of the animals that showed head acceleration in the head touch response experiment. The RNAi interfered animals are in dark red and the control animals are in blue (n=20).

The pause reaction as response to a head touch seems to appear at a spontaneous level of 4% for the RNAi animals that increases to its highest value (nearly 16%) at hits number 20, 26, and 27 (Fig. 3.8).

The hits between 20 and 26 scored a smaller percentage. The percentage of the control animals with a head pause reaction was not exceeding 5% except in the 21st and 24th hits, which were approximately 9%.

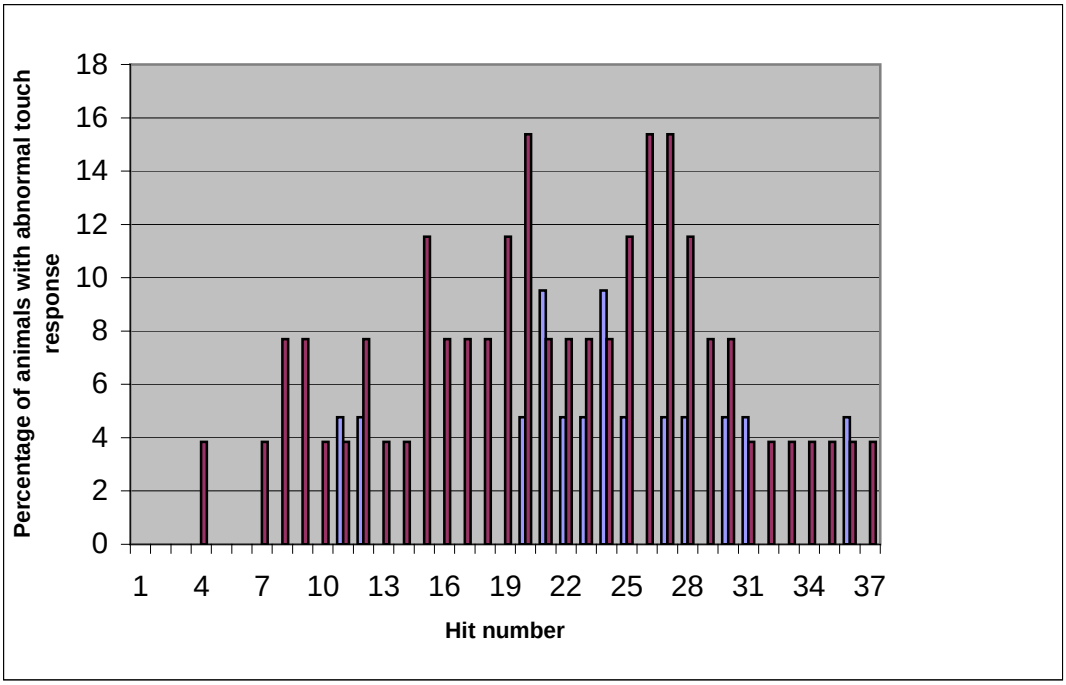

Fig. 3.8: The percentage of the animals that had head pause in the head touch response experiment. The RNAi interfered animals are in dark red and the control animals are in blue (n=20).

3.1.1.1.3 Response to the tail touch

An experiment to examine the tail touch response was done by touching the tail of the adults in the same way, rhythm and number as it was applied onto the head of the animals in the head touch response experiment. The analysis of the results of this experiment showed no backwards acceleration through the whole touch course in both traits. Furthermore, pause response of 6-7% (n=20) was scored for the control animals at hit numbers 31-35. On the other hand, no pause response was scored for the dsRNA treated animals (n=20).

3.1.1.1.4 Head touch response of L2 larvae

The percentage of the acceleration responses to the head touches that resulted from the head touching course is shown in Fig. 3.9. The animals used in this experiment were L2 larvae, which hatched from eggs that were laid 12-24 hours after microinjecting their mothers. The microinjection was done with 3.5 µg/µl *hmg-12*

dsRNA. The time between every two touches that were applied on the head of the animals was 1 second. A maximal number of 40 touches was applied to each larva.
The analysis of these results showed that there is no significant difference between the dsRNA treated animals and the control animals. Furthermore, a noticeable acceleration response was scored for the control animals at the 12th touch but for the dsRNA treated animals not before the 17th hit. The highest percentage of head acceleration in the control animals was 60% and the highest value for the dsRNA treated animals was 55%.

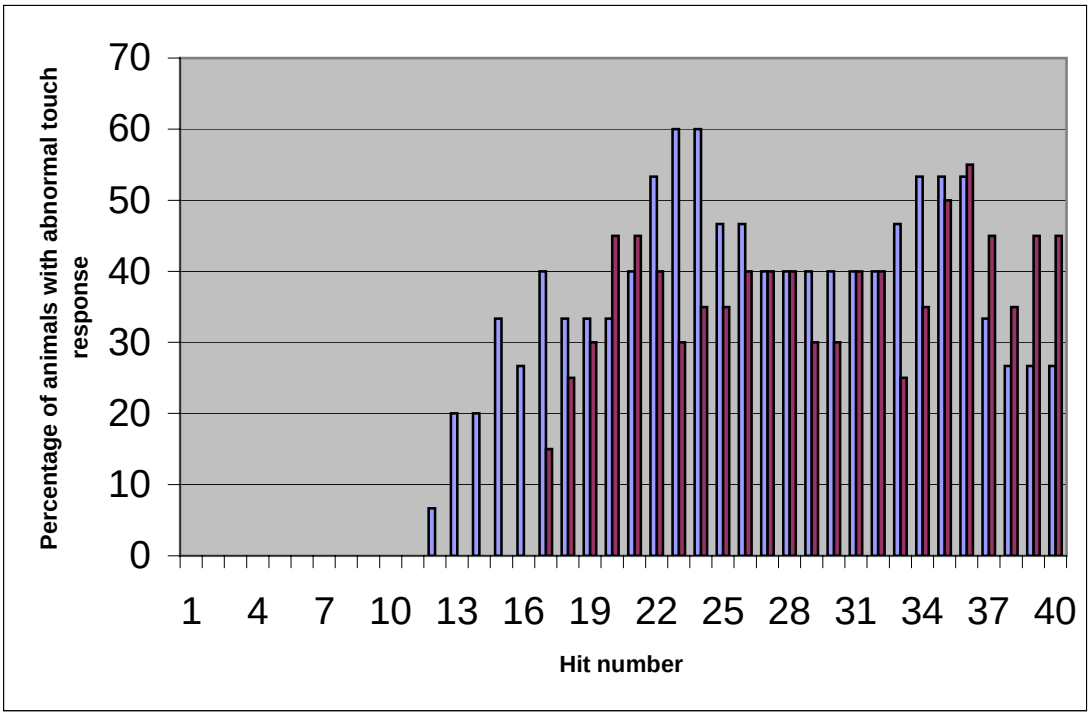

Fig 3.9: The percentage of the L2 larvae that showed head acceleration in the head touch response experiment. The RNAi animals are in dark red (n=20) and the control animals are in blue (n=15).

3.1.1.2 Turning defect

Some of the RNAi animals showed a defect in their response of going backward after a number of head touches. The wild type was turning 180° to reorient itself with the change of the movement direction. Sixty percent of the dsRNA treated animals (n=30) were turning only half of this angle (only 90°).

3.1.1.3 Uncoordination

Some of the F1 offspring of the *hmg-12* dsRNA injected P0, 60% (n=30) of the adults and 45% (n=20) of the L4 stage, were uncoordinated in their movement. This uncoordination appeared as an alteration of the normal movement but the worms were able to move (Fig. 3.10).

The uncoordinated animals left an abnormal track behind. The curves of that track were sometimes more flat than the curves of the control animals. Generally, the direction of the movement of the dsRNA treated animals was not straight but rather in uncompleted or distorted circles (Fig. 3.10).

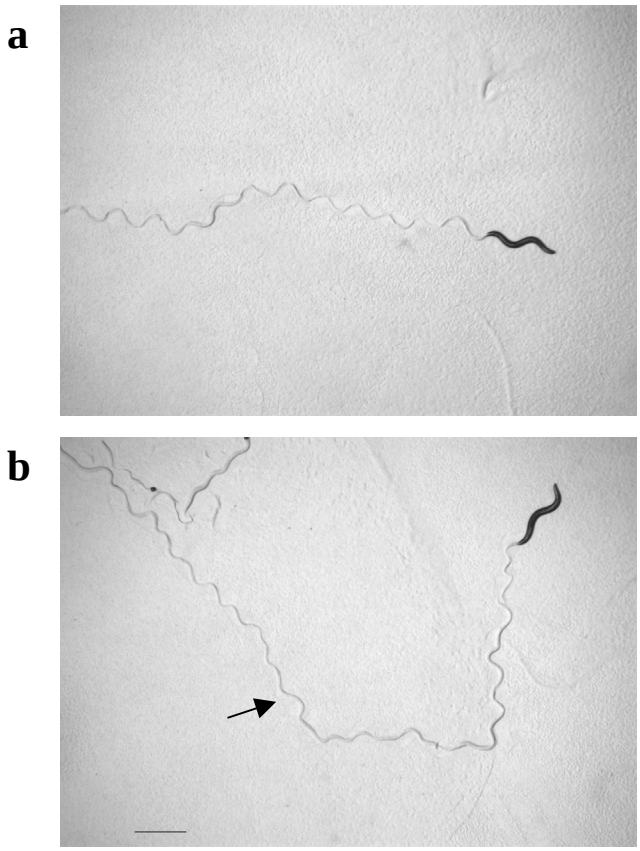

Fig. 3.10: The uncoordinated movement of a RNA-interfered animal. Panel (a) shows the track of the movement of a wild type animal and panel (b) shows the track of the RNA-interfered animal. The black bar in panel b is equivalent to 1 mm in length.

3.1.1.4 Fast foraging activity

In 30% (n=10) of the dsRNA treated animals, the foraging movement of the head was faster than in the control animals.

3.1.1.5 Partial egg laying defect

At least 45% of the adult F1 (n=11) hermaphrodites that were raised from *hmg-12* dsRNA injected P0, were partially egg laying defective. These adults laid eggs for about 24 hours at 20°C and then stopped laying eggs. As a consequence, they were bloated with eggs and died from internally hatching larvae.

Interestingly, this partial egg-laying defect was also noticed in P0 animals that were microinjected with *hmg-12* dsRNA. In order to avoid this direct effect of the microinjection process to the gonads, L4 larvae were microinjected anywhere in the body but not in the gonads. Then, they were incubated at 20°C. They laid few eggs and stopped laying eggs after 24 hour. Their bodies were bloated with eggs as it is shown in Fig. 3.11.

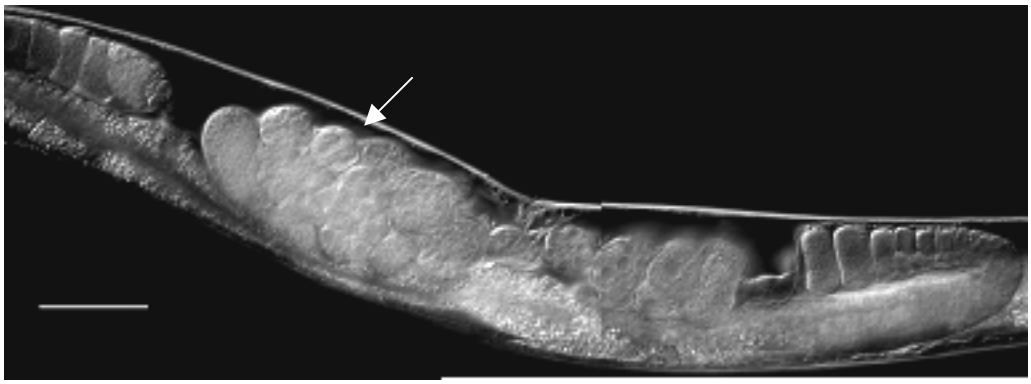

Fig. 3.11: The bloated gonad of a *hmg-12* RNAi adult N2. The arrow points to the gonad arm that was bloated with eggs. The white bar is equivalent to 10 μm in length.

3.1.1.6 Embryonic and oocyte lethality

The F1 generation of the 15 wild type adults that were microinjected with 3.5 μg/μl *hmg-12* dsRNA, and incubated at 20°C, showed in average 7% arrested embryos and oocytes (n=348). It was done by taking out the mothers from the agar plates and incubating the laid eggs over night on 20°C. The egg was counted dead if it was not hatching after the incubation time.

3.1.2 Feeding of *hmg-12* dsRNA to N2 animals

Feeding the N2 animals with *hmg-12* dsRNA resulted in the same phenotypes that appeared as a result of microinjecting the worms with *hmg-12* dsRNA. Only the head-touch response defect did not appear. 90% of the worms moved uncoordinated, a higher percentage than in case of the microinjection treatment.

35% of the animals showed hyperactive head movement, a slightly higher percentage than in the microinjection experiment. Also, some animals had a partial egg laying defect and the turning defect appeared in the animal population in a lower percentage than in the dsRNA microinjection (30%).

3.1.2.1 Effect of *hmg-12* dsRNA feeding on chemotaxis

The animals that were used in this experiment were previously synchronized in their development. This experiment was done to test the ability of chemosensory neurons of the adult animals that were fed with *hmg-12* dsRNA to sense isoamyl alcohol (1% isoamyl alcohol diluted in M9 buffer supplemented with sodium azide).

In this experiment, the animals that were raised on *hmg-12* dsRNA didn't show a considerable difference in their ability to sense the Isoamyl alcohol in comparison to the control animals. The percentage of the RNAi-treated animals that sensed the Isoamyl alcohol was 77.3% (94 out of total 124 animals), and it was 70% (50 out of 80 animals) for the control animals.

In a separate experiment, the ability of *hmg-12* RNAi L1 larvae in comparison with the *hmg-12* RNAi adults to sense isoamyl alcohol was tested by the same previously mentioned procedure. The results of this experiment showed that 80% (20 out of 25 larvae) of the control was attracted to the Isoamyl alcohol spot. However, 40% (24 of 60 larvae) of the *hmg-12* RNAi L1 larvae were attracted to the isoamyl alcohol. A percentage of control adults 81.8% (90 out of 110 animals) were attracted to the isoamyl alcohol and 75.8% (47 out of 62 animals).

3.1.3 Microinjection of *hmg-12* dsRNAi into *him-8*

The microinjection of a *him-8* strain with 3 μg/μl *hmg-12* dsRNA was done to check the sex ratio of these animals. They were fed with the *hmg-12* dsRNA after microinjecting them. This experiment was done at two different temperatures, 20 and 25°C, to see if there was a temperature sensitive phenotype. The percentage of the

dsRNA treated males was 23.6% (139 out of 588 animals) and for the control animals 29.9% (246 out of 822 animals).

A test for the *him-8* male fertility was performed. This test was done on tiny plates supplemented with a small loan of OP50 in the center of the plates. Males from the two different traits, RNAi and control, were incubated separately for 4 days with N2 hermaphrodites. The results showed that 77% (27 out of 35 males) of the males were infertile. The infertile animals were observed with the microscope.

The observation of the infertile animals showed that 40% (4 out of 10 males) of the males had a distortion in their gonad (Fig. 3.12 panel (a)), 2 of these males had a male tail defect (Fig. 3.12 panel (b)), and the rest of the animals did not show any morphological abnormality.

The arrow in Fig. 3.12 (a) is pointing to the distorted part of the gonad. The pharynx appeared swallowed at the bulb. In panel (b) of Fig. 3.12, an uncompleted development of a male tail is shown. The male tail did not have spicules and its fan was clearly incomplete. Beside these observations in the reproductive system, there were some animals that showed a malformation of their pharynx (Fig. 3.13).

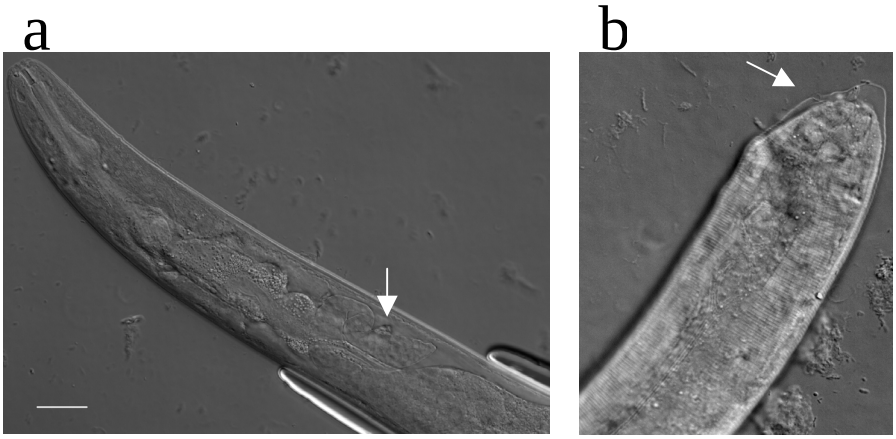

Fig. 3.12: The male-gonad and male-tail phenotypes that resulted from *hmg-12* RNAi microinjection of *him-8* strain. The arrow in panel (a) points to the defective part of the male gonad. The arrow in panel (b) points to the male fan that didn't complete its development.

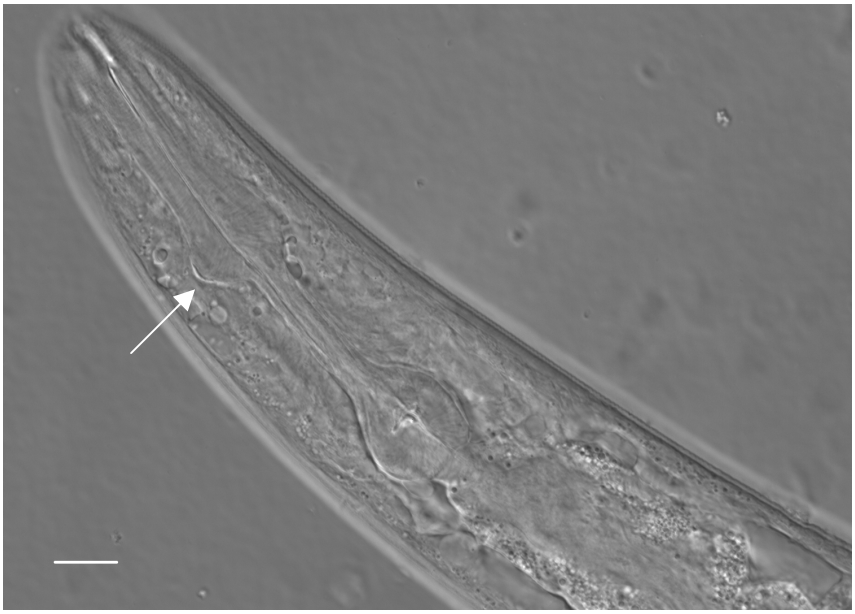

Fig. 3.13: The pharynx morphological phenotype that resulted from *hmg-12* RNAi microinjection of *him-8*. The arrow points to the part of the pharynx that had malformation.

Another test was done to know whether the infertility that appeared on the mating plates was a source of male infertility, or indirect effect of abnormality from the *hmg-12* RNAi males to sense the bacterial loan spotted in the middle of the plate. Having males that can't be attracted to the bacterial spot will let them crawl away from the bacterial spot, which is normally where the hermaphrodites stay, hence decreasing the chance of mating.

This was tested by a chemotaxis test of F1 animals of *him-8* animals that were exposed to *hmg-12* dsRNA microinjection and another trait that was exposed to *hmg-1.1* RNAi. The results odf both traits were compared to the results from the control trait. OP50 bacterial food was used as an attractant in this experiment.

The percentages of the control animals in comparison with *hmg-12* RNAi and *hmg-1.1* RNAi animals were calculated and the results of the test are shown in Table 3.1. The percentage of the control males that were attracted to the becaterial spot was 34% (25 mlaes out of 73 animals). This percentage was more than the total male percentage in the control animals, which was 29% (27 males out of 93 animals) and the male percentage on the M9 buffer, which was 10% (2 males out of 20 animals).

On the other side, the percentage of the *hmg-12* RNAi males that were attracted to the bacterial spot was 27% (5 males out of 22). This percentage was slightly less than

the male percentage in the starting population from this trait, which was 28.6% (12 males out of 42 animals) and considerably less than the percentage of the males that were around the M9 spot, which was 35% (7 males out of 20).

As a third trait, hmg-1.1 RNAi animals were checked. It showed that hmg-1.1 RNAi males were normal and comparable with the control animals in their ability to sense the bacterial food (Table 3.1). This shows that the *hmg-12* RNAi males had a slight defect in their chemosensation of the baterial food in comparison with the control and the hmg-1.1 RNAi animals.

Table 3.1: Test of the chemosensation of the *hmg-12* RNAi- and *hmg-1.1* RNAi-animals from *him-8* mutant for the bacterial food.

	Total animal no.		**On food**		**On M9 buffer**	
	Total	**Males**	**Total**	**Males**	**Total**	**Males**
Control	93	27 (29%)	73	25 (34%)	20	2 (10%)
***hmg-12* RNAi**	42	12 (28.6%)	22	5 (27%)	20	7 (35%)
***hmg-1.1* RNAi**	27	13 (48%)	15	9 (60%)	12	4 (33%)

3.1.4 Microinjection of *hmg-12* dsRNAi into KP987 (*glr-1::gfp)*:

The strain KP987 that carries an integrated transgene of *glr-1::gfp* was used to explore the possibility of having a developmental RNAi effect on one of the nerve cells that show expression in this strain. The cells that show GFP fluorescence in this strain are: AIB, AVA, AVB, AVD, AVE, RIM, AVG, AVJ, DVC, PVC, PVQ, RIG, RIS, RMD, RME, SMD, and URY (Hart, A *et al.*, 1995).

The microinjection was done with 3 µg/µl *hmg-12* dsRNA into the gonad of the strain KP987. The animals that were microinjected with the dsRNA showed GFP expression in all nerve cells expressing *glr-1::gfp*. However, in a small percentage of the animals (6%) (3 out of 50 animals), the fluorescence signal of the *glr-1::gfp* in at least one of the AVD nerve cells (AVDL or AVDR) was fainter than in the control (Fig. 3.14).

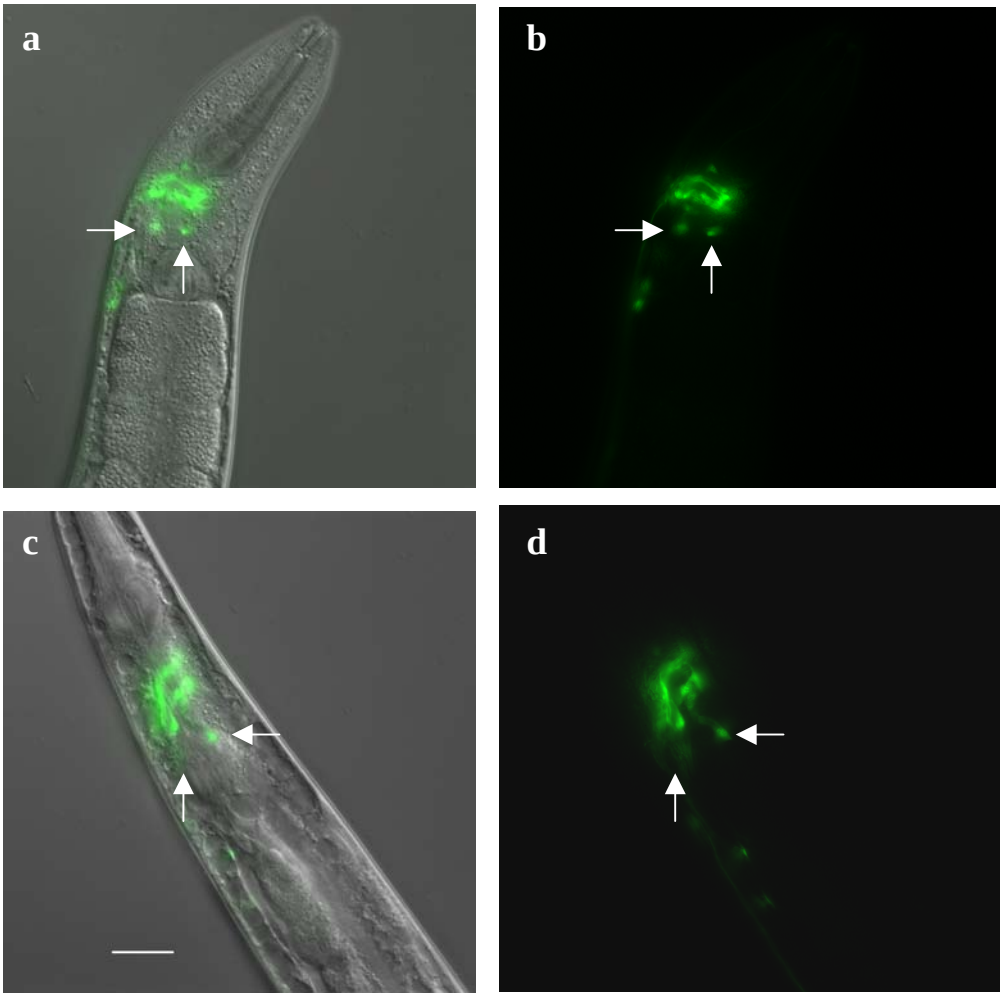

Fig. 3.14: The expression pattern of the KP987 strain with and without *hmg-12* dsRNA microinjection. (a) and (b) show the *glr-1::gfp* expression in a control animal. The arrows point to the AVDL and AVDR nerve cells. (c) and (d) show the *glr-1::gfp* expression in the F1 generation of the dsRNA treated animals. (b and d) show the fluorescent expression and (a and c) are the micrograph of the fluorescence and the Nomarski-DIC. The vertical arrow points to the AVD nerve cell with fainter *glr-1::gfp* expression.

3.1.5 Expression pattern of *hmg-12*

3.1.5.1 Expression pattern of *hmg-12* in EC700 and EC701 strains

Both of the EC700 and EC701 strains have an extrachromosomal array of *hmg-12::gfp*. The expression of that array results in partial HMG-12 protein that lacks 85 of its amino acid residues fused to GFP. These strains were inspected with the

microscope to analyze the *hmg-12::gfp* expression in different cell during development.

3.1.5.2 Expression pattern in L1 and L2

The expression was noticed in the L1 and L2 larval stages in the pharynx and the precursor cells of the somatic gonads (Fig. 3.15, a-d). In Fig. 3.15, panel (a) shows the expression in L2 stage by using the fluorescence microscope and panel (b) shows the same animal with Nomarski-DIC. Panel (c) shows a higher magnification of the somatic gonad precursor cells of the same animal.

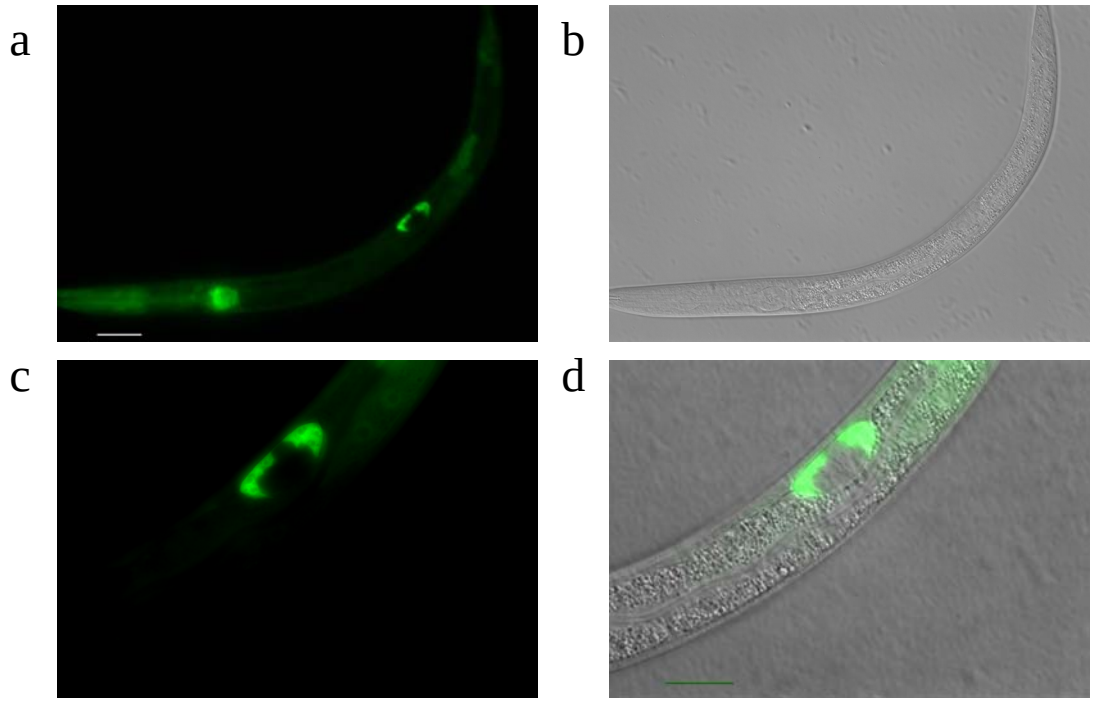

Fig 3.15: The expression pattern of *hmg-12::gfp* in the L2 stage of EC701. Panel (a) shows the overall *hmg-12::gfp* expression in the body. The white bar in panel (a) is equivalent to 25 µm (b) corresponding Nomarski-DIC photomicrographe (c) and (d) show in a higher magnification of the gonad precursor cells. The bar in panel (d) is equivalent to 10 µm.

3.1.5.3 Expression pattern in the dauer larva

In the dauer larva *hmg-12::gfp* is expressed in the pharynx and in the body muscles (Fig. 3.16). No expression was noticed in the intestine.

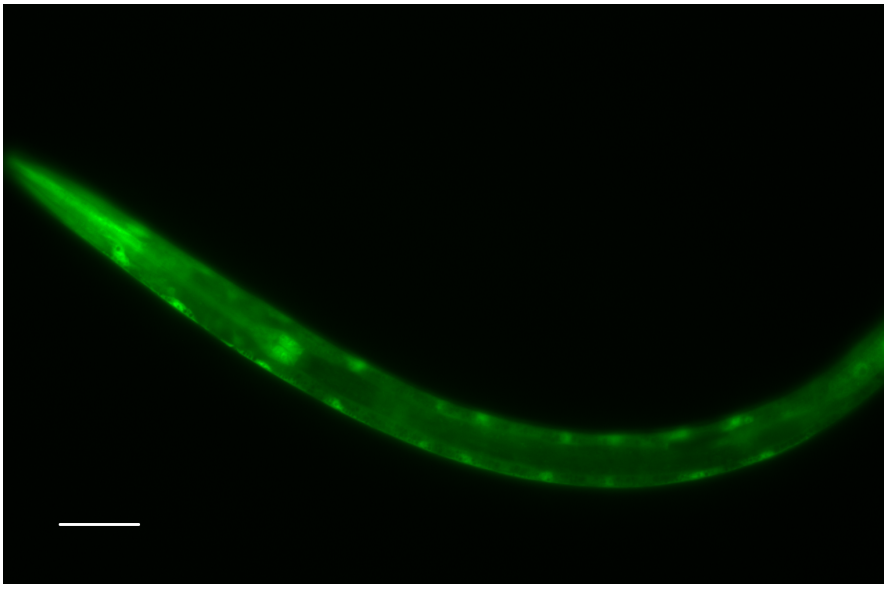

Fig. 3.16: Expression of *hmg-12::gfp* in the dauer stage of EC700. The white bar is equivalent to 25 µm.

3.1.5.4 Expression pattern in the hermaphrodites

The microscopic observation showed that *hmg-12::gfp* is expressed in many different cells in the body of the adults. It was clearly detected in both the nucleus and the cytoplasm of every cell in that it was expressed at. It was expressed in the pharynx, the intestine, the vulva, and some nerve cells. There was no expression in the gonads (Fig. 3.17).

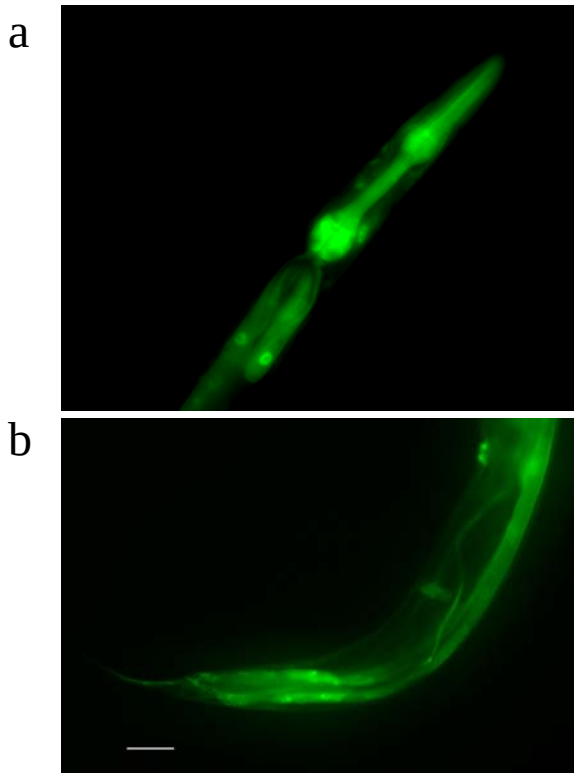

Fig. 3.17: The expression of *hmg-12::gfp* in the strain EC700. (a) shows the expression in the pharynx and the intestinal cells. (b) shows the expression in the abdominal part of the body. The arrow points to the vulva. The white bar in panel (b) is equivalent to 50 µm.

3.1.6 Expression pattern in EC705

The EC705 strain is a strain that carries an extrachromosomal array of *hmg-12::eyfp* transgene. The expression pattern of *hmg-12::eyfp* in EC705 was limited to the nuclei. It appeared in many different cells through out the animals' bodies. It was expressed in the intestine, the pharynx and some cells in the tail. Fig. 3.18 shows the fluorescence of *hmg-12::eyfp* in the head. It appeared in the pharynx tissues and in some nerve cells near the pharynx. The expression in the tail was limited to a small number of cells.

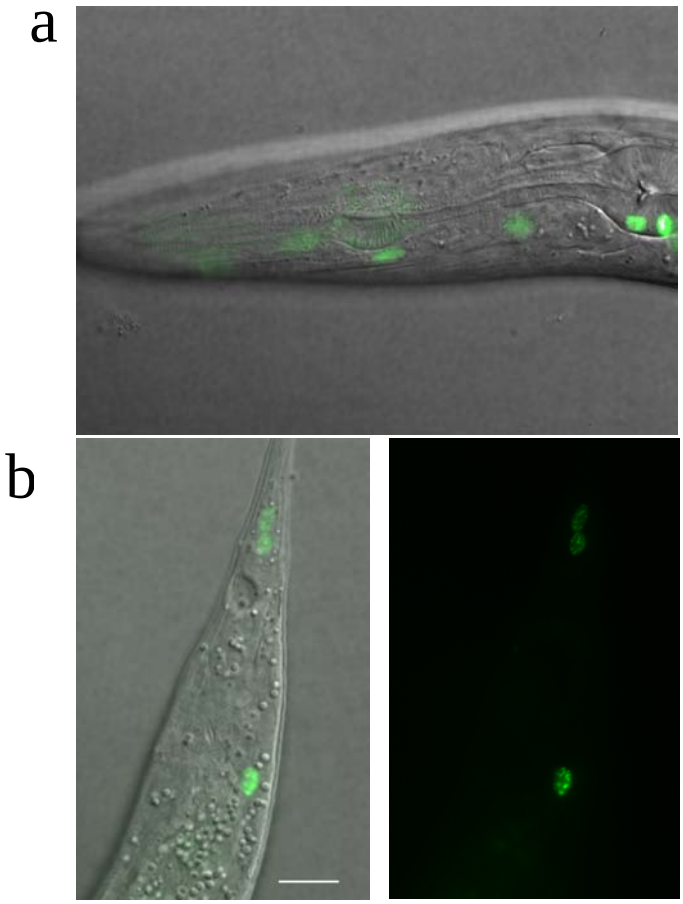

Fig. 3.18: the *hmg-12::eyfp* expression in the head and tail of the strain EC705. (a) Shows the overlaying between the fluorescent expression and the Nomarski-DIC observation in the head. (b) shows the expression in the tail, the photo on the right side shows the observation with the fluorescence microscope and the photo on the left side is overlaying of fluorescent expression with the Nomarski observation. The white scale par in panel (b) is equivalent to 10 µm in length.

hmg-12::eyfp is strongly expressed in one of the nerve ring cells. The position of this cell corresponds to that of the nerve cell AVD interneuron (Fig. 3.19).

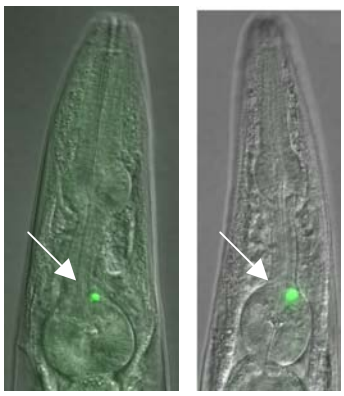

Fig. 3.19: The expression of *hmg-12::eyfp* in the head area of an EC705 adult. The arrow points to the cell, which is probably an AVD nerve cell.

3.1.7 Depletion of *hmg-12* in EC700

This experiment was done to check the effect of the *hmg-12* dsRNA feeding on the expression of *hmg-12.* The results showed that the RNAi animals (n=17) had a lower intensity of the *hmg-12::gfp* fluorescence than the observed fluorescence in the body of the control animals (Fig. 3.20). The expression of *hmg-12::gfp* was not lost in specific cells after dsRNA feeding.

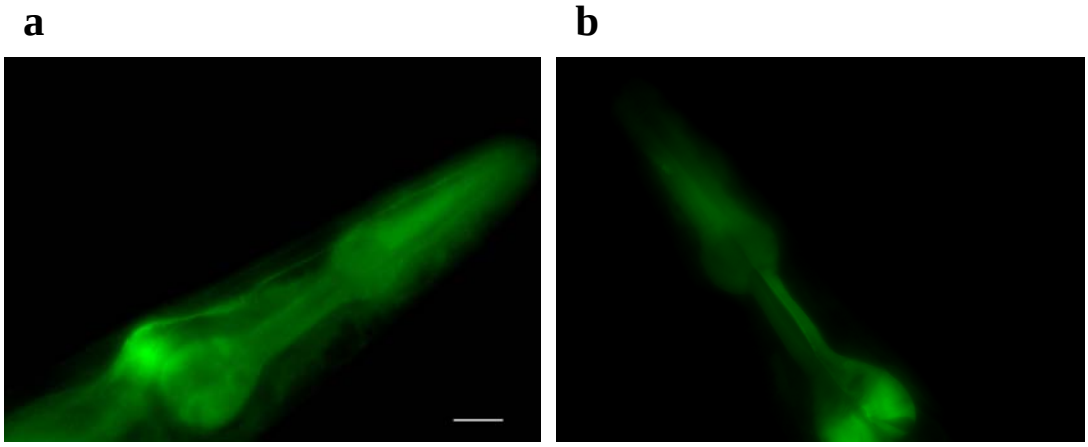

Fig 3.20: Depletion of *hmg-12* by feeding EC700 animals with hmg-12 dsRNA. (a) Control animal. (b) RNAi animal. Scale bar is 25 μm.

3.1.8 Immunostaining of HMG-12

An immunostaining experiment was done using rabbit polyclonal antibody against HMG-12. The antibody was used in a concentration of 1:100. The immunostaining showed that HMG-12 is localized in the germline nuclei (Fig. 3.21). The protein seems to be concentrated in small dots, The worms showed also a clear staining of the intestinal nuclei (Fig. 3.22).

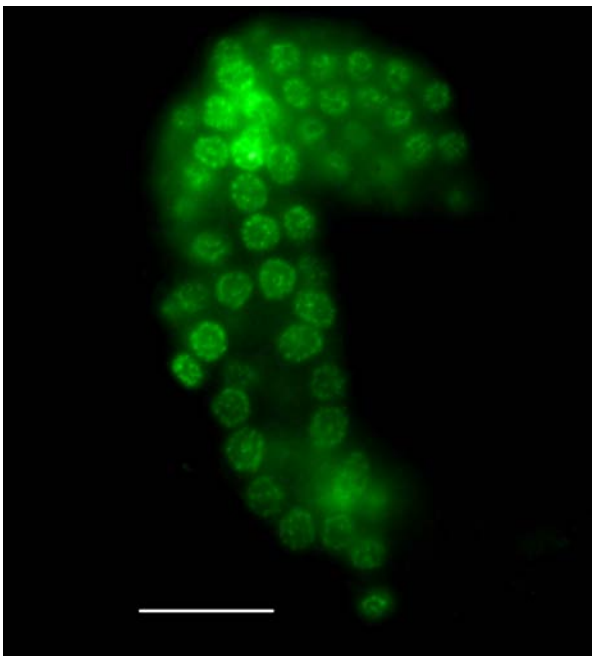

Figure 3.21: The immunostaining of HMG-12 in the gonads of a wild type animal. The scale bar in the photo is equivalent to 10 µm in length.

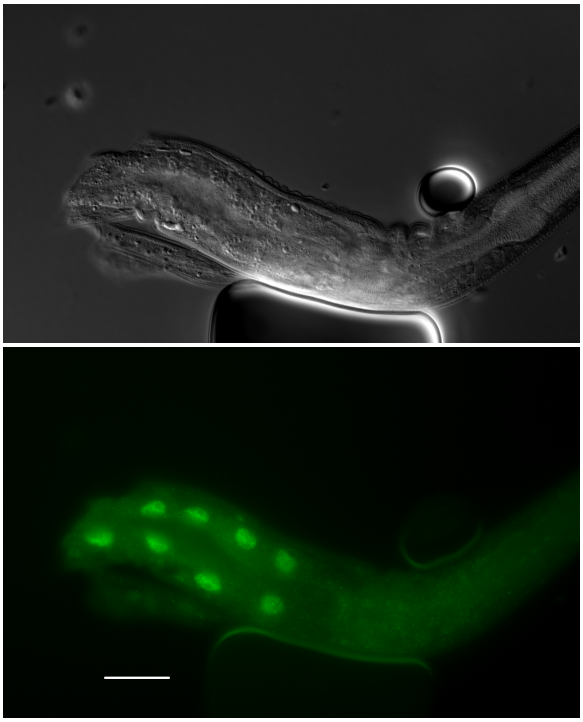

Fig. 3.22: The immunostaining of HMG-12 in the intestine of the N2 animals. HMG-12 is detected in the intestinal nuclei. The scale bar equals 25 µm.

3.2 Studies on *hmg-1.1*

3.2.1 Phenotypes that resulted from *hmg-1.1* RNA interference (RNAi)

The RNA interference (RNAi) was used in this study to explore the functions of *hmg-1.1* in C. *elegans*. The dsRNA was applied to different *C. elegans* strains with two methods, dsRNA feeding and dsRNA microinjection.

3.2.1.1 Phenotypes that resulted from *hmg-1.1* dsRNA feeding

In the standard method of feeding *hmg-1.1* dsRNA, *C. elegans* was raised on agar plates seeded with the *E. coli* strain HT115, which contained the HMG-1.1 cDNA cloned into the dsRNA producing vector L4440. The results were scored by direct observation of the F1 animals that were laid 12 hours or later after the starting point of feeding of P0 animals.

The observation was done by comparing the behaviour and morphology of the animals that were fed with dsRNA with control animals fed on a bacterial strain that contained only L4440 vector without the *hmg-1.1* cDNA.

The individual method of dsRNA feeding and scoring was conducted similar to the standard method. The main difference was that F1 worms were cultured individually on standard agar plates supplemented with OP50 bacteria or dsRNA feeding plates.

In some cases, some of the offspring of the individually cultured F1 worms were transferred individually onto new plates and observed. This method allowed many new observations. However, the observed phenotypes resulted from a relatively smaller number of animals because of the difficulties to follow a large number of animals and their offspring.

The collective culturing and scoring of dsRNA fed animals was used only in case of a need of scoring phenotypes on a very big number of F1 animals. It was used mainly to examine the F1 animals' reaction toward stresses.

3.2.1.1.1 Phenotypes from *hmg-1.1* dsRNA feeding of N2 animals

3.2.1.1.1.1 Necrotic-like structures

The most dominant phenotype that resulted from the depletion of *hmg-1.1* through feeding was the necrotic-like phenotype. This phenotype was observed in many parts of the animals in all stages. The severity and the shape of the necrotic areas were different based on where they appeared in the body of the animal. This phenotype was scored in 90% of the HMG-1.1 depleted animals (45 out of 50 animals). Only some small vacuoles appeared in a small percentage (< 10%, n=40) of the N2 control animals.

The necrotic areas start as small vacuoles-like structures in separate areas and grow through development. This growth brings them nearer to each other and later different areas can fuse to form a bigger cavity. Usually these necrotic-like areas started as small vacuoles mainly in the head of the early larval stages. In adults, they are located in many parts of the body. Sometimes, they build a continuous groove as it is shown in Fig. 3.20 (b and C).

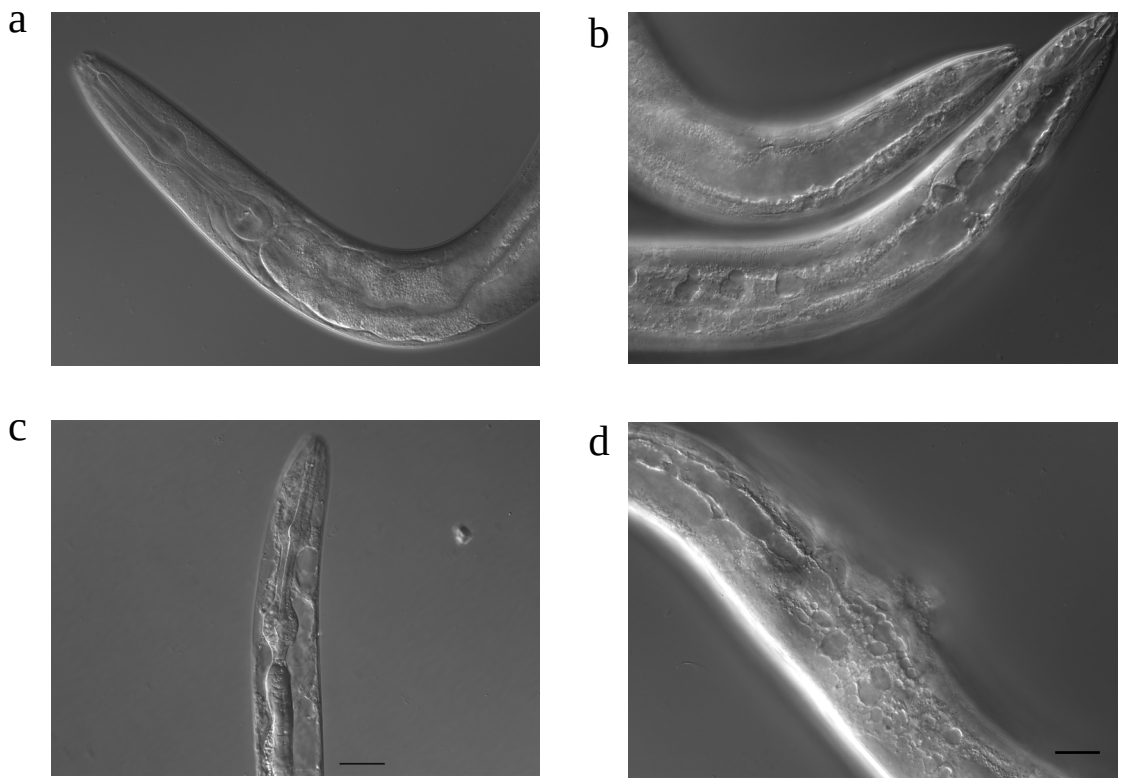

Fig. 3.20: The necrotic-like phenotype of N2 animals fed with *hmg-1.1* dsRNA. (a) Head area of N2 control animal. (b, c, and d) the Necrotic-like phenotypes in different severity and different regions of the body. The scale bar in (b) is 25 µm. (a), (b), and (d) has the same magnification and the scale bar in (d) is 10 µm.

3.2.1.1.1.2 Egg laying defects

In this experiment, 20% of the wild type hermaphrodites (4 out of 20 animals) that were fed with *hmg-1.1* dsRNA showed a partial egg-laying defect. These adults were able to lay a number of eggs, which hatched normally. Then, on the second or third day, it stopped laying eggs and became bloated from the internally accumulated eggs and embryos. After the microscopic observation, it appeared that the vulva of 50% (2 out of 4 animals) of the animals that had partial egg laying defects showed an abnormal morphology. The vulva of these adults appeared swollen and protruded (Fig. 3. 21).

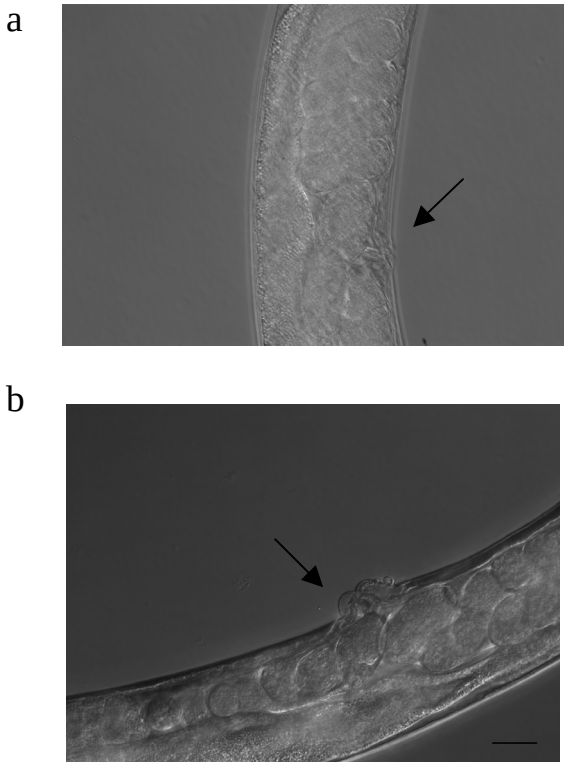

Fig. 3.21: The protruding vulva of *hmg-1.1* dsRNA fed adult. (a) Control animal. (b) The *hmg-1.1* dsRNA treated animal. The arrow points to the protruding vulva of worms that showed a partial egg-laying defect. The scale bar in (b) is 10 µm.

3.2.1.1.1.3 Gonad and germline defects

Wild type animals that were fed with *hmg-1.1* dsRNA showed malformation of the gonad in about 5% of the adult hermaphrodites (4 out of 80 animals). Their gonads had grown with extra turns in the proximal part of the gonad instead of the normal (U) shaped loop.

3.2.1.1.1.4 The effect of *hmg-1.1* dsRNA on chemotaxis

This experiment was done to measure the difference between the *hmg-1.1* dsRNA fed N2 animals and the control animals in their ability to sense volatile chemicals, isoamayl alcohol and formaldhyde. The chemotaxis test was performed on synchronized animals of the F1 generation of wild type animals that were fed with *hmg-1.1* dsRNA.

The RNAi animals were efficiently able to sense both odorants with no considerable difference compared to the control animals. 75% (480 out of 640 animals) of the

RNAi animals attracted to the isoamyl alcohol and 79% (363 out of 460 animals) attracted to the formaldhyde, while the percentages of the control animals attracted to these odorants were 81% (272 out of 281 animals) and 76% (315 out of 415 animals), respectively. The percentage of L1 larvae attracted to isoamyl alcohol was 65% (78 out of 120 larvae).

3.2.1.1.1.5 Highly variable number of laid eggs.

In this experiment the total number of laid eggs from 20 wild type animals that were fed with *hmg-1.1* dsRNA were compared with the total number of laid eggs from wild type control animals. The control animals were fed on bacteria that contained only the L4440 plasmid.

Every worm was kept individually on NGM agar plate and transferred every day to a new plate. 25% of the *hmg-1.1* dsRNA treated animals laid in average 90 eggs. That number was less than half of the average total number of eggs (n=220) that were laid by the control animals.

3.2.1.1.2 The phenotypes from *hmg-1.1* dsRNA application of *rrf-3*

The *rrf-3* strain is hypersensitive for the RNAi effect. The individual scoring method was used to score the results from the feeding of this strain. Morphological phenotypes like necrotic-like structures (100%), partial egg laying defect (33%), and gonad malformation (40%) were found (n=10).

From the microinjection, the number of *rrf-1* F1 animals that were produced from *hmg-1.1* dsRNA microinjected mothers was very low (5-12 animals), which were mainly weak. 4 out of 7 animals in two separate experiments were intersexual animals. These animals were infertile. These animals had an incomplete male-tail, with no fan and incomplete specules. Furthermore, these animals contained a morphologically and functionally altered hermaphrodite gonad end with a differentiated vulva (Fig. 3.22).

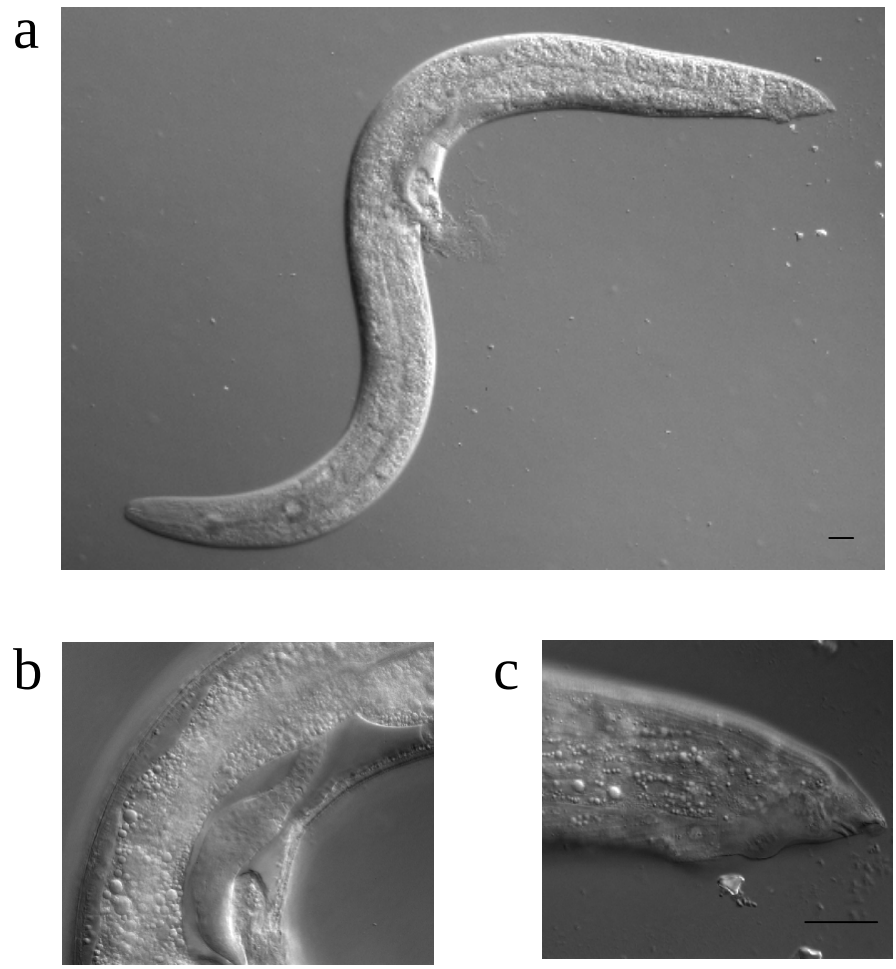

Fig. 3. 22: An intersexual animal that resulted from feeding *rrf-3* mutant strain with *hmg-1.1* dsRNA. (a) An intersexual animal. (b) Magnified view of the uterus. (c) Magnified view of the tail showing the incomplete male tail. The scale bar is50 µm.

3.2.1.1.3 The *hmg-1.1* dsRNA microinjection effect on *him-8*

3.2.1.1.3.1 Gonad and germline defects

Some of the adults that were microinjected with *hmg-1.1* dsRNA developed different kinds of gonad and germline morphological and functional defects. These defects appeared in 15% (6 out of 40 animals) of the animals; the percentage was calculated as a sum of the scored number of the animals that had any of the hermaphrodite gonad and germline defects.

The morphology of the hermaphrodite gonad was abnormal, the proximal part was often grown with extra curves which caused the distal tip cell not to be located in its normal position, the gonad was constricted in the middle of the proximal part, and the uterus appeared smaller than the normal uterus.

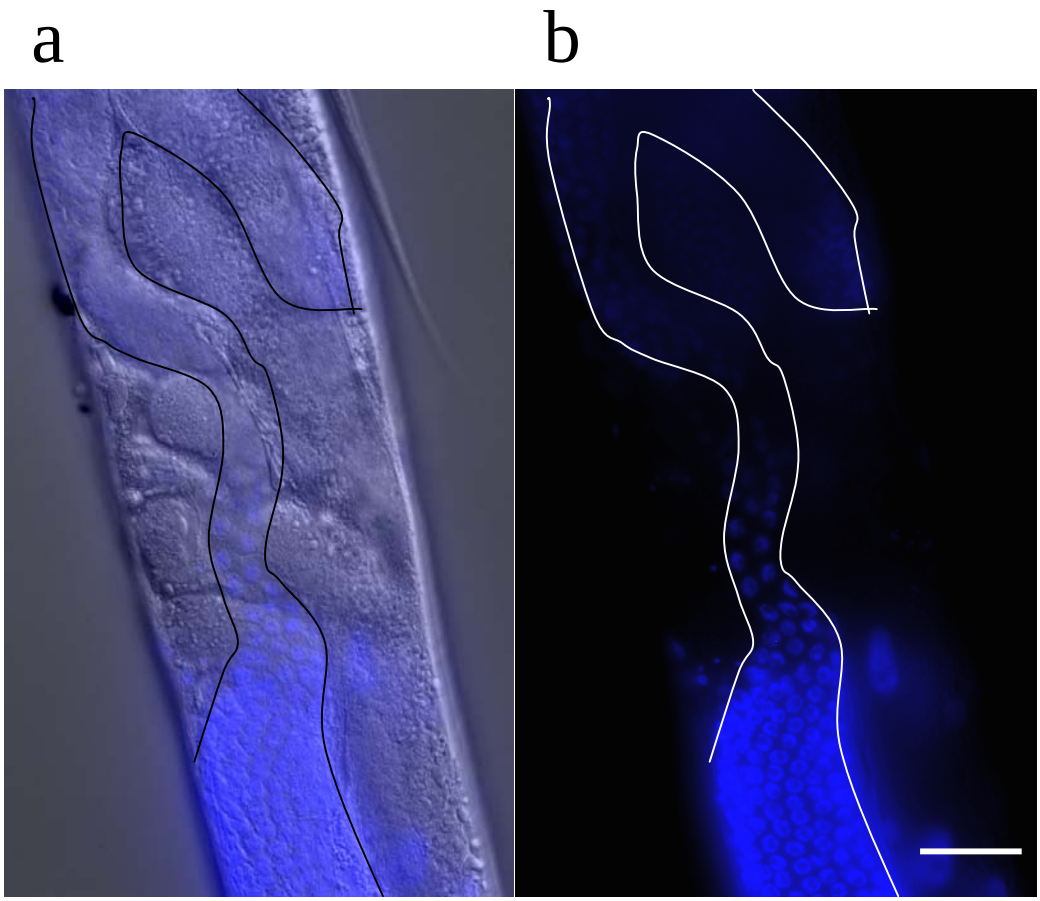

Fig. 3.23: The constricted gonad of a *him-8* hermaphrodite microinjected with *hmg-1.1* dsRNA. (a) the hermaphrodite gonad stained with DAPI staining. (b) The overlaying of the DAPI staining and the Nomarski-DIC micrographs. The scale bar is 25 µm.

The germline showed defects in the distribution and organization of its nuclei, some parts contained fewer nuclei than others, and the meiotic nuclei appeared in the area of the mitotic nuclei.

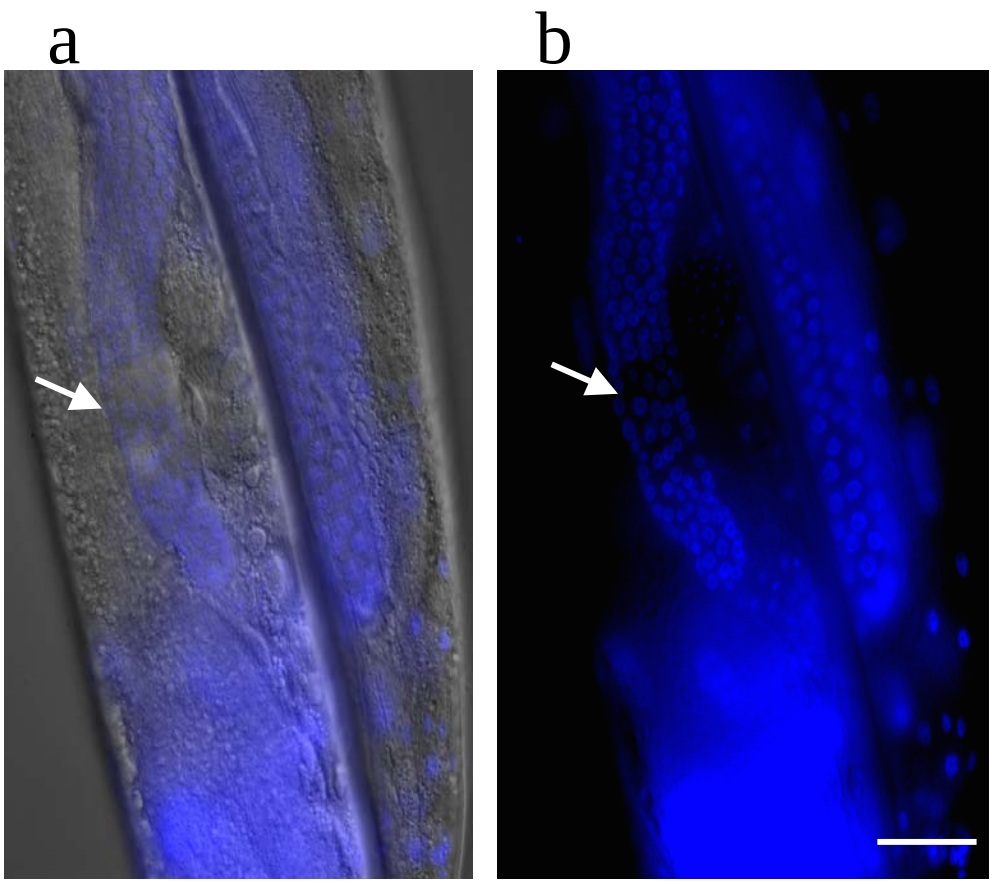

Fig. 3.24: The disorganized germline nuclei in the gonad of a *him-8* hermaphrodite microinjected with *hmg-1.1* dsRNA. (a) the hermaphrodite gonad stained with DAPI staining. (b) the overlaying of the DAPI staining and the Nomarski-DIC micrographs. The scale bar is 25 µm.

In rare cases, the germline showed an irregular distribution of mitotic nuclei, meiotic and oocytes (Fig. 3.25). This figure shows a *him-8* hermaphrodite gonad with an irregular shape and with an irregular order of the functional components of the germline. The distal tip cell was apoptotic beside at least one other cell. Some oocytes were totally dislocated in the proximal arm of the gonad and many germline nuclei were dislocated in area near to distal part of the spermatheca. The animal shown in Fig. 3.25 had also a clear malformation of the uterus and a protruding vulva (Fig. 3.26).

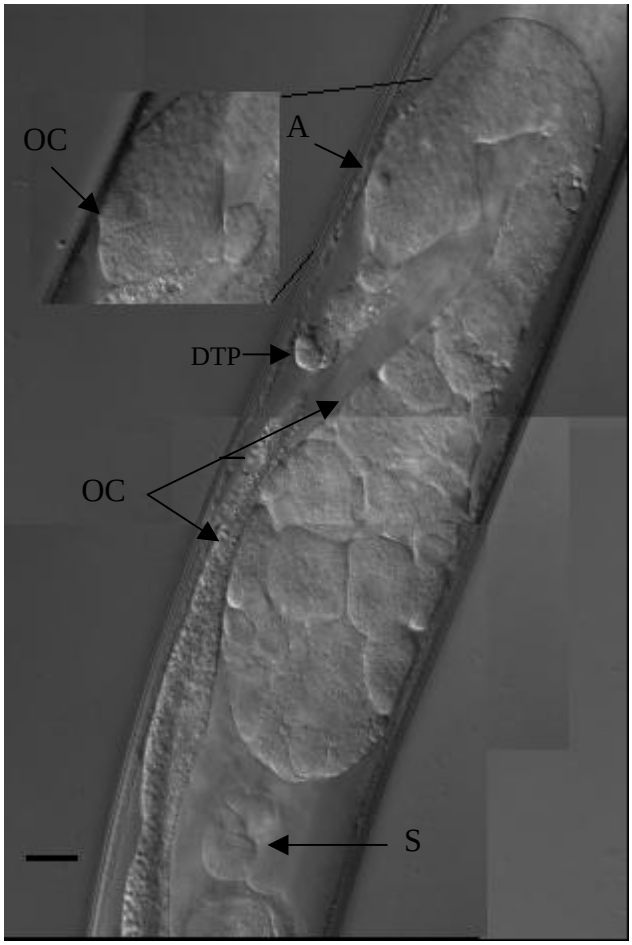

Fig. 3.25: The gonad and germline defects in a F1 hermaphrodite from *him-8* hermaphrodite that was microinjected with *hmg-1.1* dsRNA. The small view on the upper right side shows the distal part of the gonad with another focal plane. (DTP) points to the distal tip cell, (AP) apoptotic cell, (OC) oocytes, and (SP) spermatheca. The scale bar is 10 µm.

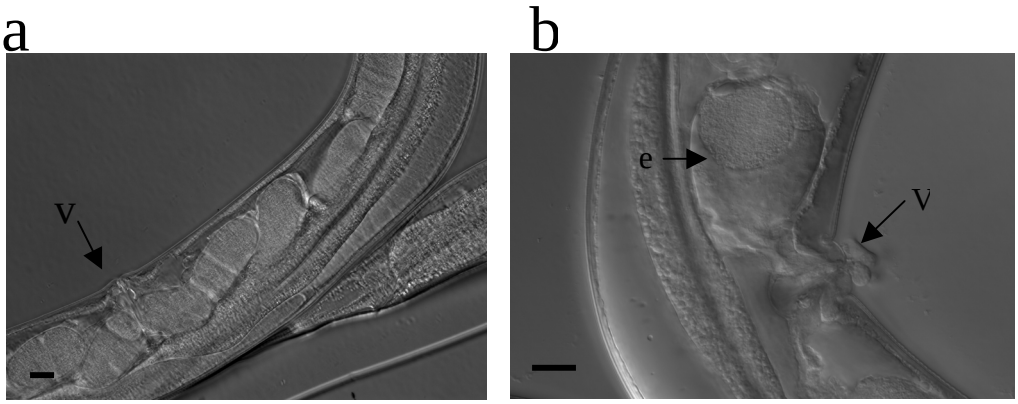

Fig. 3.26: Uterus of a *him-8* hermaphrodite microinjected with *hmg-1.1* dsRNA. (a) Control animal and (b) the RNAi treated animal. (e) Points to a single oocyte in the shrunken uterus and (V) the vulva opening. The scale bar is 10 µm.

3.2.1.1.3.2 Sex ratio of the *hmg-1.1* RNAi animals

This experiment was done by scoring the offspring of 10 hermaphrodites from RNAi animals and 10 hermaphrodites from the control animals. The early hermaphrodites from the F1 generation of *him-8* adults, which were fed with *hmg-1.1* dsRNA, and the control animals, were incubated individually and the sex ratio of their offspring (F2) was scored. In average, the male percentage was 41.3% (105 out of 245 animals) and 31.3% (117 out of 374 animals) in the RNAi animals and control animals, respectively.

Although the male percentage in RNAi animals was only 10% higher than in the control animals in the last experiment, the male percentage resulted from *hmg-1.1* dsRNA microinjection in a separate experiment showed a higher percentage. The F1 animals were categorized based on the number of their offspring. The male percentage of 5 F1 hermaphrodites laid less than 50 eggs, produced very high male percentage. After 1, 2, and 5 days from the starting time of laying eggs, the male percentages were 23% (3 males out of 13 animals), 75% (9 males out of 12 animals), and 81% (9 males out of 11 males), respectively.

These percentages were compared with the percentage of males produced by F1 of wild type animals that were microinjected with *hmg-12* dsRNA. The male percentage was 3.8% (2 males out of 53 animals).

3.2.1.1.3.3 The effect of *hmg-1.1* dsRNA microinjection on male fertility

After the microinjection of *him-8* hermaphrodites with *hmg-1.1*, the fertility of offspring males, which were laid 24-36h after microinjection, was tested. The percentage of the males that were able to make a sexual reproduction was calculated as a test for the fertility of these males. Each one of these males was incubated with two N2 hermaphrodites on NGM agar plates supplemented with a small spot of OP50 bacteria and the same was done with *him-8* males from the control trait.

The males were previously checked for their ability to sense the bacterial food and RNAi animals did not show significant difference (Table 3.1). No considerable difference between the RNAi males' fertility 50% (5 out out of 10 males) and the control animals' fertility 60% (6 out of 10 males) was detected.

3.2.1.5 Effect of stresses on the *hmg-1.1* dsRNA fed animals

3.2.1.1.5.1 Effect of the starvation stress on the *hmg-1.1* dsRNA fed animals

The collective scoring method was used in this experiment. This experiment was done to measure if the *hmg-1.1* dsRNA treated L1 larvae have the same capability to tolerate the starvation stress comparing with the control animals. The results showed that the *hmg-1.1* RNAi treated animals were more susceptible to starvation stress than the control animals. Higher percentages of *hmg-1.1* RNAi treated animals died much earlier in the control trait than the respective control animals (Fig. 3.27). The average number of larvae that were counted in each count was (50 larvae).

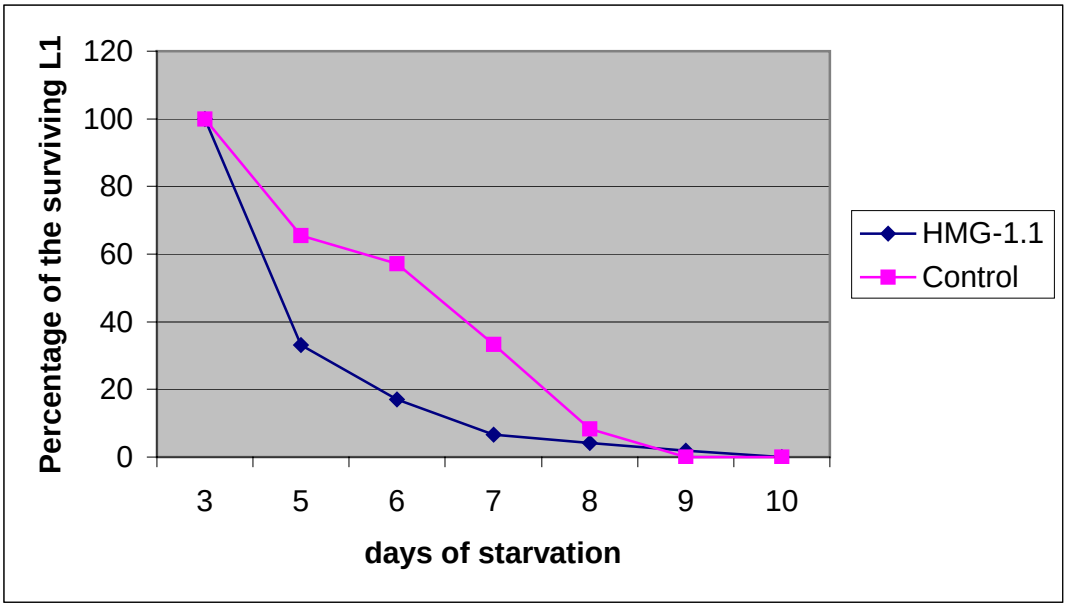

Fig. 3.27: Starvation effect on wild type L1 larvae fed with *hmg-1.1* dsRNA. X-axis is the days of starvation and Y-axis is the percentage of the surviving L1. The control animals are in red and the *hmg-1.1* dsRNA fed animals are in blue.

To prove that the effect of starvation stress, which was resulted from feeding of N2 animals with *hmg-1.1* dsRNA, was a specific effect of *hmg-1.1* dsRNA feeding, N2 animals were fed with two other dsRNA separately, *hmg-11* dsRNA and *hmg-12* dsRNA. The results of this experiment showed that only the starved *hmg-1.1* RNAi L1 larvae died earlier than the control animals.

The animals from the feeding of the other two dsRNA were less sensitive to the starvation stress than the control animals. It was astonishing that the L1 that were fed with *hmg-11* showed a higher tolerance to starvation stress than the control animals.

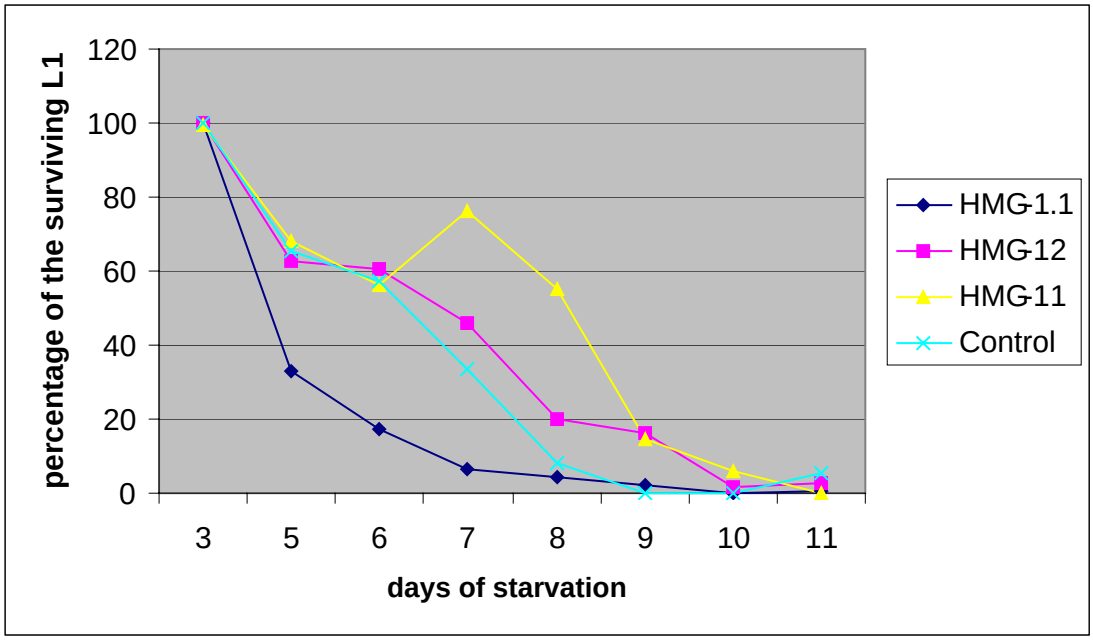

Fig. 3.28: Comparison between the starvation effect on wild type L1 stage larvae after the depletion of their HMG-1.1, HMG-11, or HMG-12 by feeding protocol. X-axis is the days of starvation and Y-axis is the percentage of the surviving L1.

From the figure 3.28, it can be observed that day 5 of starvation is a critical day when a big difference between the percentage of surviving L1 larvae in *hmg-1.1* RNAi and control traits occurred. At the same time, a reasonable percentage of animals were still alive in both traits could still be scored. So, some surviving larvae from the day 5 of starvation were selected from both traits and inspected by Nomarski-DIC. Severe necrotic-like structures were observed in all RNAi larvae (n=20), mainly posterior to the pharynx till slightly posterior to the vulva. These necrotic like structures were not observed in L1 control larvae (n=20) (Fig. 3.29).

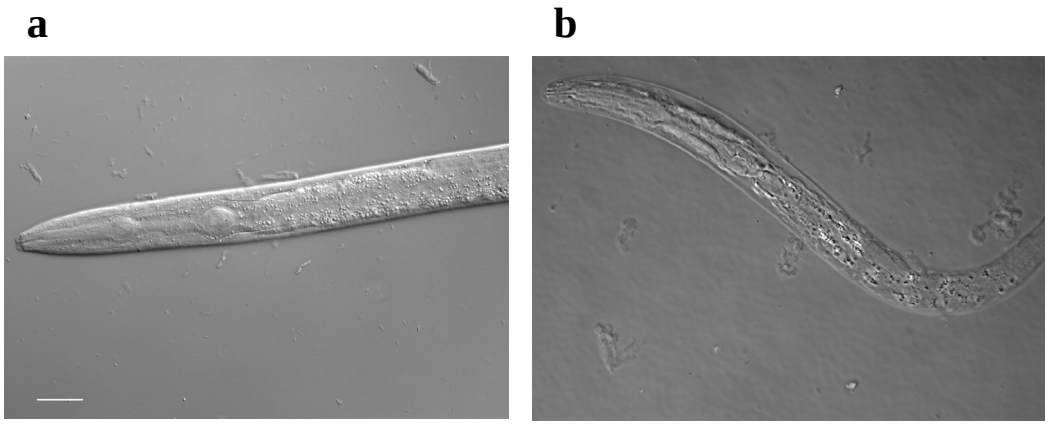

Fig. 3.29: Effect of 5 days of starvation on the *hmg-1.1* dsRNAi L1 larvae. a) Illustrates control L1 larvae. b) Illustrates *hmg-1.1* dsRNA treated L1 larvae. The scale bar in (a) is 25 µm

3.2.1.5.2 Effect of heat shock on the *hmg-1.1* dsRNA fed animals

After trying different temperatures ranging between 30-40°C, applying 35°C for 8 hours was the best combination of temperature and time to be used. This experiment was done to test the ability of the dsRNA treated wild type L1 larvae to stay alive under heat shock conditions in comparison with L1 control larvae.

Under the previously mentioned conditions 95% (38 out of 40 animals) of the RNAi animals died, which was a much higher percentage than the percentage of dead animals in the control trait 60% (30 out of 50 animals). These results showed that the RNAi animals had a lower resistance to heat shock conditions.

3.2.1.5.3 Effect of the *hmg-1.1* dsRNA feeding on the brood size of N2

Wild type animals were fed with *hmg-1.1* dsRNA and the brood size of 23 animals of their F1 was measured and compared with the control animals. It appeared that their brood size is smaller than the brood size of the control animals.

The brood size of each animal was categorized based on the total number of laid eggs. The percentages of adults in each category from both traits were calculated. As shown in Fig. 3.30, the X-axis shows the categories, each category is expressing a range of 50 eggs, and the Y-axis is showing the percentage of animals that belong to each category.

The number of animals examined in each trait was 23 animals, which were individually incubated and transferred to new plates every 2 days. Most of the animals laid eggs on the first and second plates only, and the rest laid eggs up to the fifth plates.

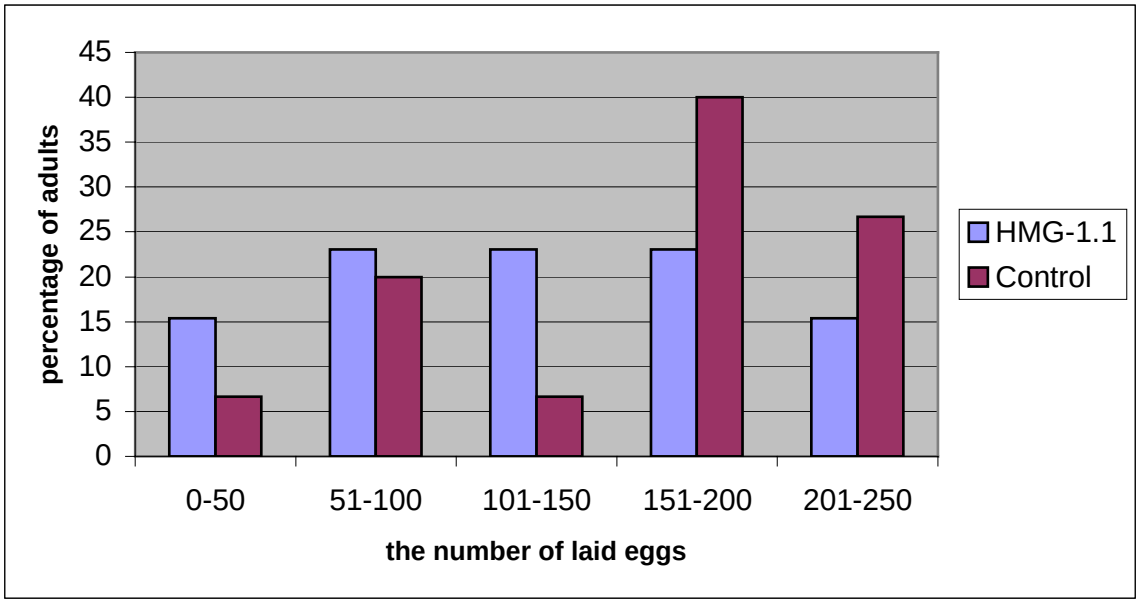

Fig. 3.30: A brood size histogram of wild type hermaphrodites postembryonically feed with *hmg-1.1* dsRNA and control animals. The X-axis shows the categories of the total number of laid eggs, and the Y-axis shows the percentage of hermaphrodites that belong to each category (n=23).

To learn more about the distribution of the egg production, the number of eggs, which were laid onto first and second plates, were separately calculated and shown in Fig. 3.31.

It appeared that the percentage of the RNAi animals that laid onto first plates a number of eggs (ranging between 0-50 eggs) onto the first plates was much higher than the percentage of the control animals belonging to the same category. RNAi animals scored as well a smaller percentage in 51-100 egg and 101-150 egg categories, and a slightly higher percentage than the control animals in the last category (151-200 egg).

The percentages from the second RNAi animals' plates were much higher than the percentages from the control animals' plates in the first category. Then, it changed to a much smaller percentage of animals than the percentage scored from the control

animals. No RNAi animals laid eggs on the second plates that belong to the third or fourth category, however, control animals continued to score percentages of animals till the third category (Fig. 3.31).

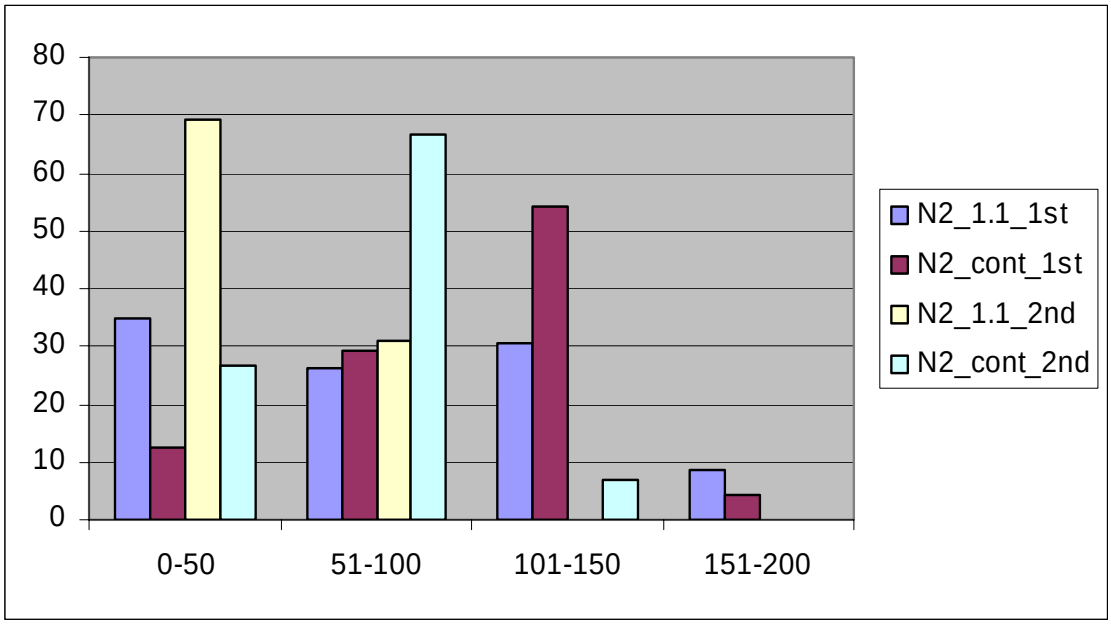

Fig. 3.31: Comparison between the percentages of hermaphrodites that laid a certain number of eggs in RNAi animals and control animals onto the first and second plates. The X-axis shows the laid-egg categories, and Y-axis shows the percentage of animals that belong to each category (n=25).

The germline of the hermaphrodites that laid a small number of eggs in the last experiments was analyzed by DAPI staining. This staining showed that there were many defects in the germline. It showed oocytes with 7 chromosome pairs; normal oocytes have 6 chromosome pairs (Fig. 3.32).

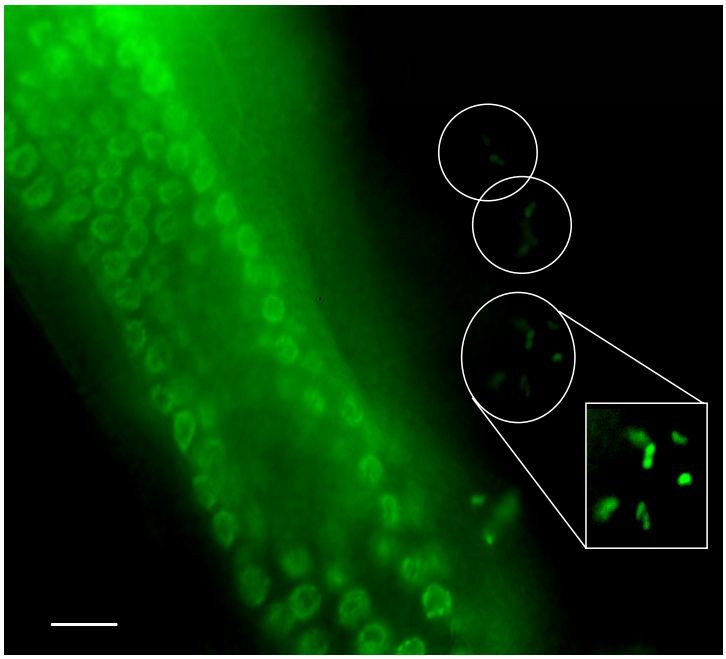

Fig. 3.32: The effect of *hmg-1.1* dsRNA microinjection on the number of chromosomes in oocytes. This micrograph shows DNA staining with DAPI recorded with the green channel. The oval and circular shapes show oocytes and the rectangle illustrates a magnification of an oocyte containing 7 chromosome pairs. Scale bar is 25 µm.

It was observed in some wild type hermaphrodites that they contain oocytes that have much higher amount of DNA than normal. These oocytes are in different stages of having endomitotic activity (Fig. 3.33). It can be observed as well that the distribution of the nuclei near to the distal part of the germline is not the same everywhere, i.e. a higher content of the germline nuclei can be observed in the area that was marked (m) in Fig. 3.33.

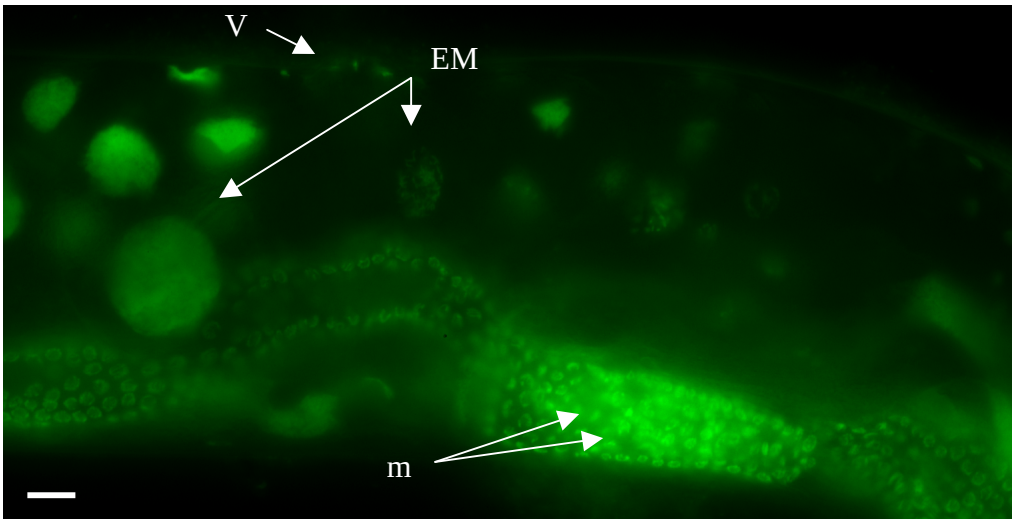

Fig. 3.33: The effect of *hmg-1.1* dsRNA microinjection on the DNA content in oocytes. (m) shows a part of the germline that have a higher content of nuclei than its surrounding area. (EM) stands for endomitotic oocytes. (V) vulva. This micrograph shows DNA staining with DAPI recorded with the green channel. Scale bar is 25 µm.

3.1.1.3 Phenotypes that resulted from microinjection

The microinjection was done with *hmg-1.1* dsRNA (3 µg/µl) in the gonads of L4 larvae or young adults. The results were scored on F1 animals that were laid 12-36 hours after the time of the microinjection.

3.1.1.4 Phenotypes that resulted from the microinjection of *him-8*

3.1.1.4.1 Male defects

him-8 Hermaphrodites were microinjected with *hmg-1.1* dsRNA and a number of their F1 males was taken to check for their fertility. These *him-8* males (n=10) were left to mate wild type hermaphrodites. Each male was incubated with 3 hermaphrodites for 3 days at 20°C on NGM agar plates supplemented with a small spot of OP50. The observation of F1 animals on these plates showed no males which shows that these males did not succeed in having a sexual reproduction with the wild type hermaphrodites. The observation of F1 animals on the mating plates of the control males showed that 50% (5 out of 10 plates) of these plates had 30-50% pf males.

The microscopic observation of the non-mating *hmg-1.1* RNAi animals morphology showed that in 40% (4 out of 10 males) of these males the sperms were trapped behind an area of necrotic-like structures inside the male gonad near to the end of the

male tail. This might be the reason to hinder the sperm from completing its way outside the male gonad (Fig. 3.34).

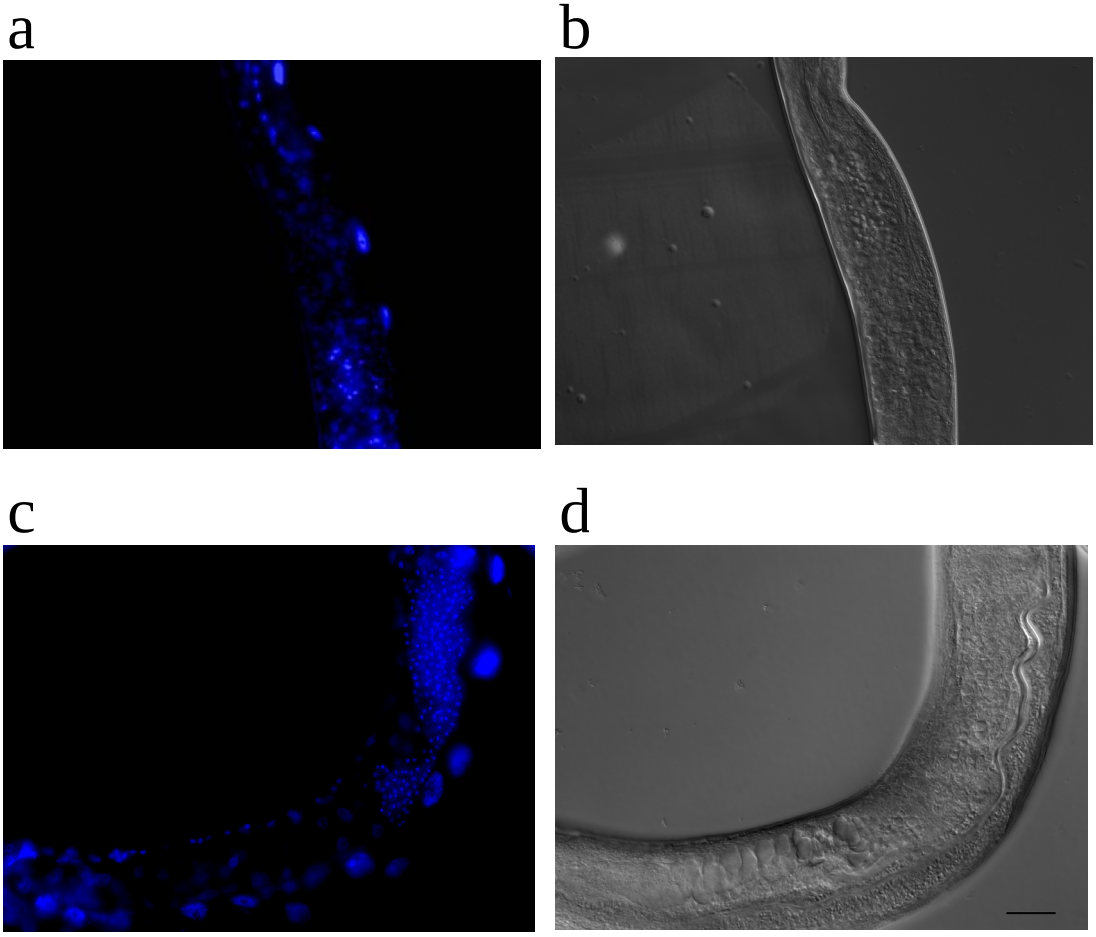

Fig. 3.34: The morphology of infertile *him-8* males treated with *hmg-1.1* dsRNA. (a,b) show the DAPI staining and the Nomarski picture of the male-tail morphology in a control male, respectively, the posterior part is up, with a scale bar of 10 µm. (c,d) the DAPI staining and the Nomarski-DIC micrograph of the male-tail morphology in a *hmg-1.1* dsRNA-treated male, respectively, the posterior part is at the left side, with a scale bar of 5 µm. The arrows in c) and d) mark the border of the area of the necrotic-like structures with no sperm in it. The sperm are mainly crowded on the sides of this region. The arrows in a) and b) show the equivalent area bordered in c) and d) with no necrotic-like strucures and with a presence of distributed sperm in it.

3.2.1.5 The relationship between *hmg-1.1* and necrosis

Several mutants of genes that play different roles in the necrotic death pathway were fed with *hmg-1.1* dsRNA to check whether the scored necrotic-like phenotype has a relationship to the necrotic pathway. The strains ZB1029 and ZB1028 are mutants of calreticulin (*crt-1).* CRT-1 as a Ca^{2+} binding protein is known to have many cellular functions including regulation of Ca^{2+} homoeostasis and chaperone activity. The *crt-1* mutant lack necrotic cell death, which therefore is thought to require the function of calreticulin and regulators of Ca^{2+} release from the endoplasmic reticulum (ER) (Xu; et al. 2001).

Feeding *crt-1* mutants showed no necrotic like structures in the body of the animals (Fig. 3.35). Generally, the *crt-1* RNAi animals were much healthier than N2 RNAi animals.

In order to examine whether HMG-1.1 depletion caused necrosis by increasing the release of Ca^{2+} from the ER by inositol-1,4,5-triphosphate receptor (InsP3R), animals from *itr-1*(sa73) mutant, a strain that lacks the InsP3R activity, was used. The animals from *itr-1*(sa73) mutant were microinjected with *hmg-1.1* dsRNA and their F1 was scored. The *hmg-1.1* RNAi caused necrotic cell death in the *itr-1* (sa73) mutant background.

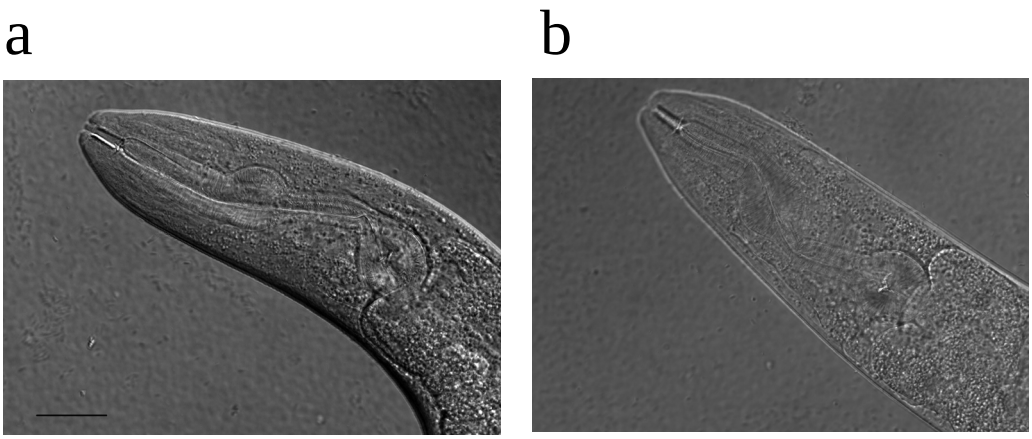

Fig 3.35: Effect of *hmg-1.1* dsRNA feeding on a *crt-1* mutant strain (ZB1029). (a) Head of RNAi adult. (b) Head of control adult. The scale bar in (a) is 10 µm.

3.2.1.5.1 The effect of L1 starvation stress on *crt-1* strain

This experiment was done using the collective scoring method. The target of this experiment was to examine whether the weakness of *hmg-1.1* RNAi animals of N2 strain resulted from general weakness out of having the necrotic-like structures in their bodies. The results showed that weakness of *hmg-1.1* RNAi animals under the conditions of starvation stress was still to be scored in the L1 of *crt-1* strain that were fed with *hmg-1.1* dsRNA (Fig. 3.36).

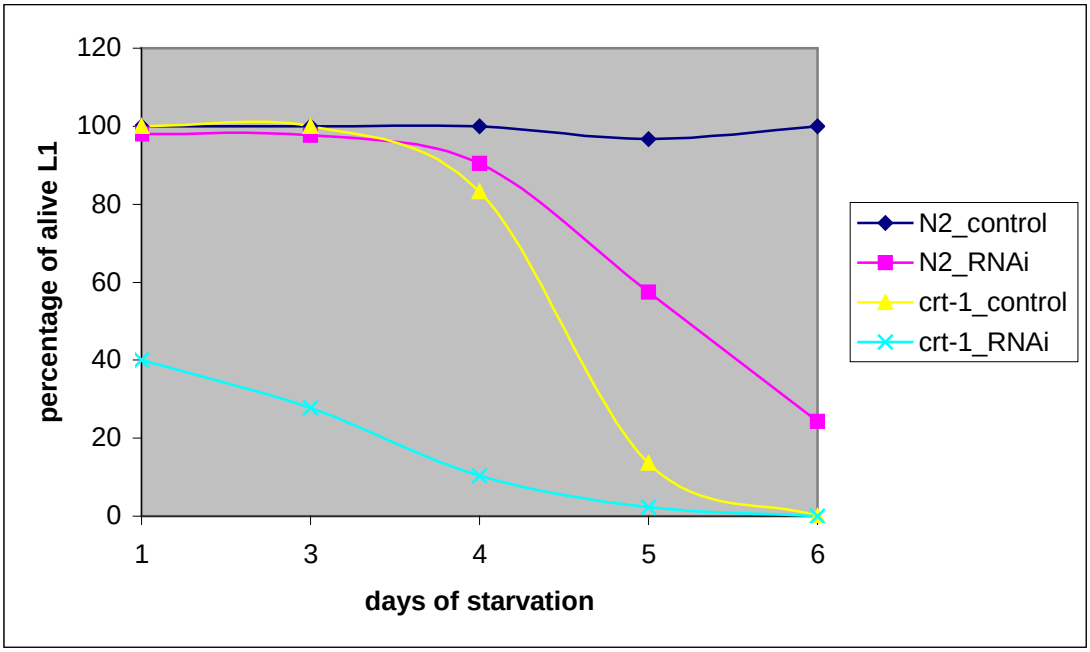

Fig 3.36: Starvation effect on *hmg-1.1* RNAi wild type strain and *crt-1* mutant L1 larvae. X-axis shows the days of starvation and Y-axis shows the percentage of surviving L1 Larvae.

cep-1 is the only homologue in *C. elegans* for *p53* in humans. To investigate a possible relationship between *hmg-1.1* and *cep-1*, HMG-1.1 was depleted in a *cep-1* mutant background by *hmg-1.1* dsRNA feeding. After 7 days of L1 larvae starvation, the scored death percentage in the control animals was 12 % (10 out of 84 animals). However, it was 28% (21 out of 75 animals) in the HMG-1.1 depleted animals, which showed an enhancement of the starvation effect after feeding with the *hmg-1.1* dsRNA.

3.2.1.5.2 The effect of *hmg-1.1* dsRNA feeding on the defecation period of N2 and *crt-1* adults

Adults from both strains, N2 and *crt-1*, were tested for changes in their defecation period with *hmg-1.1* dsRNA feeding in comparison with control animals from both strains. The results showed that the defecation period in both strains was decreased in *hmg-1.1* dsRNA fed animals in comparison with control animals.

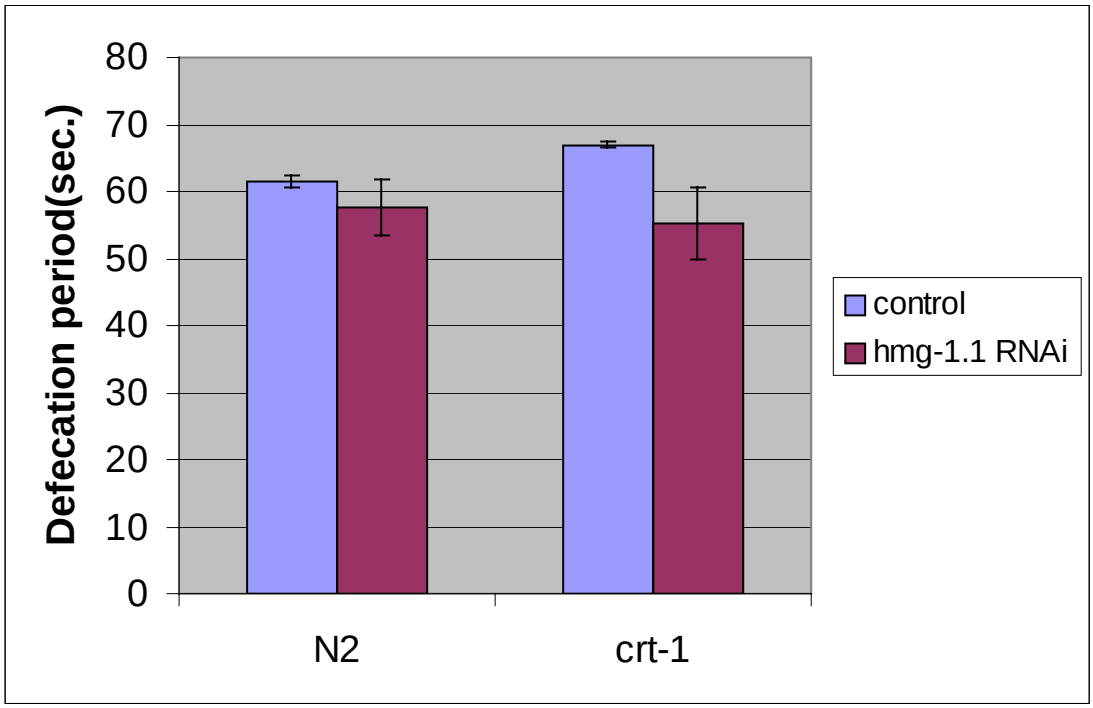

Fig. 3.37: The effect on the defecation period of N2 and *crt-1* (ZB1029) adults after feeding with *hmg-1.1* dsRNA. Y-axis shows the defecation period in seconds (n=10 from each trait).

3.2.1.5.3 The effect of the *hmg-1.1* dsRNA feeding on strains from the necrotic death pathway

Different strains from the necrotic pathway, which is shown in Fig. 4.2, were checked for the presence of the necrotic-like structures in their bodies after feeding with *hmg-1.1* dsRNA. The results showed that the necrotic-like structures were still visible in *hmg-1.1* dsRNA fed adults of *ced-5*, *ced-2*, *ced-6*, and *ced-7* (n=10 adults from each strain). The control animals of these strains showed no necrotic-like structures. Table 3.1 shows these results and the results of feeding of the *crt-1* and *itr-1* mutants that affect the necrotic cell death process.

Table 3.1: The effect of the feeding with the dsRNA of *hmg-1.1* on mutants that affect the necrotic cell death process.

	Control	***hmg-1.1* RNAi**
lin-33	Normal	Vacuolated
ced-1	Normal	Vacuolated
ced-2	Normal	Vacuolated
ced-5	Normal	Vacuolated + gonad defect
ced-6	Normal	Vacuolated
ced-7	Small vacuoles	Vacuolated
nuc-1	Normal	Vacuolated
itr-1	Normal	Vacuolated
***crt-1* (ZB1029)**	Normal	Normal
***crt-1* (ZB1028)**	Normal	Normal

3.2.1.6 studying the relationship between *hmg-1.1* and apoptosis

It was important to investigate the link between apoptosis and the phenotypes resulting from *hmg-1.1* dsRNA feeding. This was done by testing the presence of different phenotypes after feeding mutants that belong to the programmed cell death pathway with *hmg-1.1* dsRNA.

3.2.1.6.1 The effect of starvation stress on a *ced-3* mutant fed with *hmg-1.1* dsRNA

This experiment was done to check whether the effect of the starvation that was scored with the *hmg-1.1* RNAi animals have a relationship with apoptosis. Synchronized cultures of L1 larvae that had *hmg-1.1* RNAi effect from dsRNA feeding were used. The effect of starvation on these L1 larvae was compared with the resulting starvation effect on the control *ced-3* L1 larvae. The results from the *ced-3* traits were compared with the results of N2 traits for synchronized *hmg-1.1* dsRNA treated and control L1 larvae, respectively (Fig 3.38).

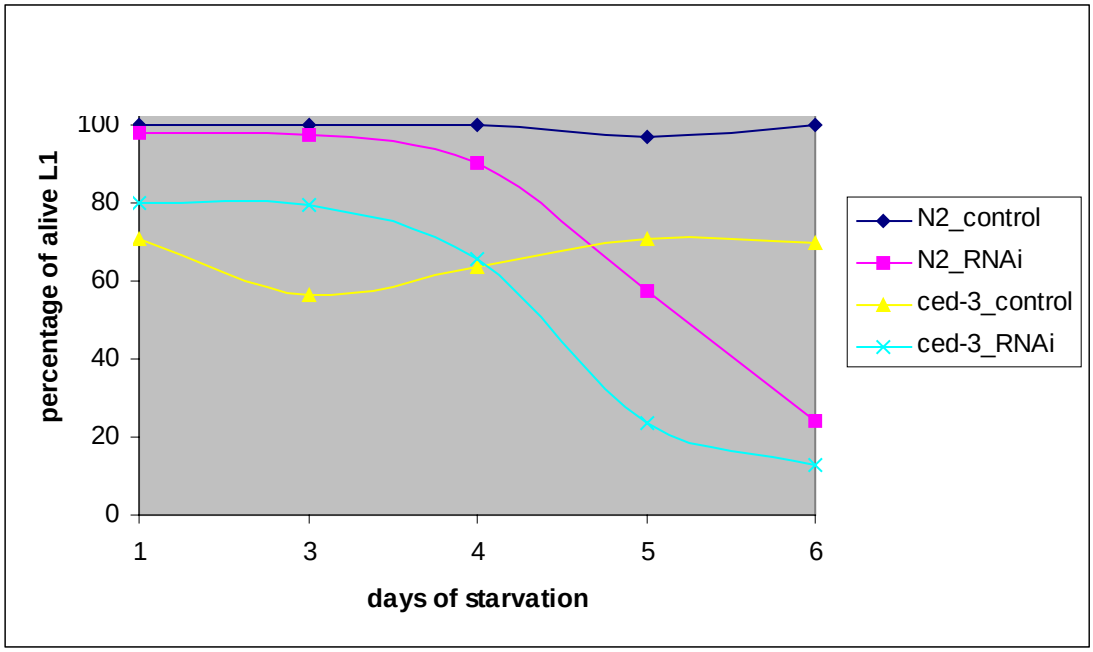

Fig 3.38: The starvation effect on *hmg-1.1* RNAi L1 larvae of N2 and a *ced-3* mutant. X-axis shows the days of starvation and Y-axis shows the percentage of L1 larvae that were still alive.

3.2.1.6.2 Effect of the *hmg-1.1* dsRNA feeding on mutants of the programmed cell death pathway

Different strains that have mutations in one of the genes that belong to the programmed cell death pathway were fed with *hmg-1.1* dsRNA. The target of this experiment was to test the link between the apoptotic death and the function of *hmg-1.1*. The RNAi fed animals were checked for the presence of cells that showed ongoing apoptosis by acridine orange staining. From each strain 10-20 worms were checked under the microscope.

To examine the possibility that the depletion of HMG-1.1 can initiate apoptotic cell death in the absence of caspase activity, a strain that lack caspase dependent apoptosis (*ced-3* mutant) was fed with *hmg-1.1* dsRNA. The results showed that the *ced-3* mutant fed with *hmg-1.1* dsRNA had healthy hermaphrodite gonads and had very few apoptotic cells (<2) in the gonad. The control animals had (Fig. 3.39). In Fig. 3.39, only one cell in the gonad showed apoptosis. There were vacuoles in the body of the RNAi animals, which were less severe in comparison with the severity in HMG-1.1 depleted wild type animals.

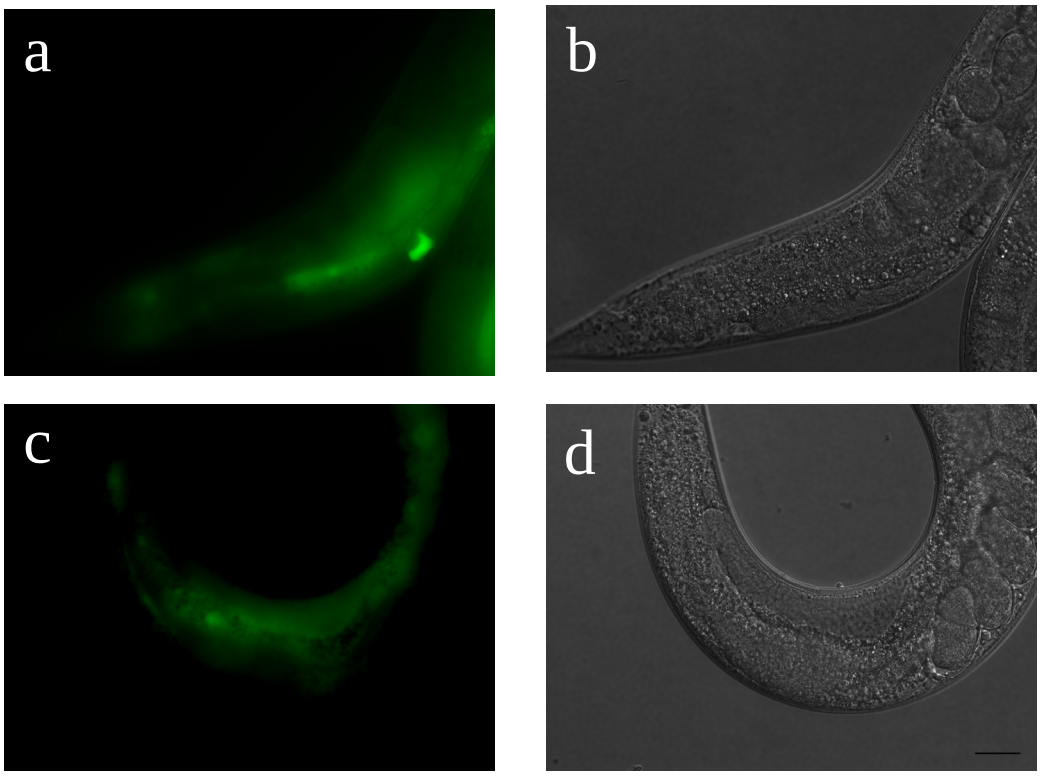

Fig. 3.39: The effect of *hmg-1.1* dsRNA feeding on *ced-3* mutant. (a) and (b) are the micrographs of RNAi animals. (c) and (d) are control animals. (a) and (c) are micrographs of acridine orange staining visualized by the fluorescence microscope. (b) and (d) shows the same animals visualized by Nomarski-DIC optics. The scale bar in (d) is 50 µm and in (b) 25 µm.

Feeding the *nuc-1* strain animals with *hmg-1.1* dsRNA resulted in a severe malformation of the germline and gonad. The HMG-1.1 depleted animals had much more cells had apoptotic activity than the control animals. Also, the HMG-1.1 depleted animals had many eggs in late developmental stages, which shows that these animals had an egg-laying defect. The control animals had healthy gonads (Fig. 3.40).

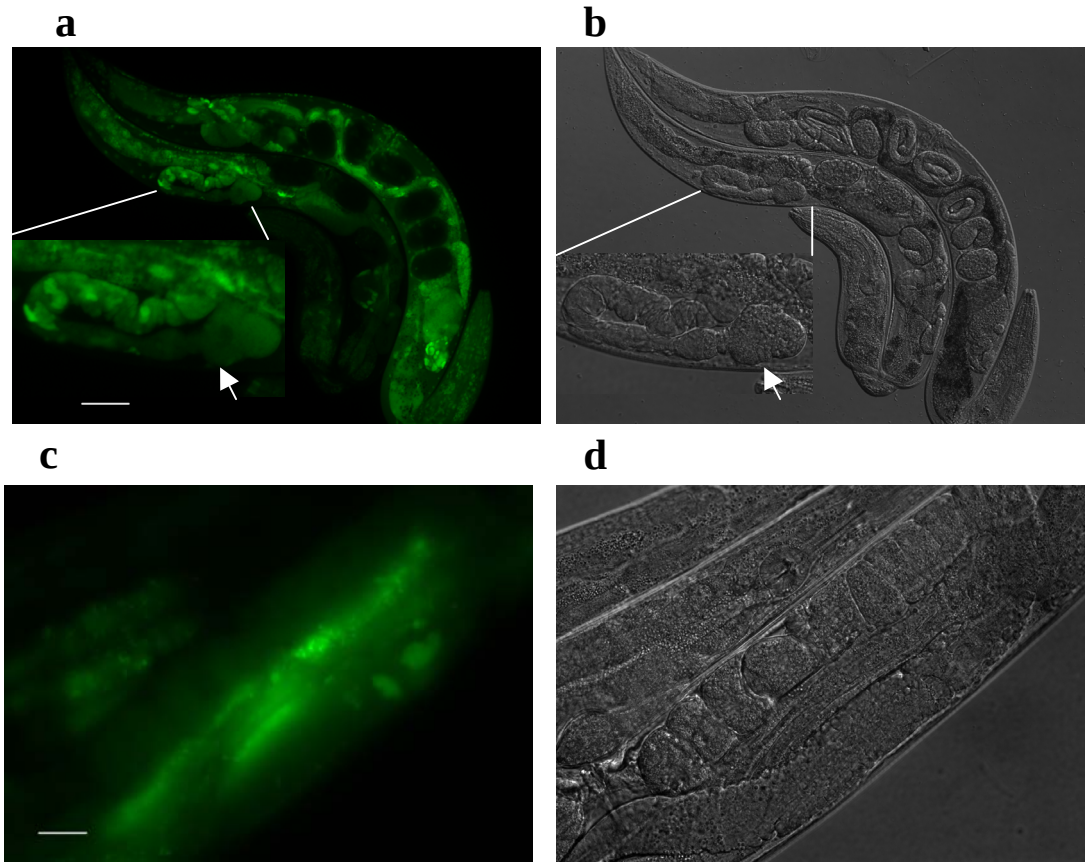

Fig. 3.40: The effect of *hmg-1.1* dsRNA feeding on *nuc-1* strain. (a) and (b) are the photos of RNAi animals. (c) and (d) are control animals. (a) and (c) are photos of acridine orange staining visualized by the fluorescence microscope. (b) and (d) shows the same animals visualized by Nomarski optics. The small windows in (a) and (b) are magnifications of the gonad in each photo and the arrows show an oocyte near the distal tip cell. The scale bar in (a) is 50 µm and in (b) 25 µm.

3.2.2 Expression pattern of *hmg-1.1* in the strain EC715

3.2.2.1 *hmg-1.1::gfp* expression in the embryos

The expression of *hmg-1.1::gfp* in embryonic development started at the two cell stage embryos (Fig. 3.41). The expression continued in most if not all of the cells through the developmental stages of the embryo till hatching.

The observation of the *hmg-1.1::gfp* expression in EC715 by LSM microscopy showed that the *hmg-1.1* expression is not stable through the cell cycle in the embryo (Fig. 3.41).

The fluorescence was seen in the nuclei beside a very slight fluorescence in the cytoplasm. The expression continued during the prophase, and it disappeared in the prometaphase in the early divisions.

To make sure that these observations were not the result of losing the focus of the nuclei during cell divisions, the focal plane was previously adjusted to have the nucleus focused before shooting any micrograph, which can be observed in the Nomarski-DIC micrograph (Fig. 3.41).

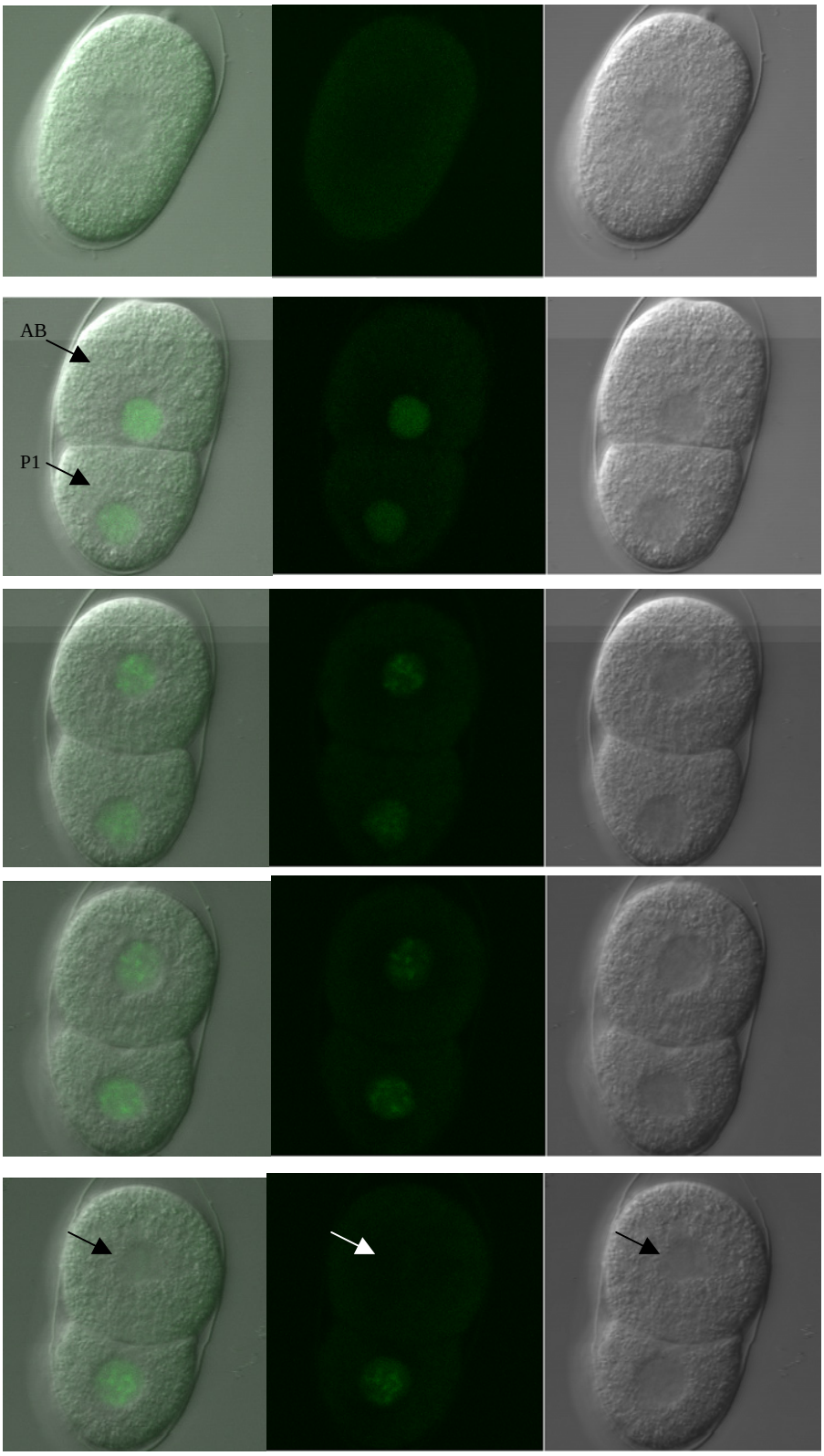

Fig. 3.41: The expression of *hmg-1.1*::*gfp* through the cell cycle. The arrow points to the nucleus that didn't show *hmg-1.1::gfp* expression.

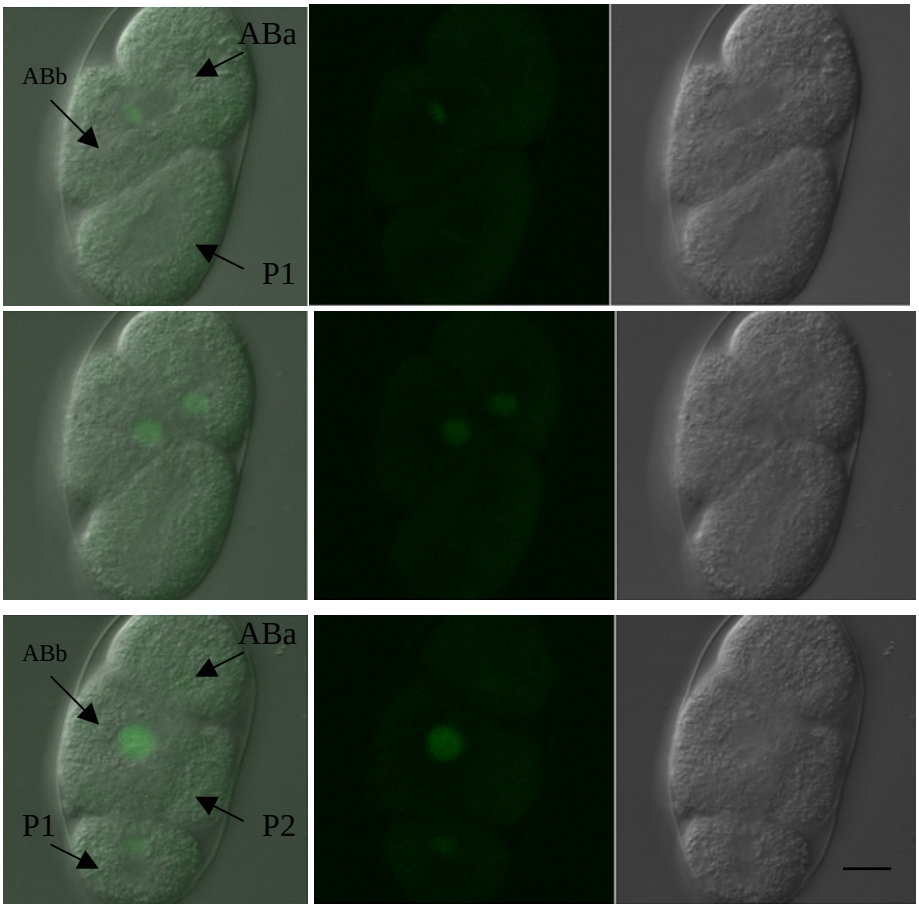

Fig. 3.41 (cont.): The photos show the reappearance of the *hmg-1.1::gfp* through the cell cycle. The scale bar is 5 µm.

The early nuclear embryonic expression of *pie-1::gfp* in AZ212 was observed with LSM microscopy. This observation gave the chance to see whether the disappearing of the fluorescence in EC715 was specific to the *hmg-1.1* expression or if it was just an artefact resulting from the fading of GFP. The fluorescence was scored in all mitotic stages in all cells, starting from 1-cell stage (P0) till 3-cell stage (P1, ABa and ABb) (Fig. 3.42).

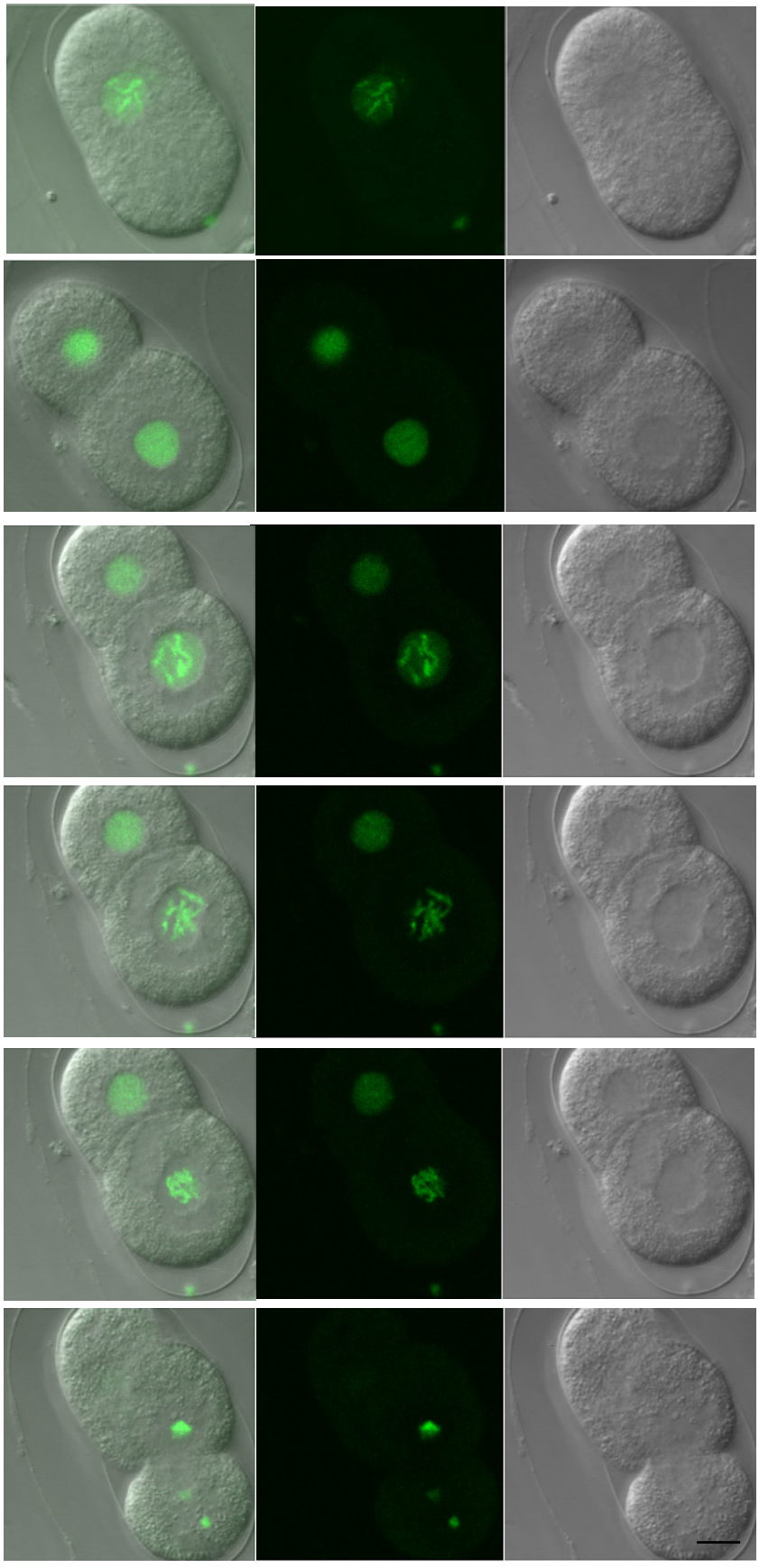

Fig. 3.42: The expression of *pie-1::gfp* (AZ212 strain) in the cell cycle of the first and second cleavages of the embryonic development. The scale bar is 5 µm.

The expression pattern of *hmg-1.1::gfp* was followed throughout the embryonic development. The figure 3.43 illustrates the abundant expression of *hmg-1.1::gfp* in most if not all of the cells.

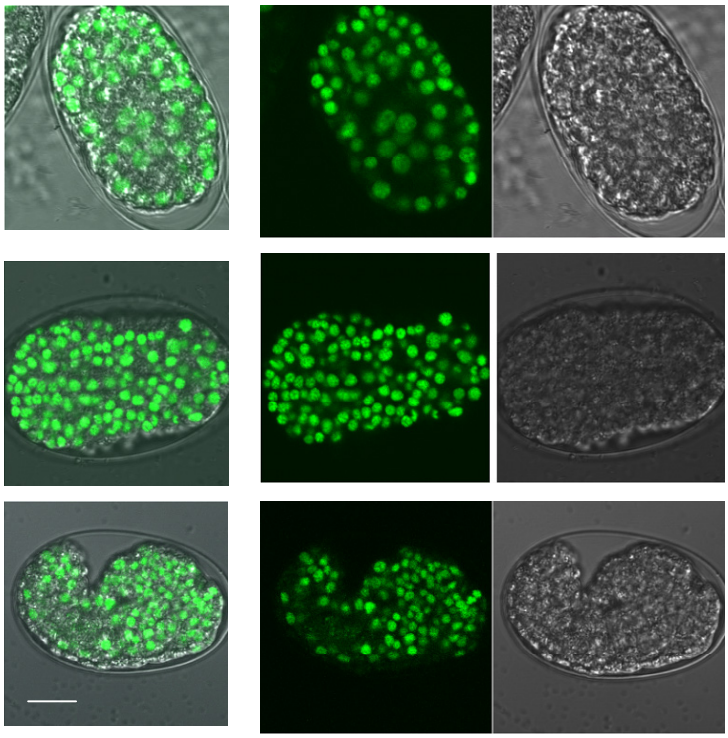

Fig 3.43: The *hmg-1.1::gfp* expression pattern in different developmental stages of embryos. The scale par is 5 µm

3.2.2.2 The *hmg-1.1::gfp* expression in the larval stages

The *hmg-1.1::gfp* expression was evident in L1 larvae in all cells (Fig. 3.44). This abundant expression was noticed in all somatic cells of the animals, but not in the germline, through the different developmental stages till it reached L4 stage.

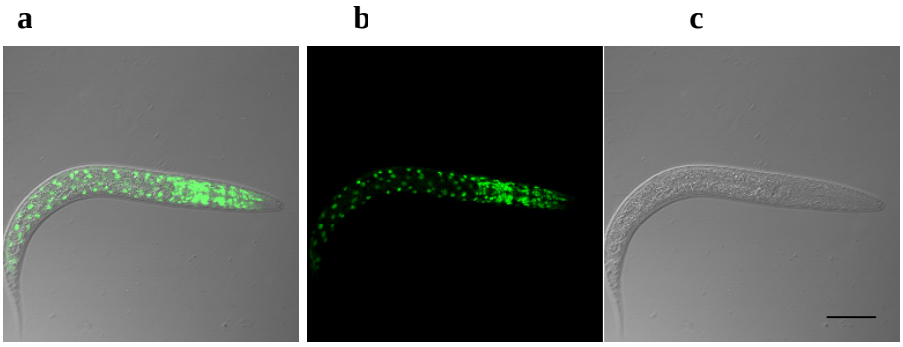

Fig. 3.44: The expression pattern of *hmg-1.1::gfp* in L1 larvae. a) is the overlaying of the fluorescence and Nomarski-DIC, b) is the fluorescence observation, and (c) is the Nomarski-DIC observation.

3.2.2.3 The *hmg-1.1::gfp* expression in the adults

The observation of the expression of the *hmg-1.1::gfp* was inspected through the developmental stages of the animals until the adult stage. The same abundant expression pattern was observed in the adult animals. Furthermore, the protein was expressed in the nuclei of the somatic cells of the spermatheca and in all nuclei of the oocytes in the germline (Fig. 3.45).

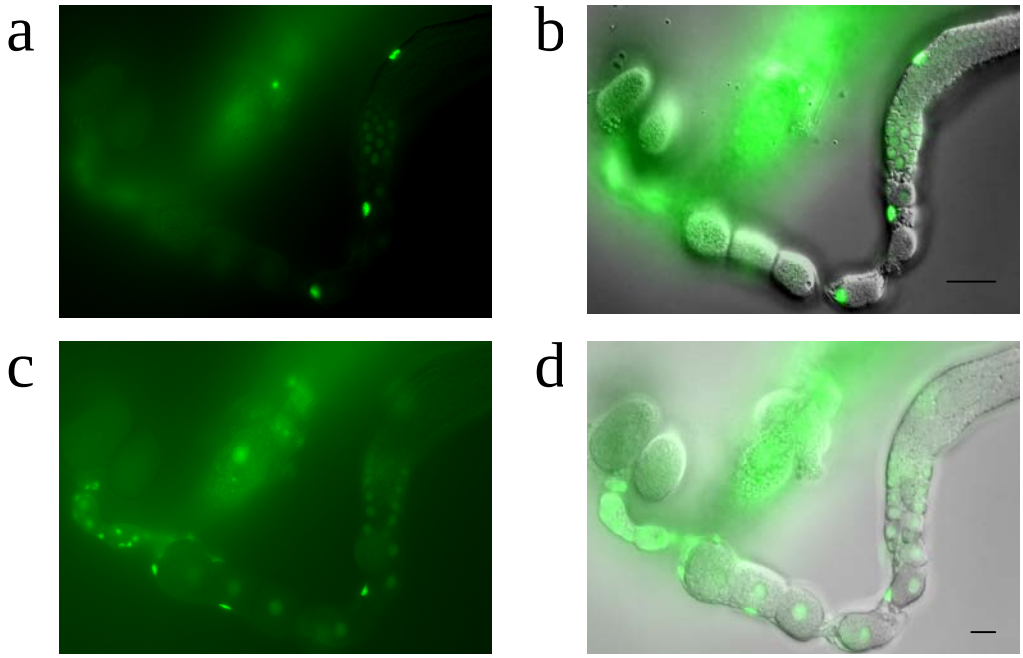

Fig. 3.45: The expression of *hmg-1.1::gfp* in the adult germline. b) and d) show the overlaying of *hmg-1.1::gfp* fluorescence a) and c) show the corresponding Nomarski-DIC. photomicrographs. The scale bar is 10 µm.

3.2.3 Effect of overexpression on the embryonic lethality

A high percentage of embryonic lethality was scored in the EC715 strain. The percentage of the dead embryos was in average 42% (109 out of 260). The percentage of the dead embryos, after feeding with *hmg-1.1* dsRNA was 26% (64 out of 245 animals).

3.2.4 Depletion of the expression in *hmg-1.1::gfp* using RNAi

The feeding of EC715 strain with the *hmg-1.1* dsRNA showed no cells that lost the expression of *hmg-1.1* but only that some of the animals had the *hmg-1.1*-gfp expression less bright than it in the control animals (Fig. 3.46).

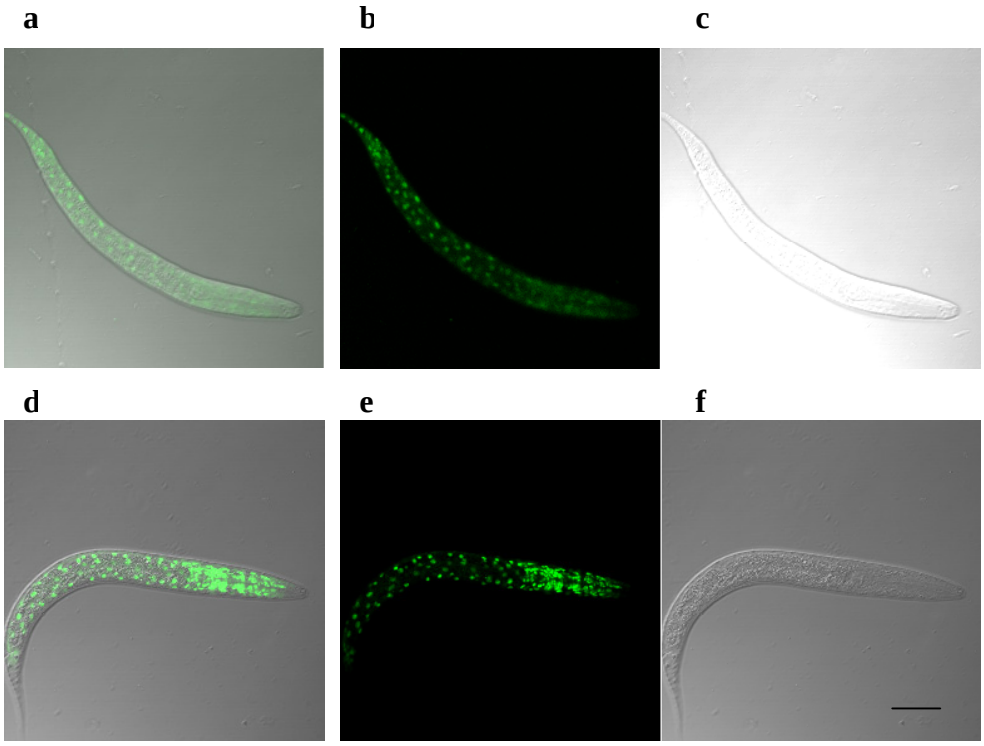

Fig. 3.46: Depletion of *hmg-1.1::gfp* expression in L1 larvae of EC715 strain after feeding with *hmg-1.1* dsRNA. a), b), and c) are the *hmg-1.1* dsRNA fed animals. d), e), and f) are the control animals. a) and d) are the overlaying of the fluorescence and. b) and e) are fluorescence observations. c) and f) are Nomarski observations.

3.2.5 Immunostaining

In this study, a polyclonal antibody that was generated in rabbit against HMG-1.1 was used. The immunostaining was done by the freeze crack method on ruptured hermaphrodites. The antibody was used with a concentration of 1:100. The immunostaining results showed that HMG-1.1 is expressed in all germline nuclei (Fig. 3.47).

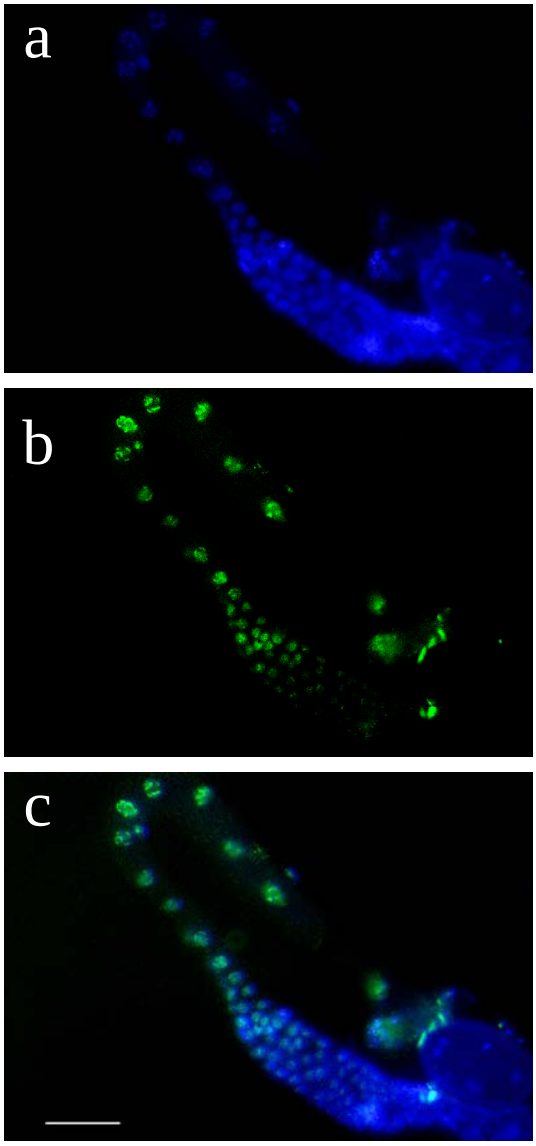

Fig. 3.47: Immunostaining of HMG-1.1 in a hermaphrodite germline. (a) is the DAPI staining micrograph. (b) is the immunostaing of HMG-1.1. (c) is the overlaying of the immunostaing of HMG-1.1 and DAPI staining.

HMG-1.1 was immunostained in the embryos of wild type animals with the previously mentioned antibody. Fig 3.48 shows the results of the immunostaining of a 16 cell-stage embryo in two different focal planes. It appeared from that embryo that HMG-1.1 is associated with chromosomes in the prophase, metaphase of mitosis in this stage of the embryonic development with a possible expression in the cytoblasm during the prophase.

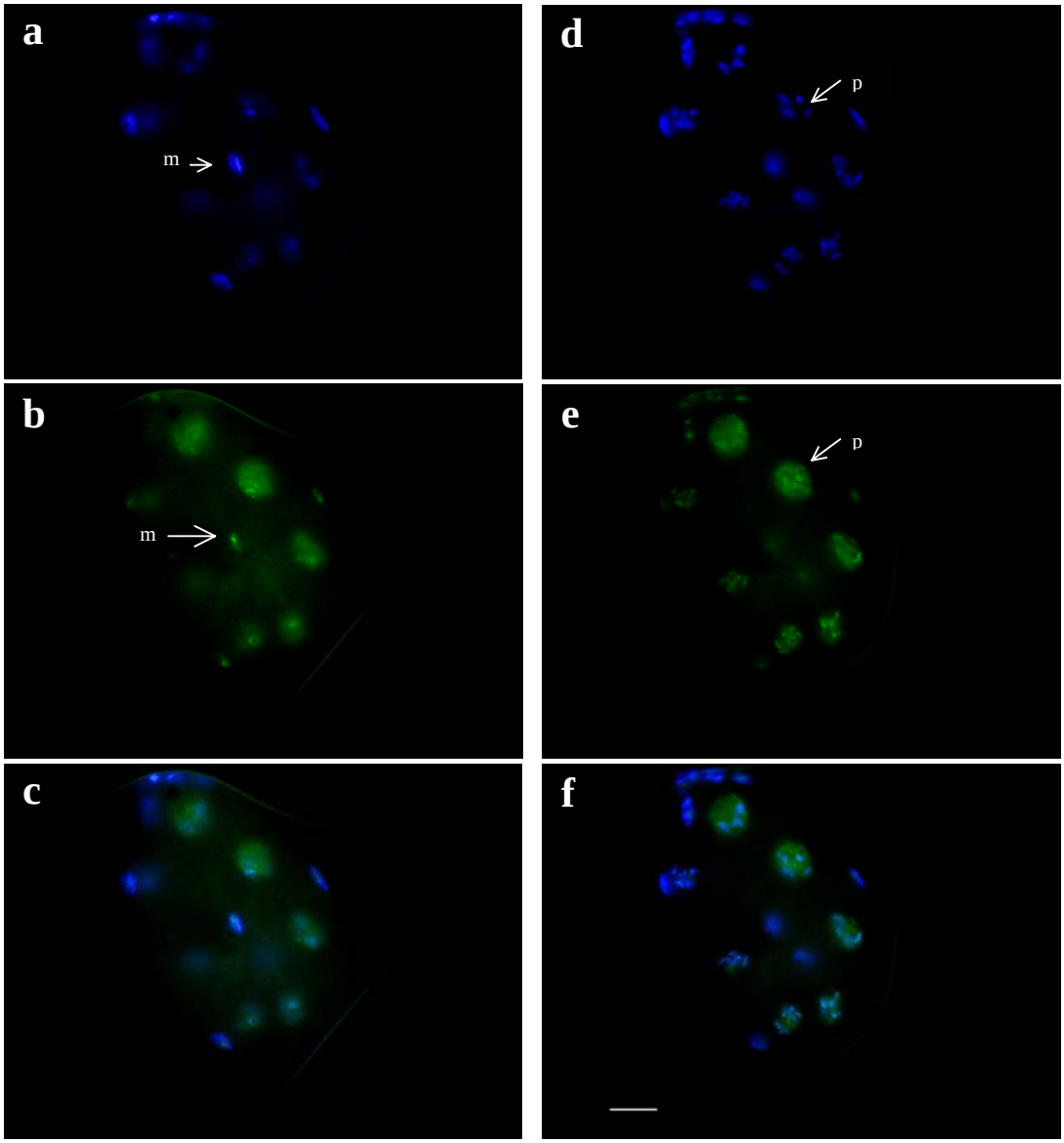

Fig.3.48: Immunostaining of HMG-1.1 in a 16 cell-stage embryo. All of the photos are from the same embryo. (a), b), and c) were taken in a focal plane different from (d), (e), and (f). (c) and (f) are the overlaying of the DAPI staining of the DNA and HMG-1.1 immunostaining. (b) and (e) HMG-1.1 immunostaining. (a) and (d) DAPI staining of the DNA. (m) is a nuclei in a metaphase and (p) is a nuclei in a prophase. The scale bar in (d) is 5 μm.

4. Discussion

4.1 Studies of the HMG-12 functions

The depletion of HMG-12 gene by applying its dsRNA, either by feeding or injecting it into the body of the worms was important to explore the functions of *hmg-12*. On the other side, combining some observations of the *hmg-12* expression in the strains that had an extrachromosomal array of *hmg-12* fused to *gfp* was used to explain some phenotypes that resulted from *hmg-12* dsRNA application.

4.1.1 Touch-response defect of RNAi animals

Testing and analyzing the nature of the touch response of the RNAi animals showed considerable differences compared with the control animals. Up to 45% of the *hmg-12* RNA interfered N2 adults showed abnormal response toward a head touch at the hit number 19 in comparison with nearly 15% of the control animals. The defect was clearly from a defect in the head response that causes head acceleration after a head touch. On the other side, this difference in behavior didn't appear in the L2 larval stage.

Furthermore, analyzing the behaviour of the control animals and its differences between the different experiments led to gain more knowledge about the touch response circuitries in the wild type animals.

4.1.1.1 Nature of the touch response behaviour in the control N2 animals

Applying the touch courses in different ways (head, head-tail, and tail) showed many interesting features about the touch response of the N2 strain. Furthermore, analyzing the touch response in each of the different experiments enabled us to learn more about the nature of the relationship between the anterior and the posterior touch circuits in the wild type animals through development.

Based on the studies of Chalfie and Thomson, (1979) and Chalfie and Sulston, (1981), there are six touch receptor cells called microtubule cells that are responsible for the response to gentle touches onto the body of the animals. Three of these cells, AVM (Anterior Ventral Microtubule), ALMR (Anterior Lateral Microtubule on the right side of the animal) and ALML (Anterior Lateral Microtubule on the left side of the animal), are responsible for the head touch response, and the other three cells,

PVM (Posterior Ventral Microtubule), PLMR (Posterior Lateral Microtubule on the Right side of the animal), and PLML (Posterior Lateral Microtubule on the Right side of the animal), are responsible for the tail touch response.

The intensive laser ablation study by Chalfie *et al*., 1985, provided a lot of information about other neurons that function in both circuits and the relationships between the different neurons. It described the possible function of a number of neurons, interneurons, and motor neurons that are supposed to play specific roles in the neural circuitry for the touch-induced movement (Fig. 4.1).

In the study of chalfie and his colleagues, individual neurons or pairs of neurons were ablated in a systematic way. The selection of these neurons was done based on previous knowledge about the connectivity between these neurons from electron microscopy micrographs.

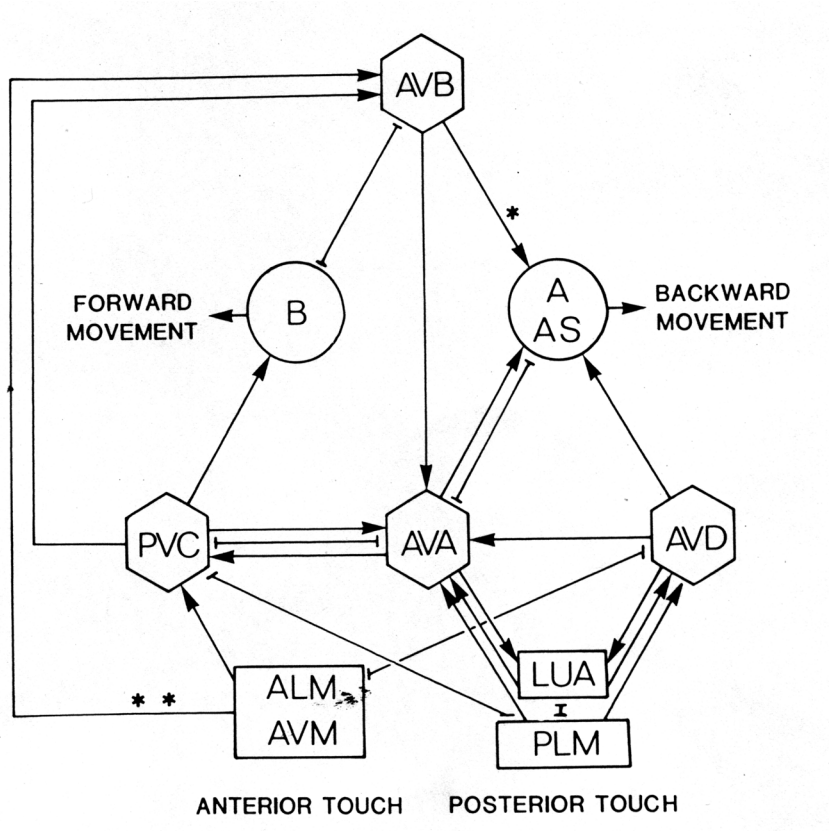

Fig. 4.1: Neural circuitry for touch induced movement. This circuitry is taken from Chalfie *et al*., (1985). Arrows are the chemical synapses and lines with blunt end are gap junctions. AVB forms chemical synapses only with the AS cells not with the A cells (*). Only AVM of the anterior touch cells chemically synapses onto AVB (**)

which is formed late in development. Touch cells and the touch cell connectors are designated by rectangles, the interneurons designated by hexagons and the motor neurons are designated by circles.

Killing the AVD interneuron in late larvae and adults resulted in early habituation after a very few touches instead of tens of touches in case of the control animals. However, killing the AVD interneuron in the early larvae caused anterior touch insensitivity (Chalfie, *et al*., 1985).

In another study on ALM$^-$ adults, it was suggested that AVM mediates a very weak touch response to head touch in adults, i.e., the animals moved after some but not all head touches. However, performing the same experiment on ALM$^-$ early-hatched larvae caused a lack of anterior touch response, and 35-40 hours after hatching these larvae regained partial touch response (Chalfie and Sulston 1981).

This means that the postembryonic development of the anterior touch circuitry has effects on the touch response behaviour of N2 animals. The main postembryonic change in the anterior touch circuit is the development of the AVM cell and its neural connectivity. Studying the postembryonic AVM development, which ends up to form a supplementary neural circuit to the anterior touch response circuitry, might lead to understand the role of development in the function of the anterior touch circuitry.

The AVM cell develops in the first larval stage and its neural connectivity develops through the animal development. Approximately after 46-51 h of development, just prior to the young adult stage, AVM develops to make a portion of the touch circuit mediating backward movement becomes functional (Chiba and Rankin 1990).

AVM builds at least two kinds of connections that can mediate touch sensitivity: functional gap junctions to both AVD and ALM, and chemical synapses to AVB. Although the development of AVM and its chemical synapses to AVB represent a major alteration in the anterior touch circuitry, it was not possible to identify the reason for these changes by the laser ablation experiment (Chalfie *et al*., 1985).

In this study, the results of the head-touch experiments showed that repeated head touches could cause abnormal head touch responses in the control animals. However, the percentages of these animals were small and the abnormal responses were not continuous. The results of the L2 head touch showed much higher percentages of acceleration head response that reached 60%.

In different experiments (Chiba and Rankin, 1990), the percentage of the worms that were accelerating was different from one developmental stage to the other after

tap-application with the highest percentage of acceleration found in L2 larvae but it had no score in any developmental stage in case of making a head touch. Both taps and touches in this experiment were applied to each animal as two stimuli, 7-15 minutes apart. Hence, it can be suggested that the difference between my results and their results concerning the head touch would be caused by the difference in the stimuli application. In our experiment, the stimuli application was composed of many more touches applied in shorter time than it was in the experiment of Chiba and Rankin, 1990.

It could be the reason behind the acceleration effect needed the excitation of the tail to appear which would strengthen the posterior touch circuit. In another experiment, two head touches were not enough to show the acceleration effect; i.e. all animals moved backward in response to these touches.

In our head touch experiment on L2, it appeared that the acceleration reaction needed 11 hits to appear and about 25 hits to appear in more than 50% of the animals (Fig. 3.9). The late score of the acceleration phenotype might be explained as a result of the weakening of the head touch circuit after this number of touches. Taking all together, it can be concluded that the appearance of the acceleration phenotype after touching the head needs a weak anterior neural signal, a strong posterior signal, or both together.

This showed that the different effect on the head touch circuitry resulted from completing its development by adding the AVM supplementary circuitry. However, this was still not enough as a source of the abnormal head response in adults.

On the other hand, the results of the head-tail touch experiment clarified a possible interaction between the anterior- and the posterior-touch circuitry. These results showed that the antagonism between these two circuitries is not only in the nature of their activity but might rise from an active communication or effect between each other.

The progress of the touch course showed a progressive increase of the percentage of the animals that had an abnormal tail response by accelerating backward after touching the tail (Fig. 3.3), which reached nearly 40%. However, the percentages of the animals with the abnormal head acceleration reaction did not show a progressive gain of abnormalities (Fig. 3.4), which reached their highest value near 15%.

These results showed that the stimulated anterior-touch circuitry in adults has the capability to overrun the antagonistic effect of the stimulated posterior touch circuitry.

This is clearly not the case in the early larvae, where the posterior touch circuitry was capable to overcome the anterior neural signals by accelerating the animal forward even after touching their head for few touches.

In other words, the completion of the anterior touch circuitry development by the addition of the AVM cells and their connections might be needed as an anterior-touch circuitry supplement to be able to overcome the posterior touch circuitry. It is not clear what could be the reason behind the preference of the anterior touch response circuitry or why this preference might not be needed in the early larvae.

Furthermore, the role that this supplementary circuitry plays in shaping the touch response behaviour is still unclear. Three assumptions are possible as follows: Either it plays its role through adding to the strength of the anterior touch circuitry or by deteriorating the posterior touch circuitry or both.

Finding that *avr-15* and *eat-4* are required for AVM function when the AVD neurons have been previously killed showed that these genes are required for functional AVM chemical synapses. It was suggested based on results from several experiments that *avr-14* and *eat-4* are components of glutamatergic synapses (Riddle *et al*., 1997). These results lead to the assumption that AVM is glutamatergic and that the AVM-to-AVB synapses are functional and inhibitory as it was suggested by Chalfie *et al*. 1985.

Finally, adding these findings to results of this study about the supplementary anterior touch circuitry can lead us to favour one assumption about the nature of this circuitry. We suggest that the development of AVM connections is needed to strengthen the anterior touch circuitry in adults by inhibitory signals toward the posterior touch circuitry.

More about the nature of this supplementary circuitry on the overall touch response can be clarified from the tail response in the head-tail touch experiment. It appeared that the progress of the touch course caused abnormality in the tail response. The percentage of animals that responded with backward acceleration was increasing consistently till it reached about 40% of the animals at the end of the touch course (Fig. 3.3).

The backward acceleration after touching the tail can have more than one source. However, two possible mechanisms can lead to this observation based on the antagonism between the anterior- and posterior circuits, either a sustained antagonistic effect from the anterior neural circuit or fatigue in the posterior circuit. The results of

the tail-touch experiment showed that all the animals were moving forward after the tail touches till the end the touch course. These results proved that the backward acceleration after the tail touches in the head-tail experiment was with no doubt caused by the antagonistic effect from the anterior touch circuit.

4.1.1.2 Nature of the touch response behaviour in HMG-12 RNAi animals

In this part, we will discuss the phenotypes that resulted from the HMG-12 RNAi animals in the different touch-response experiments. These phenotypes were the results of possible neurological defect(s) in the HMG-12-depleted animals. In the head-tail touch response experiment, the response of the RNAi animals in the adult stage to the head touch response was clearly altered in comparison with the response of the control animals (Fig. 3.2).

The abnormal response of the animals was classified into two different types of abnormality: head acceleration- and pause response. The percentages of the RNAi animals that responded by head acceleration were higher than the corresponding percentages in the control animals throughout the whole touch course in the head-tail touch experiment (Fig. 3.4). These results proved a possible presence of neural defects in one or both of the touch-response circuits in the head of the HMG-12 depleted animals.

The other type of response, the pause response, showed no relevant changes in the progress of the touch course in the head-tail touch response (Fig. 3.5). The head acceleration response was the main factor that caused the higher percentages of abnormal head response in the RNAi animals.

On the other side, it was quite clear that the abnormality, which resulted from the head in the head touch response experiment, was mainly due to pause response (Fig 3.8) rather than acceleration response (Fig 3.7). This appeared after analysing separately the nature of the abnormal response in the head.

The observation, which resulted from laser ablation tests (Chalfie, *et al*., 1985), that AVD^{-} adults responded to the head touch by faster habituation could explain the mentioned head-response abnormalities of the HMG-12 depleted adults in comparison with the control animals.

The results of depleting HMG-12 in the strain KP987 were fitting to a certain degree to the previous assumption. The strain KP987 that contains *glr-1::gfp* was microinjected with *hmg-12* dsRNA to study the effect of HMG-12 depletion on the

development of some cells that involved in touch sensitivity and the effect on *glr-1* expression.

The HMG-12 depleted animals of the strain KP987 showed no effect in the differentiation of the touch neurons that express *glr-1::gfp* or in the intensity of the GLR-1::GFP fluorescence. There was only a very slight negative effect on the *glr-1* expression in the AVD cells in a small percentage of the animals (Fig. 3.13).

The problem here was that a possible defect in the AVD cell alone is not enough to explain the differences in the nature of the head-response abnormality between the head-tail experiment and the head touch experiment. The head-response abnormality in the head-tail touch experiment consisted mainly of acceleration response, however, in the head-touch experiment it consisted mainly of pause response. This difference in the head responses between the two experiments means that there must be a lack of a neuronal signal that was caused by the tail touch, which varied the head response depending on touching the tail or not.

The analysis of the tail-touch response in the head-tail touch experiment for both HMG-12-depleted and control adults helped in the investigation of the nature of the head-touch defect. This investigation took into consideration the relationship between the head and tail neural circuitries of the touch-response movement.

In contrary with what was noticed on the control adults where the abnormality of their tail-touch response was increasing through the touch course, the abnormal touch-response of the HMG-12-depleted adults was generally inconsiderable (Fig. 3.3). In the tail-touch experiment the increase of abnormal tail-touch responses was not scored for both traits, as the percentage of the animals showing abnormal tail-touch response kept around 0% in both traits.

This proved clearly that the tail-touch response falls under antagonistic effect from the anterior touch-response circuitry in the control animals. This antagonism was previously suggested by the nature of both circuitries but it was never proved quantitatively.

Furthermore, the nature of the previously mentioned antagonism was altered in the HMG-12-depleted adults. From that point, it appeared that the abnormality in the head touch response is resulting from a systematic defect rather than a defect only in the AVD interneuron.

Also, on the view of this interpretation of the RNAi animals, it is possible to explain the difference of the head-touch abnormalities between the head-tail touch experiment

and the head-touch experiment. In the head-tail touch experiment, applying the touches excited the posterior-touch circuit. It seems that the tail excitation was enough for the posterior circuit to overcome the anterior circuit; i.e. the progress of the touches caused early acceleration (Fig. 3.4).

However, in the head touch experiment there was no previous posterior excitation. So, the animals had only their spontaneous locomotion as an antagonistic effect from the posterior circuit against the anterior-touch circuit. The forward movement could only balance the weakened backward movement and resulted in pausing the animals (Fig- 3.8) rather than pushing it to accelerate (Fig. 3.7).

Furthermore, weakened antagonistic backward signals from the abnormal anterior-touch circuit of the HMG-12-depleted animals against the posterior-touch circuit signals in the head-tail touch experiment led to very small percentages of animals which showed tail reaction abnormalities (Fig. 3.3).

The head-touch response of HMG-12-depleted L2 larvae was analyzed to check for a possible link between the touch-response phenotype and the development of the animals. Testing L2 larvae for that phenotype can draw a link between these touch-response abnormalities and the anterior touch circuitry changes during the maturation of the animals. As previously mentioned, the chemical synapses connections that connect AVM neuron with its interneurons are postembryonically formed through the animal development in late L4 larval stage (Chalfie, *et al*. 1985).

The data analysis of the head-touch experiment performed on L2 larvae helped in clarifying more details about the source of the touch response abnormality of the animals that had HMG-12 depletion. It showed high percentages of animals that responded to the head touch by acceleration. These animals didn’t show any considerable score of pause touch-response. The resulting acceleration response showed no considerable difference between the HMG-12-depleted and the control larvae. Based on these results, it appears that the development of the anterior touch circuitry is necessary for the head touch abnormality resulting from HMG-12 depletion.

Another phenotype that was scored in HMG-12 depleted animals is the uncoordinated movement. It was shown that the ablation of the AVB cell resulted in uncoordinated forward movement while the backward movement was normal (Chalfie, *et al.*, 1985). This was exactly the same description of the uncoordinated movement that the HMG-12 depleted animals showed. Comparing my results with the

results of ablating the AVB cell showed a connection between HMG-12 depletion and the development of the anterior touch circuitry, i.e. the AVB neuron is one of the neurons in the postembryonic AVM supplementary circuit. Furthermore, in both cases it matches the nature of movement of the animals while showing the turning defect.

After collecting these details about the touch response phenotypes in HMG-12 depleted animals, it appeared that these results helped to understand the behaviour of the touch response in N2 animals and the change in behaviour after depleting the HMG-12 from the wild type animals.

In N2, it seems that the mature animals need to develop an extra antagonistic supplementary circuit for their anterior neural circuitry for the touch-induced movement against two posterior neural forces: the posterior neural circuitry for the touch-induced movement and the spontaneous locomotion circuitries.

For that reason, the postembryonic neuronal connections for the AVM cell could be needed. The effect of this extra force of the anterior touch response circuitry was visible in the tail response in the head-tail touch experiment (Fig. 3.3). The strong effect of the spontaneous locomotion movement appeared stronger than the weak anterior touch response neural circuitry for the touch-induced movement in L2 larvae because a high percentage of animals showed head acceleration (Fig. 3.9). On the other side, it appeared that the anterior-touch response neural circuitry of the HMG-12 depleted adults might have lost its extra force over the neural posterior forces (Fig. 3.2).

The observation that resulted from the AVD^- adults was that these adults had a faster habituation for anterior touches, and that the adults that were AVD^-/AVA^- reacted with a pause touch response. Beside these specific types of responses, both types of neuronally ablated worms showed a positive response to the anterior touches in adults and a negative response in the larvae (Chalfie, *et al*. 1985).

In the mentioned study habituation is defined as a tendency to have shorter distance of backward movement with the progress of the touch course. These observations can lead to suggest that the anterior touch neural circuitry in AVD^- adults still has the force to push the animals backward but the same circuitry in AVD^-/AVA^- adults lost that antagonistic effect over the backward circuitry and was only able only to induce a pause reaction in the adult animals.

However, these behaviours can be the result of two different reasons. One of them is a direct loss of force in the anterior touch neural circuitry, the other an extra

antagonistic effect from the posterior touch neural circuitry. In another laser ablation test (Kitamura, *et al*. 2001), it appeared that PVCLR$^-$ animals are not slow in habituation. So, Kitamura *et al.* concluded that it is unlikely that habituation is the result of an antagonistic effect of forward and backward movement.

Another conclusion from the same publication stated that it is likely that the habituation occurs at AVM to AVBLR, or AVB to AVARL. This would mean that the previously mentioned difference in the behaviour between AVD$^-$ and AVD$^-$/AVA$^-$ resulted from a direct loss of function in the anterior touch circuitry rather than from an indirect loss resulting from an extra antagonistic effect from the posterior touch circuitry.

Beside what was previously concluded, the postembryonic development of connecting AVM to its interneurons is made as a source of strengthening the anterior touch circuitry over the antagonistic posterior touch circuitry. It can be concluded as well that *hmg-12* has a functional role in this circuit because its depletion has a negative effect on the function of the anterior neural circuitry.

The pattern of the scored abnormal behaviour that resulted from the HMG-12 depletion in comparison with that of the control animals was different. The percentages of the animals, which showed abnormal reaction resulted in one big curve through the 40 hits in Fig. 3.2, however, the percentages of the control animals reached a peak each 5-10 hit. It was interesting to see that the HMG-12 depleted animals in Fig. 3.3 showed the same pattern as the control in Fig. 3.2. This might indicate that the 5-10 hits-cycles are kind of restoration cycles that happen in each circuitry separately.

An increasing antagonistic effect from the head in Fig.3.3 in the control animals disrupted this cycle. Furthermore, a defect in the head of the HMG-12 depleted animals resulted in relaxing this cycle in Fig. 3.2 and for the same reason, depleting HMG-12, this cycle was restored in the tail of the RNAi animals (Fig. 3.3).

From these observations it can be concluded that the effect of HMG-12 depletion in the head touch neural circuitry results from a defect in the chemical synaptic function in the anterior neural touch circuit. This fits with the fact that all neural connections that are made postembryonically from AVM are chemical synapses.

4.1.2 The relationship between HMG-12 functions and the germline:

The results of this study showed that HMG-1.1 has an abundant expression in the somatic goand and the germline nuclei. This expression was clear from the transgenic animals that have *hmg-12::gfp* and from the immunostaning of HMG-12. This reflects that HMG-12 plays a role in the germline functions.

The depletion of HMG-12 showed percentage of animals that had egg laying defects and embryoninc death. The recently released information about *hmg-12* mutant (tm0798) showed sterility and lethality, which might go along with the results of this study. However, the penetrance of the germline phenotypes in our study was low and didn't cause complete sterility like the case in the *hmg-12* mutant. This might have resulted from the weak depletion of such an abundant protein which was shown by inspecting the fluorescence of *hmg-12::gfp* after *hmg-12* depletion.

4.2 Studies of the functions of HMG-1.1

In order to study the gene functions of *hmg-1.1*, the *hmg-1.1* dsRNA was applied to the animals by microinjection and feeding. These techniques demonstrated the effect of depleting HMG-1.1. Also, transgenic animals that carry integrated copy of *hmg-1.1* fused to green fluorescent protein (gfp) were investigated to study the expression pattern of *hmg-1.1*. Furthermore, using a polyclonal antibody against HMG-1.1 helped to determine the cells where HMG-1.1 functions.

4.2.1 The relationship between HMG-1.1 and necrosis

The most reproducible and penetrating phenotype, which was scored in the HMG-1.1 depleted animals, was the necrotic-like phenotype. This phenotype appeared in all larval stages and adults treated by feeding or microinjecting the *hmg-1.1* dsRNA. The severity of this phenotype was different among animals in the same experiment. Also, the nature and the position of the necrotic-like cell death showed a considerable level of variability among animals (Fig. 3.20). Fig. 4.2 shows the apoptotic- and the necrotic pathways in C. *elegans*.

It was not possible to link the differences in that phenotype that appeared in different animals with environmental conditions like incubating at different temperatures, different chemical composition of the incubating media or feeding with different strains of bacterial food. It appeared that the vacuoles that result from

necrotic like cell death have an accumulating nature with the ability to fuse because adults showed bigger and a higher number of vacuoles than early larval stages.

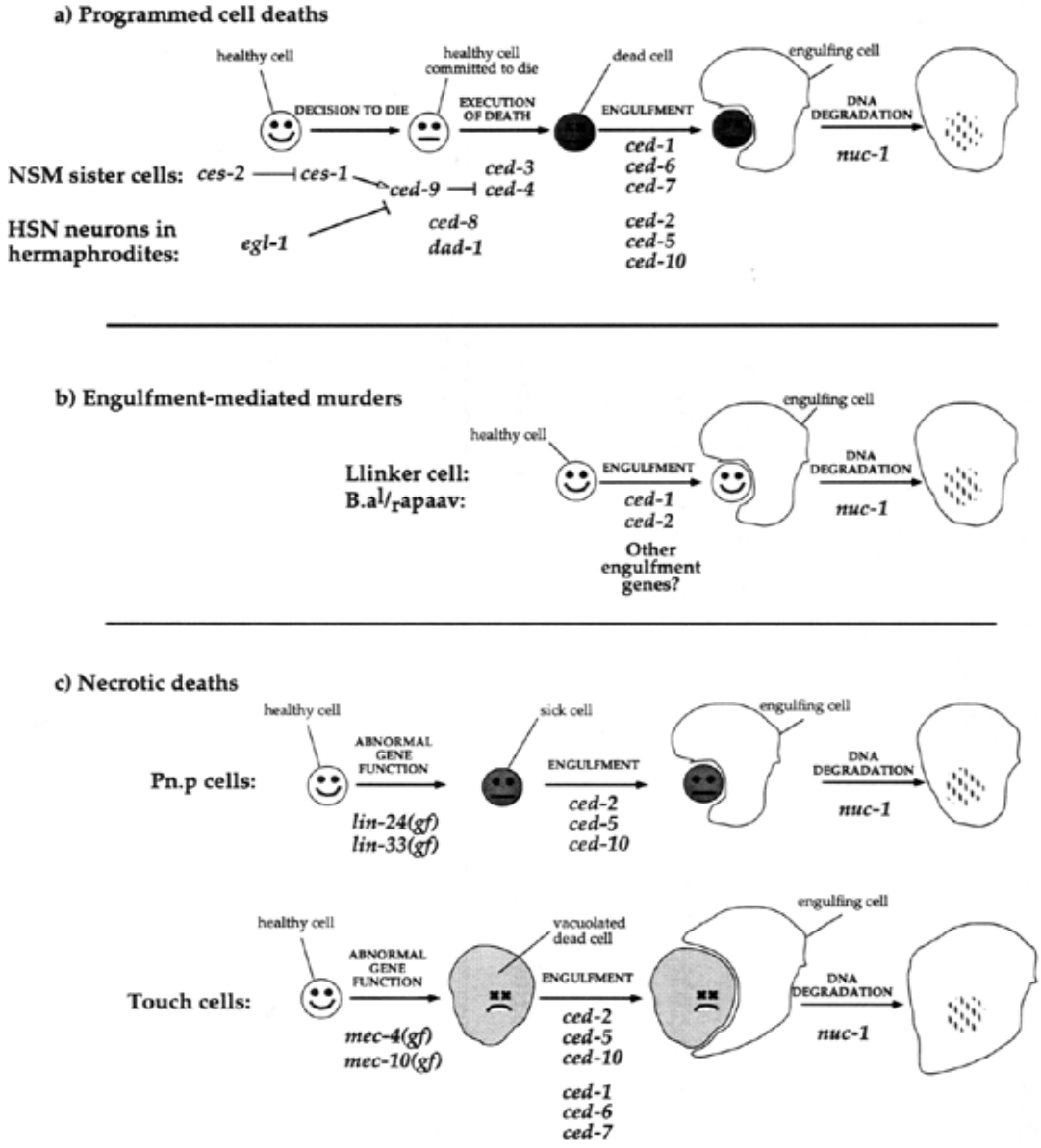

Fig. 4.2: The apoptotic- and necrotic-cell death pathways in *c. elegans*. (a) shows the apoptotic pathway, (b) shows the engulfment-mediated murders, and (C) shows the necrotic cell death. This figure is taken from Riddle, *et al.* (1997).

This observation led to an assumption that these vacuoles either formed as a result of generating an accumulating destructive signal enhanced actively by the depletion of HMG-1.1 or by lacking one of the protective cell components that would be needed

by the cells to face certain conditions. The lack of this protection could lead to increased cell sensitivity that might kill the cells. So, both the accumulative nature in the first assumption, or the random need for these cell components in the second assumption can be the reason that these necrotic like cell death appear in variable positions with variable sizes.

The structure and the location of the necrotic-like cell death that appeared in the HMG-1.1 depleted and starved L1 larvae incubated in M9 buffer differed from what was seen in animals that were incubated on agar plates. The vacuoles in the larvae that were incubated in the buffer formed a continuous area on both sides of the animals. This continuous area was mainly posterior to the head of the animals (Fig. 3.29).

On the other side, the vacuoles, which appeared in the body of the larvae that were incubated on NGM agar plates, had a higher tendency to occur in the head than to appear in the middle of the animal's body. Also, it appeared as separated vacuoles rather than as a continuous defected area (Fig. 3.20).

That observation can lead to assume a link between the nature of the movement and the formation of these necrotic-like vacuoles and their position. The worms that were reared on agar plates moved slower and foraged using mainly their head muscles. However, the larvae incubated in M9 buffer with shacking had to swim all the time. It can be possible that HMG-1.1 is involved in a signaling process to other cell-components informing about the metabolic status in the body-wall muscles and hence the possible need for energy. So, depleting HMG-1.1 by RNAi might disturb needed signals that distribute or redistribute the metabolites based on the need.

In this study, *crt-1* (calreticulin) mutants were used to investigate the link between the vacuoles resulting from *hmg-1.1* RNAi and the necrotic cell death pathway. Calreticulin functions are critical for the animals in the process of necrotic cell death (Xu *et al*., 2001). Calreticulin is a Ca^{2+} binding/storing protein found primarily in the lumen of the endoplasmic reticulum (ER) that serves both as a molecular chaperon and as a central regulator of Ca^{2+} homeostasis (Michalak *et al*., 1999; Llewellyn *et al*., 2000). In *C. elegans*, *crt-1* mutation was able to suppress the necrotic cell death, which results from HMG-1.1 depletion.

Feeding *crt-1* mutants with *hmg-1.1* RNAi did not result in the formation of vacuoles. The *crt-1* ability to suppress forming vacuoles proved a possible link between the necrotic-like structure resulting from the HMG-1.1 depletion and the necrotic cell death pathway.

Some mutants, *ced-1, ced-2, ced-5, ced-6, ced-7,* and *nuc-1,* in the necrotic death pathways and the engulfment-mediated murders was used to investigate the nature of the vacuoles, which resulted from HMG-1.1 depletion. The genes *ced-1, ced-5, ced-2, ced-6,* and *ced-7* are involved in the engulfment process, and *nuc-1* is involved in DNA degradation of the cells that were already engulfed (Hengartner, 1997).

HMG-1.1 depletion caused vacuoles in all of these mutants. However, it was less severe in the mutants that lack the engulfment process than in the HMG-1.1 RNAi wild-type animals. This means that these vacuoles did not result from the engulfment process using these genes through the previously mentioned pathway. This might mean that other genes are responsible for the engulfment of the sick or died cells resulted from HMG-1.1 depletion.

It was suggested by Ahnn and Fire (1994), based on their finding that a large number of deficiencies result, in homozygous state, in arrested embryos, which contain unengulfed cell corpses, that many more genes than already known function in engulfment. That might mean that mechanism producing the HMG-1.1 depletion necrotic-like death does not follow the known necrotic cell death pathways and the engulfment-mediated murders.

After all, there is still an assumption that repressing the necrotic-like death in *nuc-1* background of HMG-1.1 depleted animals might be specific to *crt-1* function itself. *crt-1* function as Ca^{2+} binding/storing protein in the endoplasmic reticulum (ER), which works as a central regulator of Ca^{2+} homeostasis. The stored Ca^{2+} in the ER is regulated by calnexin homolog (*cnx-1*), the ER Ca^{2+} release channel inositol triphosphate receptor channel (InsP3R), *itr-1* (Dal Santo *et al*., 1999), and the ER Ca^{2+} release channel ryanodine receptor channel RyR *unc-68* (Maryon *et al*., 1996). The released Ca^{2+} is returned from the cytoplasm to the ER by the Sarco-endoplasmic reticulum Ca^{2+} ATPase, SERCA (Pozzan *et al*., 1994).

Causing necrosis in the *itr-1* (sa73) background by the depletion of HMG-1.1 showed that the necrotic cell death caused by the depletion of HMG-1.1 is not a result of over release of Ca^{2+} from the ER by InsP3R. On the other side, it was not a result of a hyperactive plasma membrane Ca^{2+} channel because *crt-1* mutations do not protect against necrosis induced by that hyperactivity (Xu, 2001).

It was found that SERCA, based on the phenotypes resulted from its mutant (*sca-1*) and depletion with RNAi, is required for larval development, and muscle function and that from its depletion caused necrotic-like death (Zwaal, *et al*., 2001). It was found

that applying thapsigargin to wild type animals inhibited the SERCA ER Ca^{2+} re-uptake pump and induces the release of ER Ca^{2+} via an InsP3 receptor independent mechanism (Takemura *et al*., 1989).

The phenotypes scored on the wild type animals after the application of thapsigargin were very similar to the phenotypes that resulted from the HMG-1.1 depletion. Application of the thapsigargin caused protruding vulvae and maldevelopment in the germline, which contained endomitotic oocytes or oocytes with multiple nuclei resulting in a reduced production of progeny. Beside these phenotypes, it caused defects in the animals' movement and their defecation period.

Furthermore, it was shown that thapsigargin driven Ca^{2+} induced vacuoles that resemble necrotic-like cell death in random cells (Xu, *et al*., 2001). Xu and his colleagues concluded that elevation of Ca^{2+} concentration itself could be cytotoxic in nematodes and supported a model in which a critical rise in Ca^{2+} concentration is a causative factor in neurotoxicity, which causes necrotic-like cell death. These results were matching the results of Choi, (1992) and Leist and Nicotera (1998) that Ca^{2+} functions in pivotal ways in mammalian cell death.

Finally, from these results and our results we may conclude that HMG-1.1 depletion mimics the effect of thapsigargin in elevating the Ca^{2+} concentration in producing many of their resulting phenotypes. It doesn't seems that HMG-1.1 has an active role in releasing the stored Ca^{2+} from the ER because depleting HMG-1.1 in *crt-1* background didn't cause elevation in Ca^{2+} concentration hence no necrotic-like cell death was scored.

In fact, two other assumptions seem more convenient. At first, HMG-1.1 may down regulate by the Ca^{2+} concentration, which means that activation of HMG-1.1 expression would leads to lower concentration of Ca^{2+}, which consequently causes necrotic-like cell death. As a second possibility, HMG-1.1 has the function to protect the cells from initiating necrotic-like cell death response by short or weak elevation of Ca^{2+} concentration, which can be unnecessary for the cells to take the decision to die.

The second assumption might go along with the previously mentioned observation of the difference in the vacuole location between HMG-1.1 depleted L1 larva that were starved on agar plates or incubated in M9 buffer. It seems necessary to have a certain concentration of HMG-1.1 in the cells near to the strongly active muscles to protect these cells from dieing or getting engulfed by neighboring cells.

The last assumption might draw the attention still to the possible link between the ER functions and HMG-1.1 functions because of the role of the released Ca^{2+} From ER in the muscles activity.

4.2.2 The relationship between HMG-1.1 and apoptosis

After a number of publications showed that HMG1 has a function in the programmed cell death in humans, it was interesting to test whether HMG-1.1 has the same function in *C. elegans*. Scaffidi, *et al*. (2002) showed that HMG1 protein is firmly immobilized in the chromatin of the cells that undergo apoptosis and released from it so late in the process of the secondary necrosis.

However, HMG1 releases itself from the necrotic cells. Bustin, 2002 showed that HMG1 signals to multiple cellular components in a differential way, so that its signals to neighboring cells can be distinguishing between dead cells as a part of the programmed cell death or necrotic-like cell death.

In this study, RNAi feeding was used to investigate the effect of HMG-1.1 depletion on the programmed cell death by different mutants of the programmed cell death pathway. The depletion of HMG-1.1 in *nuc-1* background showed a much higher number of corpses in both somatic cells and germline than the number of the corpses in the control animals. This might show an initiation of programmed cells death in both somatic cells and germline by depleting HMG-1.1 in cells, which normally should show no apoptotic activity.

On the other side, this can explain the enormous number of resulted phenotypes that were highly variable quantitavly and qualitatively that resulted from HMG-1.1 depletion. With the lack of the apoptotic cell-death signals from apoptotic cells to neighboring non-apoptotic cells many random phenotypes can appear. For example, the endomitotic oocytes and misallocated nuclei in the germline, which were statistically much different between experiments and not all the time correlated, can result from death of different somatic sheath cells (McCarter, *et al*., 1997).

Furthermore, to check whether the apoptotic cells that resulted in the HMG-1.1 depleted animals are caspase dependent, we depleted HMG-1.1 in a *ced-3* background. There were no apoptotic cells that were scored in these animals, which prove that the cells died from apoptosis after depleting HMG-1.1 were caspase

dependent. So, that it is justified to say that this apoptotic-cell death happened in a caspase-dependent manner.

The HMG-1.1 depletion in the mutant strains that lack the genes involved in cell engulfment did not show considerable differences in comparison to the control animals. This might show a possibility that the engulfment process for the cells that died from apoptosis after HMG-1.1 depletion might be engulfed by any other engulfment genes.

This actually can match the results of the HMG1 functions in apoptosis in humans. It seems that depleting HMG-1.1 in *C. elegans* resembles the effect of immobilizing HMG1 to the chromatins in apoptotic cells in mammals.

At last, it was proved that Ca^{2+} concentration in the cytoplasm could promote apoptosis (Orrenius, *et al*., 2003). This can take us back to our previous assumption about the link between the HMG-1.1 functions and Ca^{2+} concentration. HMG-1.1 needs the caspase activity to functions in the apoptotic pathway. It seems that depleting HMG-1.1 lead to distributing the cell death signal from an apoptotic cell to the neighboring non-apoptotic cells.

4.2.3 HMG-1.1 and cell cycle

It was noticed from the microscopic study of the EC715 strain, which contains an integrated copy of *hmg-1.1::gfp*, and the immunostaining with HMG-1.1 antibody that HMG-1.1 is not expressed in the sperms. Also, it is expressed in all germline nuclei and oocytes till fertilization and then it disappears. Actually, we found that HMG-1.1 expression disappears in the one cell stage embryo and reappears at two cell-stage embryos.

It can be concluded from this observation that the ongoing activities after the oocytes fertilization till forming two cell-stage embryos does not need HMG-1.1 functions or include strong suppressor to HMG-1.1 expression. Taking the first assumption into consideration, it can be concluded that HMG-1.1 is functioning for signal transduction. So, it might not be needed in one cell stage embryo. However, it would not be still enough explanation. It is rather a need to suppress HMG-1.1 expression at that time-window in development.

In fact the most dramatic waves of Ca^{2+} occurs directly after fertilization triggering a number of events that drive the zygote toward its first mitotic division (Karp, 2002).

So, a possible explanation is that the sudden increase of Ca^{2+} directly after fertilization can be a reason for the full depletion of HMG-1. This is matching our previous conclusion about the link between HMG-1.1 and necrosis from one side, and the known necrotic effect of increasing the Ca^{2+} concentration in cells from the other side.

Starting from two cell-stage embryos till about 20 cell-stage embryos, we noticed that *hmg-1.1* expression is observable in the prophase, however, it disappears in the prometaphase and metaphase, and reappear in the anaphase and telophase. The observation of the *hmg-1.1::gfp* expression through the cell cycle in the early developmental stage of the embryo showed us that HMG-1.1 might have a possible role in mitosis. Scoring no considerable embryonic lethality in the HMG-1.1 depleted animals might show that low concentration of HMG-1.1 in the cells while mitosis is not critical. On the other side, the high rate of embryonic death in the strain EC715, which might have an over expression of HMG-1.1 in its cells, might reflect the danger on mitosis would appear with appear with a high concentration of HMG-1.1 rather than depleting it.

It was found in metazoans that before the start of the prometphase, the cells should be already prepared for the metaphase by having condensed chromosomes, fragmented Golgi complex and ER, and dispersed nuclear envelope (Karp, 2002). However, the breakdown of the nuclear envelope in *C. elegans* has a unique timing, which differs based on the developmental stage of the embryo.

In the early *C. elegans* embryonic development (2-24 cells) the nuclear envelope breaks down at early anaphase and mid-late anaphase. In embryos that had (>30 cells), the nuclear envelope breaks down at prometaphase and continued like that till the mid-late anaphase, just like the other metazoans (Lee, *et al*. 2000).

So, the timing that *hmg-1.1::gfp* expression disappears at can be matching our previous assumption that links the functions of *hmg-1.1* and the ER activities. It was not possible to see considerable embryonic lethality in the HMG-1.1 depleted animals. Possibly, this happened because the dsRNA application did not cause a complete HMG-1.1 depletion. However, the high percentage of the embryonic death in the EC715 strain that contains an integrated copy of *hmg-1.1::gfp* might reflect a defect in mitosis resulting from over expression of *hmg-1.1*. The main observation about these dead embryos was that they were embryos that had (> 40 cells).

Previous studies based on immunofluorescence analysis indicated that HMG1 dissociates from mitotic chromosomes (Falciola *et al*., 1997). However, in a recent study, it was found that HMG1 is associated with the mitotic chromosomes in HeLa cells (Pallier , 2003).

So that, our finding in *C. elegans* about the oscillation of the HMG-1.1 expression can be considered a unique case. It drives us to conclude that HMG-1.1 is not associated with the condensed chromosomes in the early *C. elegans* embryonic development. It would be possible that the function of HMG-1.1 while attaching to the condensed chromosomes is needed only in late divisions.

It was found that *C. elegans* has a. This finding of the unique timing of the nuclear envelope break down through mitosis in *C. elegans* was a start to ask the question about which component or a process might benefit from this timing. Finding out this point can help to understand more about the evolution of mitosis in eukaryotes. The similarity between the association of HMG-1.1 with the condensed chromosomes in *C. elegans* and HMG-1 in mammals occurred only in the late *C. elegans* embryos. Only in late C. *elegans* embryos the timing of the nuclear envelope break down is similar with the timing of its breakdown in mammalian, in prometaphase.

This might show a critical role of HMG-1.1 in *C. elegans* to facilitate the differences in the mitotic process in comparison with mammals. It means that, the HMG-1.1 association with the condensed chromosomes mimics functionally the activity of HMG1 in mammals only when there is no intact nuclear envelope in cells. It can be concluded that HMG-1.1 is a part of the unique mitotic machinery of early embryonic development in *C. elegans* and it is associated with the condensed chromosomes only in case of having the nuclear envelope broke down.

Finally, a conclusion that can results from this study is that HMG-1.1 functions have a link with the Ca^{2+} concentration driven by the ER activity. Supporting this conclusion are the results from this study and the results from the knocked out mice that lacks HMG1. The newly born *Hmg1*$^{-/-}$ mice died out of a lethal hypoglycaemia (Calogero, *et al*., 1999). It was reported that ER function is processing the preproinsulin, by removing its signal sequence and folding it, to make insulin (Boonyaratanakornkit *et al*., 1998). This means that changing in ER activity can cause insulin over concentration, which is one of the reasons to cause the hypoglycaemia.

From the results of this study, it can be assumed that HMG-1.1 function to shift up the threshold of the calcium concentration that is required to initiate cell death. This

might be required for the cell health by differentiating the calcium release dependent cell death from many other routine cell functions that would be initiated by the calcium release.

5. Abstract

High mobility group (HMG) proteins are a diverse group of nuclear proteins. HMG proteins were grouped under three families based on their structure: HMGI(Y), HMG14/17, and HMG1/2. Recent studies showed the ability of HMG proteins to bind DNA in different degrees and to interact with various proteins. The functions of HMG proteins play an important role in various developmental contexts. In this study, the functions of two *C. elegans* HMG proteins, HMG-12, which belongs to HMGI(Y) proteins, and HMG-1.1, which belongs to HMG1/2, were studied.

The depletion of HMG-12 with RNAi caused neural defect in adults. The *hmg-12* RNAi animals were uncoordinated and showed earlier acceleration after head touches in comparison with the wild type animals. It can be concluded from this study that HMG-12 plays a role in the function in the postembryonic AVM neural circuitry. These results might shed some light on the unknown function of the AVM neural circuit postembryonic development and the functions of HMG-12.

The results of this study showed that HMG-1.1 has abundant expression in all somatic cells starting from two cell stage embryos. HMG-1.1 expression disappears from the cells during prometaphase in early embryos. The HMG-1.1 depletion caused partial egg-laying defect and morphological defects in the germline. Furthermore, it caused apoptotic- and necrotic-cell death. HMG-1.1 appears to play a role in cell-survival mediated by regulating the Ca^{2+} concentration in the cells.

6. Bibliography

Agnello D, Wang H, Yang H, Tracey KJ, Ghezzi P. HMGB-1, a DNA-binding protein with cytokine activity, induces brain TNF and IL-6 production, and mediates anorexia and taste aversion. Cytokine. 2002; 18(4):231-6.

Ahnn J, Fire A. A screen for genetic loci required for body-wall muscle development during embryogenesis in *Caenorhabditis elegans*. Genetics. 1994; 137(2):483-98.

Andersson U, Wang H, Palmblad K, Aveberger AC, Bloom O, Erlandsson-Harris H, Janson A, Kokkola R, Zhang M, Yang H, Tracey KJ. High mobility group 1 protein (HMG-1) stimulates proinflammatory cytokine synthesis in human monocytes. J Exp Med. 2000; 192(4):565-70.

Andersson U, Wang H, Palmblad K, Aveberger AC, Bloom O, Erlandsson-Harris H, Janson A, Kokkola R, Zhang M, Yang H, Tracey KJ. High mobility group 1 protein (HMG-1) stimulates proinflammatory cytokine synthesis in human monocytes. J Exp Med. 2000;192(4):565-70.

Bianchi ME, Falciola L, Ferrari S, Lilley DM. The DNA binding site of HMG 1protein is composed of two similar segments (HMG boxes), both of which have counterparts in other eukaryotic regulatory proteins. EMBO J. 1992;11(3):1055-63.
Bianchi ME. Prokaryotic HU and eukaryotic HMG1: a kinked relationship. Mol Microbiol. 1994; 14(1):1-5.

Bianchi, M. E. (1995). The HMG-box domain. In “DNA-protein: structural interactions” (D. M. J. Lilley, Ed.), pp. 177-200, Oxford Univ. Press, Oxford.
Bioessays. 1993;15(8):539-46.

Boonyaratanakornkit V, Melvin V, Prendergast P, Altmann M, Ronfani L, Bianchi ME, Taraseviciene L, Nordeen SK, Allegretto EA, Edwards DP. High-mobility group chromatin proteins 1 and 2 functionally interact with steroid hormone receptors to enhance their DNA binding in vitro and transcriptional activity in mammalian cells. Mol Cell Biol. 1998 Aug;18(8):4471-87.

Brenner S. The genetics of Caenorhabditis elegans. Genetics. 1974 May;77(1):71-94.

Bradford MM. A rapid and sensitive method for the quantitation of microgram quantities of protein utilizing the principle of protein-dye binding. Anal Biochem. 1976;72:248-54.

Bustin M, Reeves R. High-mobility-group chromosomal proteins: architectural components that facilitate chromatin function. Prog Nucleic Acid Res Mol Biol. 1996;54:35-100.

Bustin M. At the crossroads of necrosis and apoptosis: signaling to multiple cellular targets by HMGB1. Sci STKE. 2002(151)

Bustin M., Lehn D. A., Landsman D., 1990: Structural features of the HMG chromosomal proteins and their genes. Bioch. Biophys. Acta. 1049: 231-243.

Bustin M. Regulation of DNA-dependent activities by the functional motifs of the high-mobility-group chromosomal proteins. Mol Cell Biol. 1999;19(8):5237-46.

Calogero S, Grassi F, Aguzzi A, Voigtlander T, Ferrier P, Ferrari S, Bianchi ME. The lack of chromosomal protein Hmg 1does not disrupt cell growth but causes lethal hypoglycaemia in newborn mice. Nat Genet. 1999;22(3):276-80.

Calogero S, Grassi F, Aguzzi A, Voigtlander T, Ferrier P, Ferrari S, Bianchi ME. The lack of chromosomal protein Hmg1 does not disrupt cell growth but causes lethal hypoglycaemia in newborn mice. Nat Genet. 1999; 22(3):276-80.

Cary PD, Shooter KV, Goodwin GH, Johns EW, Olayemi JY, Hartman PG, Bradbury EM. Does high-mobility-group non-histone protein HMG 1 interact specifically with histone H1 subfractions. Biochem J. 1979; 183(3):657-62.

Chalfie M, Sulston JE, White JG, Southgate E, Thomson JN, Brenner S. The neural circuit for touch sensitivity in *Caenorhabditis elegans*. J Neurosci. 1985; 5(4):956-64.

Chalfie M, Sulston J. Developmental genetics of the mechanosensory neurons of *Caenorhabditis elegans*. Dev Biol. 1981; 82(2):358-70.

Chalfie M, Thomson JN. Organization of neuronal microtubules in the nematode *Caenorhabditis elegans*. J Cell Biol. 1979; 82(1):278-89.

Chiba CM, Rankin CH. A developmental analysis of spontaneous and reflexive reversals in the nematode *Caenorhabditis elegans*. J Neurobiol. 1990; 21(4):543-54.

Choi DW. Excitotoxic cell death. J Neurobiol. 1992; 23(9):1261-76.

Cleary ML. Oncogenic conversion of transcription factors by chromosomal translocations. Cell. 1991*;* 66(4):619-22.

Cockwell KY, Giles IG. Software tools for motif and pattern scanning: program descriptions including a universal sequence reading algorithm. Comput Appl Biosci. 1989; 5(3):227-32.

Crane-Robinson C, Coles B, Goodwin GH. cDNA cloning of the HMGI-C phosphoprotein, a nuclear protein associated with neoplastic and undifferentiated phenotypes. Nucleic Acids Res. 1991*;*19(24):6793-7.

Dal Santo P, Logan MA, Chisholm AD, Jorgensen EM. The inositol trisphosphate receptor regulates a50 -second behavioral rhythm in *C. elegans*. Cell. 1999*;* 98(6):757-67.

Einck L, Bustin M. The intracellular distribution and function of the high mobility group chromosomal proteins. Exp Cell Res. 1985;156(2):295-310.

Falciola L, Spada F, Calogero S, Langst G, Voit R, Grummt I, Bianchi ME. High mobility group 1 protein is not stably associated with the chromosomes of somatic cells.J Cell Biol. 1997; 137(1):19-26.

Farnet CM, Bushman FD. HIV- 1cDNA integration: requirement of HMG I(Y) protein for function of preintegration complexes in vitro. Cell. 1997; 88(4):483-92.

Fire A. RNA-triggered gene silencing. Trends Genet. 1999 Sep;15(9):358-63.

Fire A, Xu S, Montgomery MK, Kostas SA, Driver SE, Mello CC. Potent and specific genetic interference by double-stranded RNA in Caenorhabditis elegans. Nature.1998; 391 (6669):806-11.

Friedmann M, Holth LT, Zoghbi HY, Reeves R. Organization, inducible-expression and chromosome localization of the human HMG-I(Y) nonhistone protein gene. Nucleic Acids Res. 1993; 21(18):4259-67.

Ge H, Roeder RG. The high mobility group protein HMG 1can reversibly inhibit class II gene transcription by interaction with the TATA-binding protein. J Biol Chem. 1994; 269(25):17136-40.

Giancotti V, Bandiera A, Buratti E, Fusco A, Marzari R, Coles B, Goodwin GH. Comparison of multiple forms of the high mobility group I proteins in rodent and human cells. Identification of the human high mobility group I-C protein. Eur J Biochem. 1991; 198(1):211-6.

Giancotti V, Bandiera A, Buratti E, Fusco A, Marzari R, Coles B, Goodwin GH. Comparison of multiple forms of the high mobility group I proteins in rodent and human cells. Identification of the human high mobility group I-C protein. Eur J Biochem. 1991; 198(1):211-6.

Giancotti V, Pani B, D'Andrea P, Berlingieri MT, Di Fiore PP, Fusco A, Vecchio G, Philp R, Crane-Robinson C, Nicolas RH, et al. Elevated levels of a specific class of nuclear phosphoproteins in cells transformed with v-ras and v-mos oncogenes and by cotransfection with c-myc and polyoma middle T genes.EMBO J. 1987;6(7):1981-7.

Goodwin GH, Brown E, Walker JM, Johns EW. The isolation of three new high mobility group nuclear proteins. Biochim Biophys Acta. 1980; 623(2):329-38.

Gubbay J, Collignon J, Koopman P, Capel B, Economou A, Munsterberg A, Vivian N, Goodfellow P, Lovell-Badge R. A gene mapping to the sex-determining region of the mouse Y chromosome is a member of a novel family of embryonically expressed genes. Nature. 1990; 346(6281):245-50.

Gupta BP, Sternberg PW. The draft genome sequence of the nematode Caenorhabditis briggsae, a companion to *C. elegans*. Genome Biol. 2003;4(12):238.

Grasser KD. Chromatin-associated HMGA and HMGB proteins: versatile co-regulators of DNA-dependent processes. Plant Mol Biol. 2003; 53(3):281-95.

Hamada H, Bustin M. Hierarchy of binding sites for chromosomal proteins HMG 1 and 2 in supercoiled deoxyribonucleic acid. Biochemistry. 1985*;* 24(6):1428-33.

Hengartner MO. Apoptosis and the shape of death. Dev Genet.1997*;* 21(4):245-8.

Hindmarsh P, Ridky T, Reeves R, Andrake M, Skalka AM, Leis J. HMG protein family members stimulate human immunodeficiency virus type 1 and avian sarcoma virus concerted DNA integration in vitro. J Virol. 1999 Apr;73(4):2994-3003.

Hughes EN, Engelsberg BN, Billings PC. Purification of nuclear proteins that bind to cisplatin-damaged DNA. Identity with high mobility group proteins 1 and 2 . J Biol Chem. 1992; 267(19):13520-7.

Huttunen HJ, Fages C, Rauvala H. Receptor for advanced glycation end products (RAGE)-mediated neurite outgrowth and activation of NF-kappaB require the cytoplasmic domain of the receptor but different downstream signaling pathways. J Biol Chem. 1999; 274(28):19919-24.

Ichikawa K, Yoshinari M, Iwase M, Wakisaka M, Doi Y, Iino K, Yamamoto M, Fujishima M. Advanced glycosylation end products induced tissue factor expression in human monocyte-like U 937cells and increased tissue factor expression in monocytes from diabetic patients.Atherosclerosis. 1998;136(2):281-7.

Imamura T, Izumi H, Nagatani G, Ise T, Nomoto M, Iwamoto Y, Kohno K. Interaction with p 53enhances binding of cisplatin-modified DNA by high mobility group 1 protein. J Biol Chem. 2001; 276(10):7534-40.

Jiang LI, Sternberg PW. An HMG1-like protein facilitates Wnt signaling in *Caenorhabditis elegans*. Genes Dev. 1999; 13(7):877-89.

Johns E. W., 1964:Preparative methods for histone fractions from calf thymus. Biochem. J. 92: 55-59.

Johns E. W., 1982: History, definitions and problems. In: JOHNS E.W. (Hrsg.): The HMG Chromosomal Proteins. London: Academic Press.

Johnson KR, Disney JE, Wyatt CR, Reeves R. Expression of mRNAs encoding mammalian chromosomal proteins HMG-I and HMG-Y during cellular proliferation. Exp Cell Res. 1990; 187(1):69-76.

Johnson KR, Lehn DA, Elton TS, Barr PJ, Reeves R. Complete murine cDNA sequence, genomic structure, and tissue expression of the high mobility group protein HMG-I(Y). J Biol Chem. 1988; 263(34):18338-42.

Johnson KR, Lehn DA, Reeves R. Alternative processing of mRNAs encoding mammalian chromosomal high-mobility-group proteins HMG-I and HMG-Y. Mol Cell Biol. 1989; 9(5):2114-23.

Kamath RS, Martinez-Campos M, Zipperlen P, Fraser AG, Ahringer J. Effectiveness of specific RNA-mediated interference through ingested double-stranded RNA in Caenorhabditis elegans. Genome Biol. 2001;2(1):1-10.

Kamath RS, Ahringer J. Genome-wide RNAi screening in Caenorhabditis elegans. Methods. 2003; 30(4):313-21.

Karp, G. (2002): Cell and molecular biology, concepts and experiments. John wiley & and son, New York, United states of America.

Kim SK, Lund J, Kiraly M, Duke K, Jiang M, Stuart JM, Eizinger A, Wylie BN, Davidson GS. A gene expression map for *Caenorhabditis elegans*. Science. 2001; 293(5537):2087-92.

Kitamura KI, Amano S, Hosono R. Contribution of neurons to habituation to mechanical stimulation in *Caenorhabditis elegans*. J Neurobiol. 2001; 46(1):29-40.

Klein-Hessling S, Schneider G, Heinfling A, Chuvpilo S, Serfling E. HMG I(Y) interferes with the DNA binding of NF-AT factors and the induction of the interleukin 4 promoter in T cells.Proc Natl Acad Sci U S A. 1996 Dec24 ;93(26):15311-6

Landsman D, Bustin M. A signature for the HMG- 1box DNA-binding proteins. Bioessays. 1993 Aug;15(8):539-46.

Lee KB, Thomas JO. The effect of the acidic tail on the DNA-binding properties of the HMG1,2 class of proteins: insights from tail switching and tail removal. J Mol Biol. 2000; 304(2):135-49.

Lee KK, Gruenbaum Y, Spann P, Liu J, Wilson KL. C. elegans nuclear envelope proteins emerin, MAN1, lamin, and nucleoporins reveal unique timing of nuclear envelope breakdown during mitosis. Mol Biol Cell. 2000 Sep;11(9):3089-99.

Leist M, Nicotera P. Apoptosis versus necrosis: the shape of neuronal cell death Results Probl Cell Differ. 1998;24:105-35.

Lin R, Hill RJ, Priess JR. POP- 1and anterior-posterior fate decisions in *C. elegans* embryos. Cell. 1998; 92(2):229-39.

Lin R, Thompson S, Priess JR. pop- 1encodes an HMG box protein required for the specification of a mesoderm precursor in early *C. elegans* embryos.Cell. 1995; 83(4):599-609.

Llewellyn DH, Johnson S, Eggleton P. Calreticulin comes of age.Trends Cell Biol. 2000; 10(9):399-402.

Lund T, Holtlund J, Fredriksen M, Laland SG. On the presence of two new high mobility group-like proteins in HeLa S3 cells. FEBS Lett. 1983; 152(2):163-7.

Maeda I, Kohara Y, Yamamoto M, Sugimoto A. Large-scale analysis of gene function in Caenorhabditis elegans by high-throughput RNAi. Curr Biol. 2001 Feb 6;11(3):171-6.

Maher JF, Nathans D. Multivalent DNA-binding properties of the HMG- 1proteins. Proc Natl Acad Sci U S A. 1996; 93(13):6716-20.

Maniatis T., Fritsch E. F., Sambrook J., 1982: Molecular Cloning: A Laboratory Manual. New York: Cold Spring Harbor Laboratory.

Maryon EB, Coronado R, Anderson P. unc-68 encodes a ryanodine receptor involved in regulating *C. elegans* body-wall muscle contraction. J Cell Biol. 1996; Pozzan T, Rizzuto R, Volpe P, Meldolesi J. Molecular and cellular physiology of intracellular calcium stores. Physiol Rev. 1994; 74(3):595-636.

McCarter J, Bartlett B, Dang T, Schedl T. Soma-germ cell interactions in *Caenorhabditis elegans*: multiple events of hermaphrodite germline development require the somatic sheath and spermathecal lineages. Dev Biol. 1997;181(2):121-43.

Meneghini MD, Ishitani T, Carter JC, Hisamoto N, Ninomiya-Tsuji J, Thorpe CJ, Hamill DR, Matsumoto K, Bowerman B. MAP kinase and Wnt pathways converge to downregulate an HMG-domain repressor in *Caenorhabditis elegans*.

Michalak M, Corbett EF, Mesaeli N, Nakamura K, Opas M. Calreticulin: one protein, one gene, many functions. Biochem J. 1999; 344 Pt 2:281-92.

Muller S, Scaffidi P, Degryse B, Bonaldi T, Ronfani L, Agresti A, Beltrame M, Bianchi ME. New EMBO members' review: the double life of HMGB1 chromatin protein: architectural factor and extracellular signal. EMBO J. 2001; 20(16):4337-40.
Nature. 1999; 399(6738):793-7.

Ner SS, Travers AA. HMG-D, the Drosophila melanogaster homologue of HMG 1 protein, is associated with early embryonic chromatin in the absence of histone H1.EMBO J. 1994; 13(8):1817-22.

Onate SA, Prendergast P, Wagner JP, Nissen M, Reeves R, Pettijohn DE, Edwards DP. The DNA-bending protein HMG-1 enhances progesterone receptor binding to its target DNA sequences. Mol Cell Biol. 1994; 14(5):3376-91.

Orrenius S, Zhivotovsky B, Nicotera P. Regulation of cell death: the calcium-apoptosis link. Nat Rev Mol Cell Biol. 2003; 4(7):552-65.

Pallier C, Scaffidi P, Chopineau-Proust S, Agresti A, Nordmann P, Bianchi ME, Marechal V. Association of chromatin proteins high mobility group box (HMGB) 1 and HMGB2 with mitotic chromosomes. Mol Biol Cell. 2003; 14(8):3414-26.

Pallier C, Scaffidi P, Chopineau-Proust S, Agresti A, Nordmann P, Bianchi ME, Marechal V. Association of chromatin proteins high mobility group box (HMGB) 1 and HMGB2 with mitotic chromosomes. Mol Biol Cell. 2003; 14(8):3414-26.

Baxevanis AD, Bryant SH, Landsman D. Homology model building of the HMG-1 box structural domain. Nucleic Acids Res. 1995 Mar 25; 23(6):1019-29.

Piano F, Schetter AJ, Morton DG, Gunsalus KC, Reinke V, Kim SK, Kemphues KJ. Gene clustering based on RNAi phenotypes of ovary-enriched genes in C. elegans. Curr Biol. 2002; 12(22):1959-64.

Piekielko A, Drung A, Rogalla P, Schwanbeck R, Heyduk T, Gerharz M, Rabbani A, Goodwin GH, Johns EW. Studies on the tissue specificity of the high-mobility-group non-histone chromosomal proteins from calf. Biochem J. 1978;173(2):497-505.

Read CM, Cary PD, Crane-Robinson C, Driscoll PC, Norman DG. Solution structure of a DNA-binding domain from HMG1. Nucleic Acids Res. 1993; 21(15):3427-36.

Riddle, D. L.; Blumenthal, T.; Meyer, B.J.; Priess, J. R. (1997): *C. elegans* **II**, Cold Spring Harbor Laboratory Press United States of America.

Rocheleau CE, Yasuda J, Shin TH, Lin R, Sawa H, Okano H, Priess JR, Davis RJ, Mello CC. WRM- 1activates the LIT- 1protein kinase to transduce anterior/posterior polarity signals in *C. elegans*. Cell. 1999*;* 97(6):717-26.

Scaffidi P, Misteli T, Bianchi ME. Release of chromatin protein HMGB 1by necrotic cells triggers inflammation. Nature. 2002 Jul11*;* 418(6894):191-5.

Schroeder DF, McGhee JD. Anterior-posterior patterning within the *Caenorhabditis elegans* endoderm. Development. 1998;125(24):4877-87.

Sheflin LG, Fucile NW, Spaulding SW. The specific interactions of HMG 1 and 2 with negatively supercoiled DNA are modulated by their acidic C-terminal domains and involve cysteine residues in their HMG1 / 2boxes. Biochemistry. 1993; 32(13):3238-48.

Shooter RA, Cooke EM, O'Farrell S, Bettelheim KA, Chandler ME, Bushrod FM. The isolation of Escherichia coli from a poultry packing station and an abattoir. J Hyg (Lond). 1974; 73(2):245-7.

Shykind BM, Kim J, Sharp PA. Activation of the TFIID-TFIIA complex with HMG-2. Genes Dev. 1995; 9(11):1354-65.

Sinclair AH, Berta P, Palmer MS, Hawkins JR, Griffiths BL, Smith MJ, Foster JW, Frischauf AM, Lovell-Badge R, Goodfellow PN. A gene from the human sex-determining region encodes a protein with homology to a conserved DNA-binding motif. Nature. 1990; 346(6281):240-4.

Smerdon MJ, Isenberg I. Interactions between the subfractons of calf thymus H1 and nonhistone chromosomal proteins HMG1 and HMG2. Biochemistry. 1976 Sep 21;15(19):4242-7.

Soullier S, Jay P, Poulat F, Vanacker JM, Berta P, Laudet V. Diversification pattern of the HMG and SOX family members during evolution. J Mol Evol. 1999; 48(5):517-27.

Strauss F, Varshavsky A. A protein binds to a satellite DNA repeat at three specific sites that would bebrought into mutual proximity by DNA folding in the nucleosome. Cell. 1984; 37(3):889-901.

Stros M, Stokrova J, Thomas JO. DNA looping by the HMG-box domains of HMG 1and modulation of DNA binding by the acidic C-terminal domain. Nucleic Acids Res. 1994; 22(6):1044-51.

Takemura H, Hughes AR, Thastrup O, Putney JW Jr. Activation of calcium entry by the tumor promoter thapsigargin in parotid acinar cells. Evidence that an intracellular calcium pool and not an inositol phosphate regulates calcium fluxes at the plasma membrane. J Biol Chem. 1989 Jul25 ;264(21):12266-71.

Thanos D, Maniatis T. Virus induction of human IFN beta gene expression requires the assembly of an enhanceosome. Cell. 1995 Dec29 ;83(7):1091-100.

Thorpe CJ, Schlesinger A, Carter JC, Bowerman B. Wnt signaling polarizes an early *C. elegans* blastomere to distinguish endoderm from mesoderm. Cell. 1997; 90(4):695-705.

Timmons L, Fire A. Specific interference by ingested dsRNA. Nature. 1998; 395(6705):854.

Tjian R, Maniatis T. Transcriptional activation: a complex puzzle with few easy pieces. Cell. 1994; 77(1):5-8.

Tremethick DJ, Molloy PL. High mobility group proteins 1 and 2 stimulate transcription in vitro by RNA polymerases II and III. J Biol Chem. 1986 May25; 261(15):6986-92.

Vaccari T, Beltrame M, Ferrari S, Bianchi ME. Hmg4, a new member of the Hmg1/2 gene family. Genomics. 1998; 49(2):247-52.

Waterman ML, Fischer WH, Jones KA. A thymus-specific member of the HMG protein family regulates the human T cell receptor C alpha enhancer. Genes Dev. 1991; 5(4):656-69.

Weir HM, Kraulis PJ, Hill CS, Raine AR, Laue ED, Thomas JO. Structure of the HMG box motif in the B-domain of HMG1. EMBO J. 1993;12(4):1311-9.

Wisniewski JR, Schwanbeck R. High mobility group I/Y: multifunctional chromosomal proteins causally involved in tumor progression and malignant transformation. Int J Mol Med. 2000; 6(4):409-19.

Xu K, Tavernarakis N, Driscoll M. Necrotic cell death in *C. elegans* requires the function of calreticulin and regulators of Ca(2+) release from the endoplasmic reticulum. Neuron. 2001; 31(6):957-71.

Zappavigna V, Falciola L, Helmer-Citterich M, Mavilio F, Bianchi ME. HMG1 interacts with HOX proteins and enhances their DNA binding and transcriptional activation. EMBO J. 1996; 15(18):4981-91.

Zhou X, Benson KF, Ashar HR, Chada K. Mutation responsible for the mouse pygmy phenotype in the developmentally regulated factor HMGI-C. Nature. 1995; 376(6543):771-4.

Zwaal RR, Van Baelen K, Groenen JT, van Geel A, Rottiers V, Kaletta T, Dode L, Raeymaekers L, Wuytack F, Bogaert T. The sarco-endoplasmic reticulum Ca^{2+} ATPase is required for development and muscle function in *Caenorhabditis elegans*. J Biol Chem. 2001; 276(47):43557-63.

Zwilling S, Konig H, Wirth T. High mobility group protein 2 functionally interacts with the POU domains of octamer transcription factors. EMBO J. 1995 Mar 15;14(6):1198-208. Genomes: a helpful cousin for our favourite worm. Curr Biol. 2004; 14(2):R75-7.

7. Abbreviations

aa	Amino acid
Amp	ampicillin, α-aminobenzylpenicillin
APS	ammonium persulfate
ATP	adenosine triphosphate
bp	base pairs
bp	band-pass
BSA	bovine serum albumin
cDNA	complementary DNA
°C	degrees Celsius
C. elegans	*Caenorhabditis elegans*
CFP	cyan fluorescence protein
CGC	Caenorhabditis Genetic Center
Cm	centimeters
Cy2	Cyanine Cy2
Cy3	Cyanine Cy3
DAPI	4´,6-diamidino-2-phenylindol
dATP	desoxyadenosine triphosphate
dCTP	desoxycitosine triphosphate
ddH2O	double-distilled water
dGTP	desoxyguanosine triphosphate
dH_2O	distilled water
ddH_2O	double distilled water
DNA	deoxyribonucleic acid
DNase	deoxyribonuclease
dsDNA	double -stranded DNA
DTC	distal tip cell
DTT	dithiotreitol
EDTA	ethylenediaminetetraacetic acid
ER	endoplasmic reticulum
e.g.	for example (Lat. *exempli gratia*)
et	*al.* et alii, and others
Ex	extrachromosomal array
F1	first generation
F2	second generation
Fig.	figure
g	gravitaty unit for centrifugation, and gram for weight
GFP	green fluorescence protein
h	hour
HCl	Hydrochloric acid
him	high incidence of males
HMG	high mobility group protein
IP3	inositol-1,4,5-triphosphat
IPTG	isopropyl-1-thio-β-D-galactopyranoside and 5-Bromo-4-chloro- 3-indolyl- β -D-glactopyranoside
Kan	kanamycin, from *Streptomyces kanamyceticus*
Kb	kilobase
Kbp	kilobase pair
KDa	kilo dalton
l	liter
L1 first	larval stage
L2	second larval stage
L3	third larval stage

L4	fourth larval stage
LB	Laura-Bertani medium
LBR	lamin B receptor
LSM 510	laser scanning microscope 510
µ	micro
m	milli
mA	milli ampere
M	Molar
min	minute & minutes
mRNA	messenger RNA
MW	molecular weight
n	nano
nm	nanometer
NMWL	nomina molecular weight limit
NA	numerical aperture
NaCl	sodium chloride
NaOH	sodium hydroxide
NGM	nematode growth medium
NH_4Ac	ammonium acetate
Nomarski -DIC	Nomarski differential interference contrast
N-Terminal	amino-terminal
OD	optical density
P0	the parents
PAGE	polyacrylamide gel electrophoresis
PBS	phosphate-buffered saline
PCR	polymerase chain reaction
RNA	ribonucleic acid
RNAi	RNA interference
RNase	ribonuclease
rpm	round per minute
s	seconds
S	Streptavidin
SERCA	Sarco-endoplasmic reticulum Ca^{2+} ATPase
ssDNA	single-stranded DNA
SDS	sodium dodecyl sulfate
TAE	tris acetate EDTA buffer
TEMED	N,N,N',N'-tetramethylethylenediamine
Tris	tris (hydroxymethyl)-aminomethane
U	units
UV	ultra-violet
v	volume
V	volts
wt wild	type
YFP yellow	fluorescence protein
-/-	homozygous mutant
+/-	heterozygous mutant
+/+	wild type animal
n^-	animal that have 'n' cell ablated

8. Acknowledgment

I would like to express my deep and sincere gratitude to my supervisor PD. Dr. E. Schulze for giving me the opportunity to prepare this thesis in the fascinating field of the developmental biology of *C. elegans*. I am grateful for his scientific supervision and his valuable suggestions for the improvement of this thesis and accepting to be my referee.

I am very thankful to Prof. Dr. T. Pieler to give me the chance, by his agreement, to be a member in the graduate school (GRK). I am appreciating the great help from Dr. B. Schulze in correcting and sharing ideas to improve the structure and layout of my thesis.

I sincerely thank Prof. Dr. U. Grossbach, for his continuous support and helpful supervision. Prof. Dr. M. Kessel for being my co-referee. I also extend my sincere thanks to PD. Dr. E. Schulze, Prof. Dr. D. Gradmann and Prof. Dr. R. Hardland for accepting to be my examiners. I would like to thank Prof. Dr. E. Wimmer, our head department, for supporting me and his agreement to use the facilities of the department to complete my thesis.

All my appreciation to Prof. Dr. M. Kessel for his great support, advice, and time that he spent to help me whenever It was needed.

I would like to thank all people in my department whom gave me all support, help, and advice. Especially, my colleagues, Dr. M. Bahrami, Dr. S. Fröde, Dr. M. Jedrusik-Bode, Mrs. F. Donkor, Mrs. V. Gehrt, and Mrs. S. Möhlmann. Special thanks to all technical assistance from Mrs. S. Pitzel and B. Lage. Also, the great help with the administrational and paper work from our secretary, Mrs. E. Blabusch and Mrs. B. Rossi.

special thanks for my friend Dr. med. B. Meraikib. Finally, I would like to give my warmest thanks to my family and my fiancée A. Graness for their great understanding and continuous support.

9. Lebenslauf

Name	Abd-elNasser Mohammed Abd-elMoneim Elashry	
Geburtsdatum	15. März 1971	
Geburtsort	El-Sharkria/Ägypten	
Nationalität	ägyptisch	
Schulausbildung	1977 - 1982	Grundschule in Kairo
	1982 - 1985	Orientierungsstufe in Kairo
	1985 - 1988	Gymnasium in Kairo
		Abitur
Studium	Oktober 1998	Master of Science, Fakultät für Landwirtschaft, Universität Kairo
	Mai 1992	Bachelor of Science, Fakultät für Landwirtschaft, Universität Kairo
Militärdienst	1992-1993	
Berufstätigkeit	1993-2000	wissenschaftlicher Mitarbeiter im Ministerium für Landwirtschaft, Giza, Ägypten
Promotion	ab August 2000	im Rahmen des Graduiertenkollegs "Molekulare Genetik der Entwicklung" im Göttinnger Zentrum für Molekulare Biowissenschaften, Abt. Entwicklungsbiologie der Georg-August-Universität Göttingen